

Establishment of a three-dimensional cell culture system to study tubular structures

A comparative study of neuronal differentiation in zebrafish
and in 2D and 3D zebrafish primary cell culture

Zur Erlangung des akademischen Grades eines
DOKTORS DER NATURWISSENSCHAFTEN
(Dr. rer. nat.)

von der KIT-Fakultät für Chemie und Biowissenschaften
des Karlsruher Instituts für Technologie (KIT)

genehmigte

DISSERTATION

von

Diplom-Biologin Simone Geyer
aus Mutlangen, Deutschland

Dekan: Prof. Dr. Willem Klopper

Referent: Associate Fellow Dr. Steffen Scholpp

Koreferent: Prof. Dr. Martin Bastmeyer

Koreferent: Priv.-Doz. Dr. Dietmar Gradl

Tag der mündlichen Prüfung: 18.12.2015

Dedicated to my parents

Erklärung der Urheberschaft

Ich erkläre hiermit an Eides statt, dass ich die vorliegende Arbeit selbstständig und ohne Benutzung anderer als der angegebenen Hilfsmittel angefertigt habe. Die aus fremden Quellen direkt oder indirekt übernommenen Gedanken sind als solche gekennzeichnet. Des Weiteren habe ich die Satzung der Universität Karlsruhe (TH) zur Sicherung guter wissenschaftlicher Praxis in der jeweils gültigen Fassung beachtet. Diese Arbeit wurde bisher weder in gleicher noch in ähnlicher Form einer anderen Prüfungsbehörde vorgelegt und auch nicht veröffentlicht.

Ort und Datum:

Unterschrift:

Karlsruhe, 04.11.2015

.....

.....

Simone Geyer

„Dream like a child, follow your heart, be honest and work hard“

(Samuel Aleksí Haber)

Abstract

The establishment and patterning of the nervous system represents a complex process during embryonic development and is still far from being completely understood. The complexity of an intact embryo hinders the elucidation of particular developmental steps. Therefore, a simplified controllable cell culture system is more suitable for the detailed dissection of neurogenesis *in vitro*. The aim of this thesis was to generate a zebrafish neural tube *in vitro* in a 3D cell culture system. Thereby, a comparative study of neuronal differentiation in the zebrafish and in 2D and 3D zebrafish primary cell culture was performed. The 3D platform, based on a polycarbonate microchannel, was formed to fit with the dimensions of a zebrafish neural tube and moreover biofunctionalized for the cultivation of cells. In this platform neurogenesis *in vitro* was investigated and compared to the *in vivo* scenario. By treatment with an inhibitor for the nodal signaling pathway, the formation of mesendodermal tissue was reduced and a population of neural progenitor cells was enriched. Therefore, the established 3D cell culture platform reflects a similar dynamic of neurogenesis like the *in vivo* scenario and is well controllable. Moreover, it was investigated if cells can be guided and cultivated in an area of interest in the microchannel. Thus, a photolithographic method was established, in which by light-inducible surface patterning a functionalized surface was created on a polycarbonate film. Cells were cultivated almost exclusively on the functionalized area and avoided non-functionalized regions due to the oligoethylenglycol (Hirschbiel and Geyer *et al.*, 2015). Thereby, a first step was made to investigate border regions, which are essential to separate particular brain parts, *in vitro*. Furthermore, based on studies which showed that the microenvironment in 2D and 3D results in altered cellular signaling, a co-cultivation study was performed with Wnt8a (an important factor for posteriorizing the neuroectoderm) and a Wnt reporter. A difference in Wnt reporter activation between cultivation in 2D and 3D was observed, whereas Wnt reporter activation was higher in 2D compared to 3D. Due to differences in 2D and 3D cultivated cells, existing 2D studies should be re-considered.

By establishment of the 3D platform, based on a microchannel, a controllable, reproducible system was generated to study the formation of tubular structures, guide cells to an area of interest and study cellular communication.

Acknowledgements/ Danksagung

This work was done at the Institute for Toxicology and Genetics at the Karlsruhe Institute of Technology.

I would like to thank Dr. Steffen Scholpp for giving me the opportunity to work in his group and on this exciting project and moreover for the introduction to zebrafish developmental neurobiology. His enthusiasm and scientific knowledge were of great support to push forward my project. Moreover, I would like to thank him for evaluating my PhD thesis.

I would like to thank Prof. Dr. Martin Bastmeyer to be my first co-referent and for evaluating my PhD thesis.

I would like to thank Dr. Dietmar Gradl to agree to be my second co-referent and for evaluating my PhD thesis.

Moreover, I would like to thank Prof. Dr. Christopher Barner-Kowollik and Dr. Astrid Hirschbiel for the fruitful collaboration and the opportunity for the shared first co-authorship. Furthermore, I thank Dr. Stefan Giselbrecht and Dr. Pavel Nikolov for the great collaboration and their effort in optimizing the microchannel. A special thanks goes to Dr. Pavel Nikolov for his great effort producing the microchannels and for reading this thesis and giving helpful suggestions.

I thank Dr. Guillaume Delaittre, Dr. Basit Yameen and Dr. Alexander Welle for collaboration.

I would like to thank Prof. Dr. Christopher Barner-Kowollik, Prof. Dr. Stefan Giselbrecht, Dr. Felix Loosli and Prof. Dr. Ute Schepers for being part of my TAC committee.

Many thanks goes to Dr. Peter Walentek for reading my thesis and giving me helpful advice. Moreover, I thank him for his amicable support during my time as a PhD and diploma student. He is an inspiring example of being an outstanding scientist, conveying his fascination for developmental biology and research in general to me.

Furthermore I would like to thank Dr. Eliana Stanganello for reading my thesis, for inspiring discussions about the project and for helpful suggestions.

Many thanks goes to the entire lab – Dr. Eliana Stanganello, Benjamin Mattes, Sabrina Weber, Bernadett Boesze, Steffi Mackensen, Nathalie Geyer and Yonglong Dang - for the great work environment. A special thanks goes to Dr. Eliana Stanganello for the introduction to cell culture and confocal microscopy and Sabrina Weber for technical and personal support contributing to this work and for the help with the in situ hybridization. Furthermore, I thank Benjamin Mattes for the motivation especially during the last months and being my “Lieblingsnebensitzer”.

I would like to thank Anna Geenen to be a great Bachelor student and supporting my project during her bachelor thesis.

I would like to thank Eliana Stanganello and Kathrin Herbst for their friendship and the great time we had together in and beyond the lab. Thanks for always being there!

Ebenso danke ich Karin Leue für ihre Freundschaft, Aufheiterung und Ablenkung, die mich immer wieder motiviert hat.

Lydia Stenger danke ich für die langjährige Freundschaft, Unterstützung und Aufmunterung in guten und suboptimalen Zeiten.

Der größte Dank gilt meinen Eltern, für die herzliche und unermüdliche Unterstützung, in motivierender und auch finanzieller Weise. Sie halten mir immer den Rücken frei und ohne sie wäre die Verwirklichung des Studiums und der Promotion nicht möglich gewesen.

Publication

„Photolithographic Patterning of 3D-Formed Polycarbonate Films for Targeted Cell Guiding“

Astrid F. Hirschbiel*, ***Simone Geyer****, *Basit Yameen*, *Alexander Welle*, *Pavel Nikolov*, *Stefan Giselbrecht*, *Steffen Scholpp*, *Guillaume Delaittre* and *Christopher Barner-Kowollik*
*shared first-authorship

Adv. Mater. 2015, DOI: 10.1002/adma.201500426

Table of Contents

ABSTRACT	I
ACKNOWLEDGEMENTS	II
LIST OF PUBLICATIONS	IV
FIGURE INDEX	VII
ABBREVIATIONS	VII
SUMMARY	X
1. Introduction	- 1 -
1.1 General Introduction	- 1 -
1.2 The zebrafish as model organism	- 1 -
1.3 Embryonic development of <i>Danio rerio</i>	- 2 -
1.3.1 From Cleavage to mid-blastula transition.....	- 2 -
1.3.2 Gastrulation.....	- 2 -
1.3.3 Establishment of the central nervous system	- 4 -
1.4 The Wnt family.....	- 20 -
1.4.1 The canonical Wnt signaling pathway	- 21 -
1.5 Cell culture systems	- 23 -
1.5.9 2D Cell Culture Systems	- 26 -
1.5.10 3D Cell Culture Systems	- 28 -
1.6. Aim of this project.....	- 33 -
2. Material and Methods	- 34 -
2.1 Material	- 34 -
2.2 Methods	- 38 -
3. Results	- 46 -
3.1 Control of neurogenesis	- 46 -
3.1.1 Expression analysis of relevant dynamic markers during zebrafish embryonic development.....	- 46 -
3.1.2 Neural differentiation <i>in vivo</i>	- 49 -
3.1.3 Analysis of <i>neurogenin1</i> expression.....	- 50 -
3.1.4 Analysis of Rohon-Beard sensory neurons.....	- 51 -
3.1.5 Cultivation of neural progenitor cells <i>in vitro</i>	- 53 -
3.1.6 Control of neurogenesis in 2D	- 53 -
3.1.7 Establishment of a 3D cell culture system to generate a neural tube	- 55 -
3.1.8 Control of neurogenesis in a 3D microchannel	- 59 -
3.1.9 Comparison of <i>in vitro</i> altered neurogenesis to the <i>in vivo</i> scenario	- 61 -

3.2 Guided Cell Attachment	- 63 -
3.2.1 Synthetic strategy for the development of a functionalized wave pattern by Astrid Hirschbiel.....	- 64 -
3.2.2 Testing of adhesion capability of the functionalized wave pattern	- 64 -
3.3 Cellular signaling	- 69 -
3.3.1 Comparison of Wnt reporter activation in 2D compared to 3D.....	- 69 -
4. Discussion	- 74 -
5. References	- 90 -

Figure Index

Figure 1:	Zebrafish development.....	2
Figure 2:	Fate map of a zebrafish gastrula embryo.....	3
Figure 3:	Neural tube formation in zebrafish.....	7
Figure 4:	Neurog1 expression in Rohon-Beard sensory neurons.....	14
Figure 5:	Simplified scheme of the canonical Wnt pathway.....	22
Figure 6:	Time line of relevant events for this thesis.....	33
Figure 7:	Expression analysis of relevant dynamic markers during zebrafish embryonic development.....	47
Figure 8:	Expression of neurog1:RFP/elavl3:GFP in a 24hpf and 48hpf zebrafish embryo.....	49
Figure 9:	Inhibition of mesendoderm formation by the SB431542 Nodal Inhibitor.....	50
Figure 10:	Neurog1 in situ hybridization.....	51
Figure 11:	Analysis of Rohon-Beard sensory neurons.....	52
Figure 12:	Cultivation of neurog1:RFP cells in 2D.....	53
Figure 13:	Control of neurogenesis in 2D.....	54
Figure 14:	Production and visualization of the microchannel.....	56
Figure 15:	Biofunctionality test of the microchannel with PAC2 cells.....	56
Figure 16:	Testing of different coating conditions with and without UV-ozone treatment.....	57
Figure 17:	Vision of the establishment of a neural tube inside the microchannel.....	59
Figure 18:	Control of neurogenesis in 3D.....	60
Figure 19:	Acquisition of neurog1:RFP pos. nuclei in 2D vs. 3D.....	61
Figure 20:	Quantification of neurog1:RFP pos. nuclei of the 2D (a) and 3D (b) <i>in vitro</i> experiment and RB sensory neurons expressing neurog1 <i>in vivo</i>	62
Figure 21:	Testing of adhesion capability of the functionalized wave pattern.....	65
Figure 22:	Attachment of PAC2 fibroblast cells to a surface patterned polycarbonate film.....	66
Figure 23:	Attachment of PAC2 fibroblast cells to a surface patterned 3D polycarbonate microchannel.....	67
Figure 24:	Co-cultivation of Wnt8a-GFP and TcfmCherry/His-CFP transfected HEK293T cells in 2D and 3D.....	70
Figure 25:	Analysis of Wnt reporter activation and Tcf Intensity-Mean.....	71
Figure 26:	Neuronal differentiation.....	75
Figure 27:	Model for the formation of a boundary <i>in vitro</i>	87
Table 1:	UV only, UV ozone and coating conditions.....	58

Abbreviations

ALK receptor	activin receptor-like kinase
AS-C	Achaete scute
bHLH	basic helix loop helix
BMP	Bone morphogenetic protein
Brn3a	brain-specific homeobox/POU domain protein 3A
CCS	Cell culture system
C-Division	Crossing division
CNS	Central nervous system
COP	Cycloolefin polymer
DAPI	4',6-Diamidin-2-phenylindol
DMSO	Dimethylsulfoxid
EB	Embryoid body
ECM	Extracellular matrix
eGFP	enhanced green fluorescent protein
elavl3	ELAV like neuron-specific RNA binding protein 3
ESC	Embryonic stem cell
Espl	Enhancer of split
EVL	Enveloping layer
FCS	Fetal calf serum
GFP	Green fluorescent protein
GOF	Gain-of-function
GSK3	Glycogen synthase kinase 3
HEK293T cells	Human epithelial kidney cells
hESC	human embryonic stem cell
hPSC	human pluripotent stem cell
HuC	Human neuronal protein C
INM	Interkinetic nuclear migration
iPSC	induced pluripotent stem cell
KV	Kupffer´s vesicle
LOF	Loss-of-function
MEF	Mouse embryonic fibroblasts
MHB	midbrain hindbrain boundary

MHBC	midbrain hindbrain boundary constriction
NC	Neural crest
NEC	Neuroepithelial cell
neurog1	neurogenin 1
NI	Nodal Inhibitor
NICD	Notch intracellular domain
NPB	Neural plate border
NPC	Neural progenitor cell
NSC	Neural stem cell
NSPC	Neural stem progenitor cell
OEG	oligo(ethylene glycol)
OEP	one-eyed pinhead
Pax6	paired-homeodomain transcription factor 6
PC	Polycarbonate
PCC	Primary cell culture
PCs	Progenitor cells
PNN	Perineuronal net
pou5f3	POU domain, class 5, transcription factor 3
RB	Rohon-Beard
RGC	Radial glial cell
SC	Stem cell
SEM	Scanning electron microscopy
SFEB	serum-free culture of EB-like aggregate
Shh	Sonic hedgehog
SMART	Surface modification and replication by thermoforming
Sox2	Sex determining region Y-box 2
SoxB1 family	SRY-box containing genes
SVZ	Subventricular zone
TGF- β	Transforming growth factor beta
VZ	Ventricular zone
YSL	Yolk synthicial layer
ZLI	Zona limitans intrathalamica

Zusammenfassung

Die Bildung des Nervensystems und dessen Strukturierung stellt einen komplexen Prozess während der Embryonalentwicklung dar und ist trotz einiger *in vivo* basierter Erkenntnisse bei weitem noch nicht vollständig aufgeklärt. Die Komplexität eines intakten Embryos erschwert die Aufklärung einzelner Entwicklungsschritte. Daher ist ein vereinfachtes kontrollierbares Zellkultursystem geeigneter, um Neurogenese *in vitro* detailliert aufzuklären. Ziel dieser Arbeit war es, das Neuralrohr eines Zebrafisches *in vitro* in einem dreidimensionalen Zellkultursystem zu generieren. Dabei wurde eine vergleichende Studie zur neuronalen Differenzierung im Zebrafisch und in einer 2D und 3D Zebrafisch Primärzellkultur durchgeführt. Als Basis des 3D Zellkultursystems diente ein Mikrokanal, geformt aus einem Polycarbonatfilm, welcher den Dimensionen eines Zebrafisch Neuralrohrs entspricht. Diese Kanalstruktur wurde biofunktionalisiert um die Kultivierung von Zellen zu ermöglichen. In dieser Plattform wurde der Prozess der Neurogenese *in vitro* mit der *in vivo* Situation verglichen. Durch Behandlung mit einem Inhibitor für den Nodal-Signalweg konnte die Bildung von mesendodermalem Gewebe reduziert und eine Population von neuronalen Vorläuferzellen angereichert werden. Schlussfolgernd reflektiert die etablierte 3D Zellkultur eine ähnliche Dynamik der Neurogenese *in vivo* und repräsentiert ein gut kontrollierbares System. Darüber hinaus wurde untersucht ob Zellen gerichtet in einem bestimmten Bereich im Mikrokanal kultiviert werden können. Dafür wurde ein photolithographisches Verfahren entwickelt, wobei durch licht-induzierbare Oberflächenstrukturierung eine funktionalisierte Region auf dem Polycarbonatfilm generiert wurde. Es gelang Zellen nahezu ausschließlich in diesem Bereich zu kultivieren, wobei nicht-funktionalisierte Bereiche auf Grund des vorhandenen Oligoethylenglycols von den Zellen gemieden wurden (Hirschbiel und Geyer *et al.*, 2015). Dadurch wurde eine Grundlage geschaffen um Grenzregionen, die essentiell sind um die einzelnen Gehirnabschnitte abzugrenzen, *in vitro* zu untersuchen. Basierend auf Studien die zeigten dass die Mikroumgebung in 2D und 3D in Veränderungen zellulärer Signalkommunikation resultiert, wurde eine Co-Kultivierungsstudie mit Wnt8a (einem wichtigen Faktor zur Strukturierung des posterioren Neuroektoderms) und einem Wnt Reporter durchgeführt. Es wurde ein Unterschied in der Wnt-Reporter Aktivierung zwischen Kultivierung in 2D und 3D Zellkultur beobachtet, wobei die Wnt-Reporter Aktivierung in 2D höher war als in 3D. Durch unterschiedliches Verhalten von 2D und 3D kultivierten Zellen hinsichtlich Signalkommunikation sollten Erkenntnisse aus vorangegangenen 2D Studien überdacht werden. Durch die Etablierung dieser 3D Plattform, basierend auf einem Mikrokanal wurde ein kontrollierbares, reproduzierbares System geschaffen, um tubuläre Signalkommunikation zu beobachten.

1. Introduction

1.1 General Introduction

The most fascinating event in biology is the development of a living creature. Starting from a fertilized egg embryonic development is characterized by different conserved mechanisms, including fertilization, cleavage, gastrulation, neurulation, organogenesis and growth.

Massive cell rearrangements, proliferation and differentiation require a complex and accurately defined communication between cells over a short and long distance. The right cell type has to be generated at the right time and place. Therefore, a precisely regulation of the balance between differentiating cells and cells maintaining in the stem cells pool is crucial for successful tissue development and adult maintenance. Thus, various signaling pathways are essential to create a healthy adult organism. Although researchers gain more and more insights into the manifold processes of how a fertilized egg develops into an adult organism, the big puzzle is yet far away from being completely understood. Thus, embryonic development remains one of the most fascinating biological enigmas in biomedical research.

1.2 The zebrafish as model organism

Danio rerio represents a suitable system to study embryonic development, since fertilization takes place externally and the eggs develop into a larvae in three days. Moreover, the nervous system is already established after 48 hours post fertilization (hpf). Due to the transparency, embryonic development can be observed in the living embryo. Furthermore, a huge amount of zebrafish can be easily maintained with relatively low costs, since they are small and one female can lay hundreds of eggs. Besides, the zebrafish genome is sequenced and a number of genetic tools are available, as well as mutants and transgenic lines. Furthermore, *Danio rerio* is suitable for manipulations, e.g. microinjections, or transplantation assays. A zebrafish embryo can be raised into an adult organism in about three months (Fig.1).

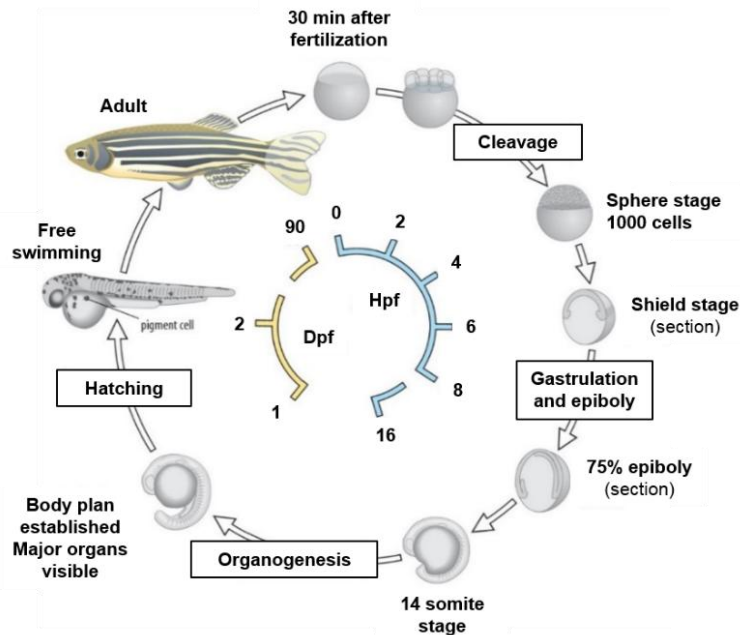


Figure 1: Zebrafish development.

The zebrafish development is characterized by cleavage, blastulation, gastrulation and neurogenesis/somitogenesis/organogenesis. The larvae hatches after about 2 days, resulting in an adult organism after 90 days. Hpf = hours post fertilization, dpf = days post fertilization.

1.3 Embryonic development of *Danio rerio*

1.3.1 From Cleavage to mid-blastula transition

The fertilized zebrafish egg undergoes discoidal meroblastic cleavage, since cleavage takes just place in the blastodisc and is incomplete due to the huge yolk mass. The dividing cells form the blastoderm which is located at the animal pole.

The onset of mid-blastula transition (MBT) can be observed at about the tenth cell division. MBT is characterized as the time point from then onwards zygotic gene transcription is active. During MBT the embryo consists of the internal and the external syncytial layer (YSL), the enveloping layer (EVL) and the periderm. The deep cells between the EVL and the YSL will mainly contribute to the formation of the embryo. (Gilbert, 6th edition).

1.3.2 Gastrulation

Gastrulation is characterized by the specification and positioning of the three germ layers ectoderm (future neural tissue and skin), mesoderm (gives rise to muscles, blood and inner organs) and endoderm (prospective gut, liver and pharynx; illustrated in the zebrafish fate map; Fig.2).

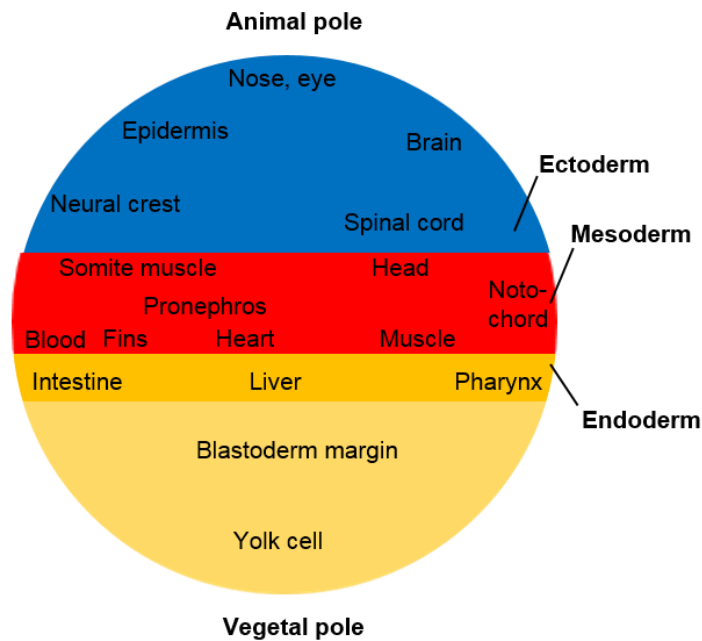


Figure 2: Fate map of a zebrafish gastrula embryo.

Gastrulation is characterized by the positioning and specification of the three germ layers ectoderm, mesoderm and endoderm. Mesoderm tissue moves inside the embryo, placing the endoderm inner-most, mesoderm in between and ectoderm outside. The endoderm will give rise to intestine, liver and pharynx; mesoderm develops into notochord, muscles, blood and inner organs and ectoderm will become future neural tissue and skin.

Moreover, the antero-posterior-, dorso-ventral- and left-right axes are established. Cell rearrangements like migration, involution and epiboly are a hallmark of this developmental step. Initially, the blastoderm cells surround the yolk during the so-called epiboly. The blastoderm thickens throughout the margin of the epibolying blastoderm, indicating the future dorsal side of the embryo. This thickening, called germ ring, consists of an outer layer – the epiblast and an inner layer – the hypoblast (Gilbert, 6th edition).

Cells from the epiblast and hypoblast intercalate on the future dorsal side of the embryo, thereby forming the embryonic shield, which is the homologous structure of the dorsal blastopore lip in amphibians, since it can generate a secondary axis when transplanted to a host embryo (Oppenheimer, 1936). Whilst epibolying the yolk, cells are also involuting at the margins and converge anteriorly and dorsally towards the embryonic shield.

By these convergent-extension movements (C&E) of the hypoblast cells form the chordamesoderm, which will give rise to the notochord. Somites develop from paraxial

mesoderm located on both sides adjacent to the chordamesoderm. Due to the C&E in the epiblast, a subset of prospective neural cells gets positioned at the dorsal midline, forming the neural keel. The embryonic shield is important in the formation of the dorso-ventral axis and it can induce the fate of the ectoderm to become neural rather than epidermal. Furthermore, the antero-posterior axis is formed by two signaling gradients. At the end of gastrulation the main body axes have been specified (Gilbert, 6th edition).

1.3.3 Establishment of the central nervous system

The establishment of the central nervous system (CNS) of an organism, including forebrain, midbrain, hindbrain and spinal cord starts at late gastrulation and continues during segmentation stages. Pivotal events of this complex process will be considered in detail in the following paragraphs.

1.3.3.1 Neural induction – The classical “neural default model” under debate

The development of the vertebrate nervous system begins with the so-called „neural induction“. The ectoderm, which normally gives rise to the epidermis of the skin, receives inductive signals from the adjacent mesoderm. Ectodermal cells respond to inducing signals, by demonstrating their competence and thus entering the “neural default program”.

The classical “neural default model” was originally discovered and shown by studies in *Xenopus laevis*. In 1924, Hans Spemann and Hilde Mangold carried out one of the most important experiments in embryology. They transplanted tissue of the dorsal lip (dorsal mesoderm) of an early gastrula embryo to an ectopic position - underneath the ventral ectoderm (presumptive ventral epidermis) in another early gastrula embryo (the host). To distinguish clearly between donor and host cells, Spemann and Mangold used two newt species; one pigmented and the other non-pigmented. Whereas the transplanted donor cells continued in a normal manner to self-differentiate, forming chordamesoderm (notochord) ectodermal cells of the host underwent immense changes which lead to the formation of a secondary body axis with a second nervous system. Only these individual cells of the dorsal lip showed the ability to induce a secondary embryo in a host embryo. Thus, organizer properties were assigned to this specific cells and they were named “the organizer”, or “Spemann organizer” (Spemann and Mangold, 1924). This implied the first evidence of the function of non-neural cells to initiate neural fate by providing inducing signals. The organizer in turn, is established by dorsal-most vegetal cells of the blastula, called the so-called “Nieuwkoop Center” (homologous to the dorsal part of the yolk cell in zebrafish). Most likely, maternal β -catenin, enriched dorsally in the embryo, forms the Nieuwkoop center.

Ventralizing signals were identified as members of the bone morphogenetic protein (BMP) family – BMP 2,4 and 7. They are able to inhibit neural induction, thus generating an

epidermal fate. If these BMP signals are blocked by their antagonists noggin, chordin or follistatin (released from Spemann's organizer), inhibition of neural induction is prevented, hence generating a neural cell fate (Schmidt *et al.*, 2013).

In zebrafish the ventralizing signal was shown to be BMP2B and the antagonizing factor was called Chordino (Kishimoto *et al.*, 1997; Schulte-Merker *et al.*, 1997).

However, recent studies in frog, mouse, chicken and zebrafish resulted in new insights and the "classical neural default model" got under debate. It seems that the model of neural induction is not "that simple" and requires a more complex interplay of signaling factors. Besides BMPs, possible involved candidates are e.g. Wnts, fibroblast growth factors (FGFs) or nodal (reviewed by Stern, 2006).

Pivotal experiments by the De Robertis lab, in which they inhibited BMP 2, 4 and 7 resulted in severe trunk defects, but still a minor dorso-ventral polarity persisted. Inhibition of another member of the BMP family, the so-called anti-dorsalizing morphogenetic factor (ADMP) at the same time resulted in the formation of a massive brain. De Robertis showed that inhibition of BMPs and elimination of the organizer showed the same consequence as eliminating the surprisingly dorsally expressed ADMP. Hence, different members of the BMP family were suggested to function in a redundancy manner (Reversade *et al.*, 2005; Stern *et al.*, 2006). Moreover, in zebrafish *follistatin-like product (fstl2)* and *noggin1* have been mentioned to act with *chordin* in a redundant way. Furthermore, FGF signaling is considered to induce posterior neuroectoderm independent of BMP signaling inhibition (Rentzsch *et al.*, 2004). The involvement of Wnts in neural induction is controversial. Surely, Wnt signaling is crucial at very early stages by accumulation β -catenin dorsally in the embryo, which determines the future dorsal side. However, at later stages the role of Wnts is unclear due to timing aspects (Stern *et al.*, 2006). Additionally, in zebrafish Homeobox gene *bozozok* and the nodal-related gene *squint (sqt)* have been shown to function in parallel to specify dorsal mesoderm and anterior neuroectoderm, thereby antagonizing the repressive function of *cyclops (cyc)* (Sirotkin *et al.*, 2000).

Besides extrinsic signals from non-neural cells intrinsic factors contribute to neural induction. On the transcriptional level, members of the SRY-box containing genes B1 (SoxB1) family - in zebrafish *sox1a/b*, *2,3,19a/b* - are redundantly crucial during blastula stages to take part in neuroectoderm fate. E.g. *sox3* has been shown to act together with FGFs thereby regulating BMP expression (Schmidt *et al.*, 2013). Other functions of SoxB1 members will be discussed later on).

Therefore, BMP signaling is definitely required but not sufficient for ectodermal cells and additionally FGFs and SoxB1 members act together to adopt a neural fate.

1.3.3.2 Neural tube formation in vertebrates

After neural induction, neural tube formation starts when the neural plate – a columnar epithelial sheet - rolls up its folds forming a neural groove, which finally fuses dorsally to build the central channel which becomes specified into brain and trunk. This main principle of primary neurulation is conserved among vertebrate species (Schoenwolf and Smith, 2000).

Additionally, posterior structures like the lumbar and tail region are generated out of mesenchymal cells by secondary neurulation (Lowery and Sive, 2004). Although neural tube formation has been extensively studied in avian, amphibian and mouse embryos (Schoenwolf and Smith, 2000; Colas and Schoenwolf, 2001), molecular mechanisms are still not understood in detail, due to molecular differences between vertebrate species (reviewed in Araya *et al.*, 2016).

Since for this thesis in particular the zebrafish neurulation is important, neurulation in *Danio rerio* will be considered in-depth.

1.3.3.3 Neural tube formation in zebrafish

The zebrafish as a teleost and its neurulation differs faintly from amniote and amphibian vertebrates. After the initiation of the neural plate (Fig.3a) at 10-11hpf the neural plate is located above the mesoderm and the notochord and covered by the EVL. Neural plate cells are still disorganized. After neural induction, the left and right sides start to converge towards the dorsal embryonic midline. At 12hpf, neuroepithelial cells (NECs) elongate and intercalate, thereby internalizing at the midline. The neural keel (Fig.3b) is formed at 13hpf. Between 15-17hpf the neural keel progresses further into the neural rod (Fig.3c), which appears as a cylindrical structure (Araya *et al.*, 2016). Neural progenitor cells (NPC)s undergo a 90° turn of the mitotic spindle, thereby crossing the midline in so-called C-divisions (Tawk *et al.*, 2007). Opposing apical proteins appear at the seam of the neural rod. Finally, at 18hpf the lumen has formed and thus a complete neural tube with proper apical/basal polarity and a lumen. Hence, the result is a proper neural tube (Fig.3d), very similar to other vertebrates (Araya *et al.*, 2016).

In amniotes like mouse and chicken, the neural plate was described as pseudostratified columnar epithelium, and in non-amniotes like *Xenopus laevis*, as a bi-layered tissue, consisting of a polarized superficial layer and an underneath nonpolarized layer. However, in zebrafish, the morphology of the neural plate is still unclear, due to controversial studies. Due to conflicting observations regarding neuroepithelial morphology, it was proposed that the teleost neural plate cells own epithelial and mesenchymal characteristics (Araya *et al.*, 2016). Moreover, neurulation in zebrafish is influenced by intrinsic and extrinsic factors.

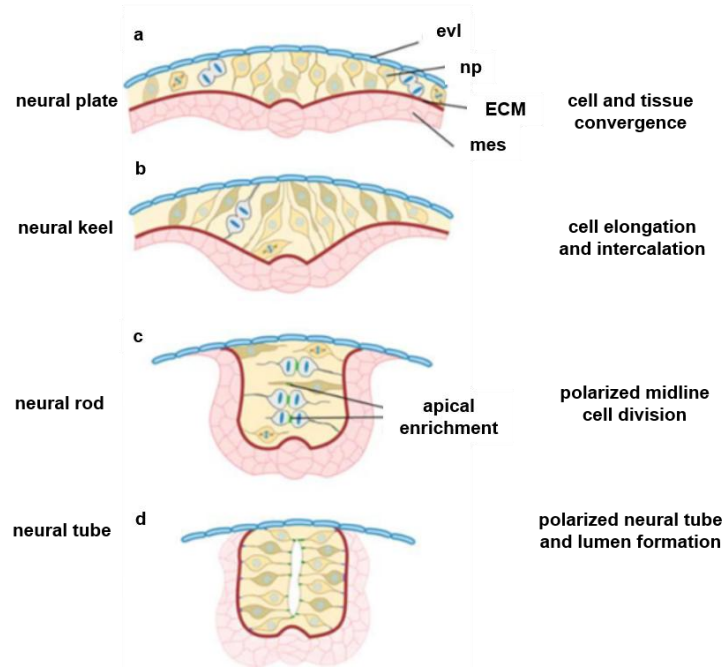


Figure 3: Neural tube formation in zebrafish. The neural tube **(a)** is formed by cell and tissue convergence and develops into a neural keel **(b)** by cell elongation and intercalation movements. At the neural rod stage **(c)** cells are already polarized and cross the midline (C-Divisions). The lumen forms secondarily resulting in the neural tube **(d)**.

Intrinsic mechanisms of zebrafish neural tissue internalization are still not clarified. However, regulated convergence movements have been demonstrated to be crucial for tissue internalization and the formation of proper neural keel and rod. The non-canonical Wnt-PCP pathway has been shown to be involved in neural tube formation in mice and amphibians. Additionally, Wnt-PCP was suggested to act during zebrafish neuroepithelial morphogenesis, since the Trilobite/strabismus mutant resulted in a wider and thicker neural primordium (Tawk *et al.*, 2007). Moreover, *n-cadherin* (*cdh2*) was considered, since absent *cdh2* in the hindbrain leads to failure of internalization of the neural primordium, resulting in an abnormal T-shaped neural tube (Hong and Brewster, 2006). Additionally, *protocadherin-19* (*pcdh19*) caused arrested neural tissue convergence and a divergent anterior neural tube morphology. Since abnormal phenotype were only observed during late keel stages, thus a precise spatio-temporal organization seems to be crucial for neural tissue internalization (Hong and Brewster, 2006; Biswas *et al.*, 2010).

Additionally, extrinsic factors influence neural plate morphogenesis, although in another manner than in other vertebrates, due to the different organization of the non-neural

ectoderm. The overlying EVL unlikely mediates influencing cues. Recently, the adjacent mesoderm was discussed to might be involved to coordinate cell movements within the neural plate, but this remains unclear (Araya *et al.*, 2014, 2016). Furthermore, since the neural plate and the underlying mesoderm are tightly in contact, the mesoderm might serve as a scaffold for the convergence of neural plate cells. The tightness may be supported by the placement of the basal proteins laminin and fibronectin, early during zebrafish gastrulation (Latimer and Jessen, 2010). Additionally, the neural plate is tightly packed between the EVL and the adjacent mesoderm, thus just a tiny duct remains for cells to move through. Thus influencing flow and shape of cells, which probably changes inner tissue-contacts mediated by cell-cell adhesion proteins, which in turn might alter physical assembly of the ECM. However, also this process has to be investigated further in detail (Araya *et al.*, 2016).

As already mentioned, mirror symmetric C-Divisions occurring at the right time and place have been shown to be involved in zebrafish neural tube development, as it was evidenced by experiments inhibiting C-Divisions. In the *trilobite* mutant, mirror symmetric C-Divisions take place in ectopic lateral locations and resulted in double neural tubes (Tawk *et al.*, 2007). Moreover, no lumen formation was observed and the neural tube appeared as disorganized structure (Quesada-Hernandez *et al.*, 2010, Žigman *et al.*, 2011). Additionally, since it was indicated that the mitotic spindle apparatus is critical for oriented cell division, involvement of the subcellular basal determinant *scribble* was discussed to control mitotic spindle orientation during zebrafish neurulation by regulation cadherin- based cell adhesion. Moreover, C-divisions occur rather due to a specified time window than local environment (Girdler *et al.*, 2013), however how cells respond to developmental time is unclear; microRNAs were considered to be involved (Araya *et al.*, 2016).

The C-divisions have been suggested to be important for the correct positioning of apical/basal proteins at the tissue midline and this might be required for lumen opening. However, C-divisions are not required in neural tube formation, but result in alterations in lumen formation. Initially, it has been shown that lumen opening starts from 17hpf onwards and extends dorsally, thus lumen formation might be dependent on the formation of the developing neuraxis. Apical adherence and junctional proteins like aPKC, Pard3, ZO-1 and β -catenin, which are located at the rod midline are placed there decreasing in amount from ventral to dorsal. Hence, a well-polarized neuroepithelial structure is crucial for lumen formation, since it has been shown that loss of aPKC or Pard6 is ongoing with a malformed lumen (Lowery and Sive, 2004, 2009). Midline C-divisions and cell polarization mechanisms are crucial to function synergistically to enhance efficiency of lumen generation. Moreover, laminin, a basal protein of the ECM, has been shown to be crucial for polarized lumen

formation (Araya *et al.*, 2016). The neural tube undergoes dorso-ventral and antero-posterior patterning due to two signaling centers. Thereby the neural tube is subdivided in forebrain, midbrain, hindbrain and spinal cord along the antero-posterior axis.

1.3.3.4 Dorso-ventral patterning of the neural tube

The mature spinal cord is characterized to handle sensory input and to organize motor output. Thereby sensory neurons are located in the dorsal half and motor neurons in the ventral half of the spinal cord whereas the interneurons are located in between. During neurulation, dorsally neural crest cells are formed and specialized glia cells which build the midline of the roof plate. The floor plate forms ventrally at the midline by specialized glial cells.

An opposed signaling gradient is patterning the neural tube along its dorso-ventral axis. The dorsal signaling center is located in the epidermal ectoderm and roof plate which secrete BMPs. The ventral neural tube is patterned by the morphogen Sonic hedgehog (shh) released from the notochord and floor plate (Patten and Placzek, 2000; Wilson and Maden, 2005).

Since in this thesis just the antero-posterior patterning will be considered, the dorso-ventral patterning will not be explained more in detail.

1.3.3.5 Antero-posterior patterning of the neural tube

According to the Nieuwkoop two-step mechanism for neural AP patterning it was suggested that 1. anterior neuroectoderm is formed by an activation signal separating non-neural from neural ectoderm and 2. patterning of the posterior neuroectoderm by a transformation signal which acts in a dose-dependent manner. Various explants and tissue recombination studies were performed to identify the “neural transformer”. E.g. in zebrafish non-axial marginal tissue was engrafted into the future head region, resulting in ectopic *krx20* expression, which is a hindbrain marker (Woo and Fraser, 1997). Several studies in *Xenopus*, chicken and zebrafish showed that it is unlikely that FGFs or retinoids (RAs) could initiate posteriorization of neuroectoderm (Erter *et al.*, 2001).

Rather Wnt signaling could be crucial to convey posterior character to a distinct neuroectoderm region. This was at first evidenced in the headless mutant, in which the repressor of Wnt target genes, *T-cell factor 3 (Tcf3)* was inhibited (Kim *et al.*, 2000).

Additionally, by expression of the Wnt antagonist *dickkopf 1 (dkk1)* in the prechordal plate, the future forebrain is protected to become posteriorized. Another Wnt inhibitor, the Homeobox gene *bozozok*, has been shown to limit posteriorization of the neuroectoderm in the late zebrafish gastrula.

Formation of head structures has been shown to be ongoing with inhibition of Wnt, Nodal and BMP - all accessible to be inhibited by Cerberus – a head inducer. A series of overexpression studies as well as expression and dominant negative analysis identified Wnt8a to be the molecular candidate transforming the posteriorizing information to the neuroectoderm. *Wnt8* is first expressed in the YSL expressed and in the blastoderm margin at early gastrulation stages. At about 70% epiboly *Wnt8* expression is restricted to ventrolaterally positions (Kelly *et al.*, 1995; Erter *et al.*, 2001). In vertebrates, the genome contains to *Wnt8* genes – *Wnt8a* and *Wnt8b*. In zebrafish, it has been shown to be a bicistronic *wnt8a* encoding both *wnt8a* transcripts` (Lekven *et al.*, 2001).

Additionally to the posteriorization of the neuroectoderm, Wnt8 has been shown to initiate the placement of the Midbrain-hindbrain boundary (MHB) by initiating the correct expression of *otx2* and *gbx1* (*wnt1*, *pax2* and *fgf8* are also involved in MHB development; Rhinn *et al.*, 2005).

Wnts act as morphogens in a dose-dependent manner and it has recently been shown that Wnt8a molecules can be transferred by filopodia from a source cell to a receiving cell (Luz *et al.*, 2014; Stanganello *et al.*, 2015) thereby activating the canonical Wnt pathway in the receiving Stanganello *et al.* hypothesized a filopodia-based direct contact model, in which transport of Wnt8a on filopodia is required to pattern the zebrafish neural plate (Stanganello *et al.*, 2015).

1.3.3.6 Neurogenesis

Neurogenesis is the process of generating new neurons in the brain. For a long time it was assumed that after birth no new neurons are formed. However, this theory was reversed by the discovery of the subventricular zone (SVZ) and the subgranular zone (SGZ) of the telencephalon as sources for neuronal birth in rodents and non-human primates. The first hints about birth of neurons in the adult brain were already mentioned in 1962 by Joseph Altman in 1962 and Michael Kaplan 1979, but their thoughts remained controversial until the 1990s. Nowadays, even more brain locations are known to produce neurons. The formation of new neurons in the human brain is still controversial.

In the zebrafish, the showpiece of proliferation and regeneration, 16 different proliferating regions were identified, including the homologous region to SVZ and the SGZ. The ability of the brain to change and adapt with experience is known as neuroplasticity. The zebrafish brain contains approx. 10^7 neurons (Schmidt *et al.*, 2013).

1.3.3.6.1 Proneural activator genes, encoding for bHLH transcription factors

After the neural induction, proneural genes which encode so-called Class II basic helix-loop-helix (bHLH) transcription factors play a fundamental role in the decision if a multipotent neural stem cell (NSC) undergoes differentiation into a neuronal or glial cell type or self-renews.

bHLH transcription factors build dimers with Class I bHLH proteins, or E-proteins. The characteristic feature of the bHLH superfamily members are the two highly conserved α -Helices, which are connected by a loop. In total, the bHLH motif contains approximately 60 amino-acid residues.

The basic domain is located at the amino-terminal end and represents the DNA-binding side. At this position the transcription factor binds to the DNA of a target gene at the E-Box (CANNTG). Thereby, particular bHLH transcription factors can either act as repressors or activators. Homo- and hetero-dimeric structures are formed with the HLH domain, located at the carboxy-terminal. The variability is due to the enormous combination potential of dimers and their binding affinities of the single monomers.

1.3.3.6.2 Activation of neurogenesis by proneural genes – lateral inhibition by Notch/Delta signaling

Neurogenesis is best explained in the fruit fly. In the late 1970s a set of genes was discovered in *Drosophila melanogaster*, regulating early steps of neural development. These genes are proneural genes of the so-called achaete-scute complex (AS-C) including *achaete (ac)*, *scute (sc)*, *lethal of scute (lsc)* and *asense (ase)* and encoding for bHLH transcription factors. AS-C factors dimerize with daughterless (DA), a bHLH protein (homologous to the vertebrate E proteins). The bHLH depicts a structural motif which is crucial for DNA binding and dimerization and is common in AS-C proneural genes. Moreover, another family of proneural genes contain *atonal (ato)* and the related *amos* (absent MD neurons and olfactory sensilla) and *cato* (cousin of *atonal*). The *ato* family members are part of another bHLH family, however they show still approx. 45% identity with bHLH domain of AS-C genes and 70% identity with AS-C themselves (Bertrand *et al.*, 2002).

Vertebrate class II bHLH genes are categorized on their homology to proneural genes of *Drosophila*, depending on if they are inside the AS-C or not. Outside the AS-C they are named e.g. *atonal*, *cato* or *amos*. In vertebrates, their homologues belong to Neurogenin proneural genes (*Neurog1*, *Neurog2* and *Neurog3*), Neurogenic differentiation genes (*NeuroD2*, *NeuroD4*, *NeuroD6*) and Olig differentiation genes (*Olig1*, *Olig2*, *Olig3*; Wilkinson *et al.*, 2013). From the AS-C just Achaete scute-like 1 (*Ascl1*) is expressed in the developing nervous system.

On the contrary to invertebrates, proneural genes in vertebrates are expressed in an already specified and self-renewing neuroepithelium (Bertrand *et al.*, 2002). The expression pattern of many neurogenesis key players - like Delta, Notch, Suppressor of Hairless, and genes of the AS-C - has also been characterized in zebrafish. Proneural genes in vertebrates have been shown to be highly heterogeneous. E.g. Gain-of-function (GOF) analysis of *neurog* genes have shown that when *neurog* genes are ectopically expressed in *Xenopus* or zebrafish embryos in the surface ectoderm, this leads to excessively produced NPCs, ectopically active notch and enhanced neuronal differentiation. Thus, like in *Drosophila*, ectopic expression or 0 mutations in proneural genes resulted in opposed phenotypes (Bertrand *et al.*, 2002).

Regulation of neurogenesis is achieved by lateral inhibition, mediated by the Notch/Delta pathway (Korzh and Strähle, 2002). Notch/Delta signaling differs from other pathways, since not just the receptor is a transmembrane protein, but also the ligand. This limits Notch signaling to direct cell-cell interactions. On the contrary, in pathways like the Wnt and HH pathway, ligands are not membrane bound and act in a diffusible manner.

In a proneural cluster all proneural genes express Delta at a low dose. When one cell of the cluster becomes selected to differentiate into a neuron or glia cell, this selected cell prevents the neighboring cells in doing so as well. The prospective neuroblast expresses Delta at a higher level than the surrounding cells, thereby initiating Notch signaling in adjacent cells. After activation of the receptor notch by the ligand Delta or Serrate/Jagged, the activated notch receptor is cleaved two times (and one more time before binding the ligand) until the Notch Intracellular domain (NICD) enters the nucleus and starts the expression of repressors – *Esp1* genes in *Drosophila* and homologs Hes/Her in vertebrates (Bertrand *et al.*, 2002).

Thus, the neighboring cells of the future neuroblast were repressed by lateral inhibition. Whereas morphogens like Wnts or Shh acting in signaling pathways cause cellular responses by a diffusion gradient (with the highest expression at the source; according to the French Flag model by Lewis Wolpert), Notch signaling is regulated by the intensity of proneural gene expression in NPCs.

When the prospective neuroblast is irreversible determined, the neural progenitor undergoes differentiation. The expression of proneural genes in NPCs is limited, since proneural genes are downregulated and NPCs leave the proliferative zone, starting to differentiate. bHLH genes have been shown to promote neural differentiation when ectopically expressed, although they are expressed later than proneural genes under their transcriptional control. Such bHLH genes have been identified in *Drosophila* and vertebrates (Bertrand *et al.*, 2002). In vertebrates, e.g. bHLH genes of the NeuroD family are expressed in immature neurons, which in turn activates the expression of markers for early neuronal differentiation, like *Elav*

like neuron-specific RNA binding protein 3 (*elavl3*; formerly HuC). Absence of Delta and Notch leads to a loss of lateral inhibition and overexpression of *elavl3* (Park *et al.*, 2000).

Since neurogenins are one of the earliest expressed proneural genes and moreover important regulators of neurogenesis, they will be considered in detail.

1.3.3.6.3 Neurogenins

Neurogenins, transcription factors which also belong to the class II bHLH family, have been shown to act as activators of neurogenesis but inhibitors of gliogenesis. Neurogenins own a highly conserved bHLH domain. Moreover, they function as heterodimers, by binding through their HLH domain to the E-box CANNTG motif. Mouse and human own the neurog homologs neurog1, neurog2 and neurog3; the chick has neurog1 and neurog2; the zebrafish neurog1 and neurog3 and the fly has just Tap (Target of Poxn; Yuan and Hassan, 2014). Whereas neurog1 and 2 show partly overlapping expression, activity of neurog3 is different, since it was shown that neurog3 is expressed much later, from about 24hpf onwards. Neurog3 expression was observed in the anterior-ventral diencephalon contributing to the hypothalamus (Wang *et al.*, 2001).

Neurog1 will be focused in detail, since it's important for this thesis.

1.3.3.6.3.1 Neurogenin1

Neurog1 represents one of the earliest proneural genes, functioning as activator of neurogenesis, but inhibitor of gliogenesis. Since *neurog1* acts as an inducer of delta and neuroD, it has been shown to be an important player in regulating lateral inhibition and thus to be a neuronal determination factor (Wang *et al.*, 2001).

1.3.3.6.3.2 Neurogenin1 expression and function as a proneural activator of neurogenesis

In *Danio rerio* and *Xenopus* – neurogenesis starts at the end of gastrulation (about 9hpf in zf), at the open neural plate stage. *Neurog1* in zebrafish and in *Xenopus* is expressed in primary neurons in the neural plate. In zebrafish, *neurog1* expression was shown to partly overlap with *elavl3* expression (which indicates early post-mitotic neurons). Misexpression of *neurog1* results in ectopic neurons in the non-neural ectoderm. Moreover, zebrafish *neurog1* is crucial for the development of all cranial ganglia.

Primary neurons include Rohon-Beard sensory neurons (RBs; Fig.4), primary interneurons (PINs) and motoneurons (PMNs). *Neurog1* expression appears in three strips, each strip containing the precursors of RBs, INs and MNs, respectively.

Misexpression of *neurog1* leads to ectopic neuron formation in the ectoderm and absent RBs (Cornell and Eisen, 2002). Moreover if *neurog1* function is down-regulated in embryos with absent Delta/Notch signaling, trunk neural crest (NC) is restored.

Hence, *neurog1* function is crucial for RB and later on neural crest-derived dorsal root ganglia ganglion (DRG) formation (although they are induced independently), whereas *neurog1* was shown to be strongly expressed in RBs and later in DRG and just shortly in NC (Cornel and Eisen, 2002). RBs develop at the neural plate border (NPB) before neurulation in developing anamniote embryos. They own some special features, since their cell bodies (which usually are found in the PNS) are located in the dorsal region of the spinal cord. RBs are innervating the skin of the embryo and are the first mechanosensory neurons acting in an embryo. Thus, factors involved in RBs` generation are supposed to be the earliest players in cell fate specification.

On the transcriptional level, *neurog1* has been shown to be involved in RB specification together with *dlx3b*, *dlx4b*, *neuroD*, *tfap2a* and *tfap2c*. RB specifiers act downstream of the NPB specifier *prdm1a*, which in turn is activated by NPB inducers BMPs and Wnts (Rossi *et al.*, 2009).

Additionally, *neurog1* is essential in dopaminergic interneurons for specifying dopaminergic progenitors in zebrafish forebrain (Yuan and Hassan, 2014). Further on, *neurog1* was shown in combination with the Notch pathway to regulate *her4*, which is involved in lateral inhibition in otic neurogenesis (Radosevic *et al.*, 2014).

Besides inhibition of zebrafish deltaA resulted in increased primary neurons and surrounding cells persisted as NSCs, *neurog1* seems to be a target of Delta- mediated inhibition (Korzsh and Strähle, 2002). Dominant-negative Delta expression results in absent *neurog1* expression in the neural plate (Korzsh and Strähle, 2002). GOF of vertebrate Her/Hes genes (inhibitors of neurogenesis), resulted in a downregulation of *neurog1* expression, but LOF of Her/Hes genes to an increase in *neurog1* expression (Schmidt *et al.*, 2013). Additionally, *neurog1* is involved in determining neural identity in the thalamus, since *neurog1* mediates generation of glutamatergic neurons in the caudal thalamus (Scholpp *et al.*, 2009).

Moreover, it was shown that overexpression of *neurog* induced ectopic expression of *elavl3*. Thus, it was supposed that *neurog* might be involved in generation of *elavl3* precursor cells (Kim *et al.*, 1997).

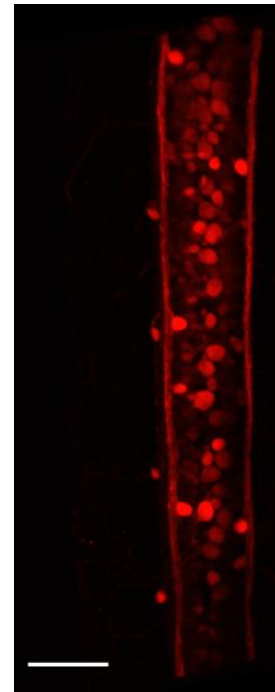


Figure 4:
neurog1:RFP
expression in
Rohon-Beard
sensory neurons.
Visualization of
neurog1:RFP
expression in Rohon
Beard sensory
neurons in the spinal
cord at 24hpf.

1.3.3.6.3.3 Transcriptional regulation of neurog1

Due to their complex tissue-specific expression pattern, neurogenins are supposed to be regulated by particular cis-regulatory elements, controlling e.g. *neurog1* expression in primary neurons. Two regions, the lateral stripe element (LSE) and the anterior neural plate element (ANPE) were identified upstream of *neurog1*. Thereby, the LSE is crucial for expression in prospective RBs and in the reticulospinal neurons in the spinal cord anlage and hindbrain. The ANPE is needed for expression in the ventral caudal cluster in the future midbrain, trigeminal ganglia and some scattered nuclei in the anterior hindbrain. *Neurog1* expression in the dorsal telencephalon has been shown to be driven by LSE in zebrafish. Moreover, the ANPE contains an E-box enabling the interaction with bHLH factors (Blader *et al.*, 2004).

Furthermore, the more proximally located LATE has been shown to mediate expression in the diencephalon and hindbrain. The area of activity of LATE overlaps with that of the paired-homeodomain transcription factor *pax6*, thus it seems that *pax6* is involved in regulating the activity of LATE. It has been shown that *pax6* binds to a conserved *pax6*-binding site in the LATE region. By knockdown of both zebrafish *pax6.1* and *pax6.2* results in a small eye phenotype and dramatically reduces endogenous *neurog1* and transgene expression. Thus, *pax6* regulates the activity of LATE directly (Blader *et al.*, 2004).

Additionally, the zinc-finger transcription factor *zic2* and the bHLH factor *her5* have been shown to negatively regulate *neurog1*. *Zic2* has a repressing function in the longitudinal stripes, thereby separating prospective MNs, INs and SNs. Her5 inhibition results in an expansion of *neurog1* and ectopic formation of a proneural area in the MHB (Blader *et al.*, 2004). Moreover, the β -catenin/Tcf complex, an intracellular transducer of canonical Wnt, promotes neurogenesis by directly binding to *neurog1* mRNA, thus leading to transcription of the protein (Yuan and Hassan, 2014).

1.3.3.6.3.4 Neurog1 is an inhibitor of gliogenesis

Neurog1 acts as inhibitor of glial differentiation. On the one hand, if *neurog1* is absent, precursors might become a glial cell. On the other hand, *neurog1* functions independently of its proneural activity, since it sequesters the CBP/p300-Smad1 coactivator complex to prevent its interaction with STAT glial differentiation factors (Yuan and Hassan, 2014).

1.3.3.7 Inhibition of neurogenesis by bHLH repressor genes: The Hairy/Enhancer of Split and Her/Hes family

bHLH repressor genes demonstrate an antagonizing function to bHLH proneural genes, which act as activators of neurogenesis. It would be dramatic if all progenitor cells would prematurely develop into neurons only and would be gone prior they have proliferated and

developed all required neuronal and glial cell types. Small and deformed brains would be the consequence. Therefore, the differentiation potential has to be prevented in some cells, thereby maintaining the stem cell pool. Thus, repressors of proneural genes are essential to regulate the ratio between selected cells which undergo differentiation and cells which persist in the stem cell pool (Philpott, 2010).

In *Drosophila*, these bHLH repressors have been identified as hairy and Enhancer of Split [E(spl)] and in vertebrates they are called Her/Hes family, thereby the Hes factors are expressed by mammals and Her factors in zebrafish. In zebrafish, *her4.1* has been shown to act in CNS and MHB and *her6* in the CNS; both dependent of notch, whereas *her5* functions at the MHB and *her9* in the CNS, both Notch- independent (Kageyama *et al.*, 2007).

1.3.3.7.1 Structure of bHLH Hes/ Her repressor genes

The structure of bHLH repressor genes delineates to be more complex than in bHLH proneural genes. Hes/ Her factors contain three conserved domains mediating transcriptional function. The BHLH, Orange and WRPW domain. Indeed, the BHLH domain owns like bHLH activators a DNA binding site and a helix-loop-helix region for dimerization. However, Hes/Her factors hold a proline residue in the middle of the basic region. Usually, bHLH factors bind to target genes with the so-called CANNTG E-box. Due to the proline residue in the E-box however, bHLH repressors bind to other target sequences at the so-called class C site CACG(C/A)G or the N box CACNAG with highest affinity. Dimerization is regulated by the Orange domain, since it selects partners to form heterodimers. Moreover, the C-terminal WRPW domain, which contains the tetrapeptide Trp-Arg-Pro-Trp, is responsible for repressing transcription. Hes/Her factors are polyubiquitylated and have short half-lives (Jones, 2004; Kageyama *et al.*, 2007).

1.3.3.7.2 Inhibition of neurogenesis by Hes/ Her repressor genes

The Hes/ Her factors can repress their targets either in an active or passive way. Active repression occurs by direct binding of the WRPW domain to co-repressors encoded by the Transducin-like E(spl) (TLE) genes/*Groucho-related gene* (Grg); homologous to *Drosophila groucho*. Probably, the Hes/ Her-Groucho homolog complex represses transcription by inactivation of chromatin, like in *Drosophila*. Passive repression is mediated by the Class C site, where other bHLH repressors called Hey (Hes- related with YRPW mitif1) can bind, like Hey1 and 2. Thus, heterodimers are formed (bHLH factors can also build homodimers). Hence, Hes/ Her factors mediate a dominant-negative effect on E-box binding bHLH activators (Kageyama *et al.*, 2007). The Hes/ Her genes (or hairy E(spl) in *Drosophila*) are expressed in cells with active notch signaling and inhibit neurogenesis, thus maintaining

some cells in the progenitor pool. Hes/ Her factors target members of the achaete-scute-like complex genes, thereby repressing them.

In zebrafish, *her3* and *her9* are expressed in inter-proneuronal domains, where they repress proneural genes like *neurog1*. *Her3* and *her9* are Notch independent. Rather they are controlled by upstream located factors, including BMPs, thus controlling neurogenesis in inter-proneuronal domains (Bae *et al.*, 2005).

1.3.3.7.3 Hes/ Her genes regulate boundary formation

By expression of Hes/ Her proteins in some cells, these cells reside in the stem cell pool. The regulation which cells are allowed to differentiate into a neuron or glia cell type and which remain stem cells plays an important role in boundary formation by maintaining organizer populations. Hes/ Her proteins have been shown to be crucial for the organizer formation of the zona limitans intrathalamica (ZLI), the boundary between the thalamus and the prethalamus and the located at the midbrain-hindbrain boundary (MHB) between the midbrain and the hindbrain (also called isthmus; Scholpp *et al.*, 2009).

Her5 in zebrafish has been shown to function in the MHB by repression of neurogenesis independently of Notch signaling (Geling *et al.*, 2003). Moreover, *her6* plays an essential role in thalamus development. It was shown that when *her6* is absent, glutamatergic neurons are formed, initiated by premature neurog1. GOF of *her6* leads to Ascl1- mediated GABAergic neurons (Scholpp *et al.*, 2009).

Boundary formation requires some special features of neuroepithelial or radial glial cells, respectively; e.g. slowed down proliferation and delayed or absent neurogenesis. In two adjacent compartments (with a boundary region in between), a higher expression of a Her/ Hes gene in one compartment and a lower expression of Hes/ Her in the other compartment has been shown, thus oscillating in these cells; e.g. Hes1 expressing cells. Proneural genes are ectopically expressed in boundaries when Hes genes are absent. Hence, organizer activity is lost due to ectopic neurogenesis. In zebrafish, *her3* and *her5* inhibit neurogenesis and are involved in MHB formation (Kageyama *et al.*, 2007). Cell migration occurs only within a compartment, thereby cells don't cross the boundary between two adjacent compartments (Kiecker and Lumsden, 2005).

1.3.4 SOXB1 family members are essential for inhibition of neurogenesis and maintenance of the stem cell pool by regulation of pou5f3 (Oct3/4) expression

The SOX genes encode for a group of transcription factors which share a HMG-type (high mobility group) box, responsible for DNA binding. Members of the Sox family are highly conserved among vertebrates.

Beside the SoxB family, also SoxC,D,E and F are existing and involved in neurogenesis and gliogenesis (reviewed in Reiprich and Wegner, 2015); but only the SOXB family will be considered.

SoxB genes are subdivided in *SoxB1* (containing *Sox1-3*) with an activator function and *SoxB2* (*Sox14, Sox21*) with a repressor function (Karnavas *et al.*, 2013). The B1 SOX transcription factors are involved in several steps during embryonic development.

In zebrafish the SoxB1 family includes *sox1a/1b/2/3/19a/9b*. Recently, the role of these zebrafish SoxB1 family members was investigated by quadruple knockdowns of *sox2/3/19a/9b* which evidenced a redundant function in early development. Whereas *sox3/19a/9b* is expressed in the entire blastoderm at first, expression progressively disappears at the margin after 30% epiboly. At the shield stage, *sox2/3/19a/9b* is expressed in the prospective ectoderm and then in the future neuroectoderm. E.g. it was shown that B1 genes in the blastula are involved in the regulation of *bmp2/7* regarding dorso-ventral patterning. Moreover B1 *sox* regulates the expression of *pcdh18a/b* and non-canonical *wnt11* which in concert acts during gastrulation in convergence and extension (C&E) movements.

During neurogenesis, SoxB1 members regulate Hes/Her bHLH repressors and the activation of region-specific transcription factor genes; e.g. *zic1*. Additionally, many signaling pathway genes need SoxB1 for their expression; e.g. *oep* in nodal signaling.

Quadruple knockdown of *sox2/3/19a/9b* resulted in absent *neurog1* (a bHLH proneural activator) and *her3* expression (a bHLH repressor). However, *ascl1a* was upregulated broadly at 75% epiboly in the neuroectoderm. Hence, a precise interaction of neuronal differentiation programs, including bHLH genes and regulatory networks is enormously influenced by B1 *sox*. Additionally, an involvement of the SoxB2 subgroup in the continuing neurogenesis was mentioned. Sox14 and Sox21 own repressor functions. Sox21 may antagonize activity of SoxB1 proteins, allowing cells to progress into mature neurons (Wegner, 2011).

Additionally, interaction of B1 SOX proteins with octamer binding transcription factor (Oct) 3/4 (*pou5f3* in zebrafish) was mentioned in activation of transcriptional repressor genes which inhibit further differentiation of NPCs (Okuda *et al.*, 2010). An important feature of B1 SOX is the interaction with co-DNA binding partner factors to specific sequences, thus they are involved in the regulation of various cell states (Okuda *et al.*, 2010). The SOX2-Oct3/4 complex was identified to perform an enhancer activity, thereby regulating the expression of pluripotent stem cell specific genes like *Nanog*, *Oct3/4* and *Sox2* itself (Masui *et al.*, 2007).

1.3.4.1 The role of Sox2

The most prominent member of the B1 Sox family is surely Sox2 (Sex determining region Y-box 2). Sox2 is crucial for the generation of embryonic stem cells (ESCs), maintaining their pluripotency and guaranteeing their self-renewal (Wegner, 2011; Karnavas *et al.*, 2013). Moreover, initially Sox2 was shown to reprogram already differentiated cells (mouse fibroblasts) to induced pluripotent stem cells (iPSCs) in concert with Oct3/4, c-Myc, and Klf4, under ES cell culture conditions. The iPSCs showed characteristics of ESCs and expressed specific markers (Takahashi and Yamanaka, 2006). Following studies indicated that not all of these factors are required, e.g. c-Myc is not needed (Mauksch *et al.*, 2013). Even Sox2 alone might be sufficient to reprogram cells to a pluripotent state, as it was shown by induction of NSCs from mouse fibroblasts on a mitotically inactive feeder layer (Ring *et al.*, 2012); thus Sox2 might be a master regulator for reprogramming to a neural precursor state (Graham *et al.*, 2003; Mauksch *et al.*, 2013).

Sox2 is expressed in the prospective ectoderm and later on strongly in the neuroectoderm and in NPCs. In some NPCs it can be found as well in neurogenic niches of the adult brain. During the final cell cycle exit and shortly before differentiation, Sox2 is down-regulated in NSPCs and thus not anymore expressed in immature neurons. Hence, Sox2 is essential for the maintenance of NSC properties in functions, thereby interacting with various pathways, like Shh and Notch signaling. Overexpression leads to the persistence of precursor cells and blocked up-regulation of neuronal markers, whereas overexpression of dominant-negative Sox2 resulted in cell-cycle exit of cells and prematurely differentiation. At this point, it has to be mentioned, that (at least in mammals) ESCs switch on Sox3 and Sox1 when receiving the neural lineage, thus a redundant function of Sox2, Sox1 and Sox3 has to be considered (Wegner, 2011; Karnavas *et al.*, 2013).

Notably, only a knockout of Sox2 results in embryonic lethality, whereas knockdown of Sox1 or Sox3 caused only mild abnormalities. A Sox2 knockdown in zebrafish depicted mild malformations (Zhang and Cui, 2014).

In summary, Sox2 is a key transcription factors in embryogenesis, thereby involved in various processes. Sox2 (like other Sox members) mediates its regulatory function by binding an interaction partner, e.g. Oct4. Together with Oct4, Sox2 initiates other factors to activate pluripotent gene expression. Moreover, Sox2 is involved in neural induction and the maintenance of NPC characteristics during neural differentiation. Sox is not anymore expressed in immature neurons. Extrinsically, Sox2 is affected e.g. by the Notch and Shh pathway (Zhang and Cui, 2014).

1.3.5 Maturation of neurons

During the establishment of the CNS, selected NPCs differentiate into neurons or glial cells like astrocytes and oligodendrocytes, whereas other NECs self-renew and reside in the stem cells pool. Maturation of neurons is mediated by two different steps, the specification and the commitment step.

The specification step occurs in the ventricular zone (VZ). There cells with up-regulated Notch receptors remain as NSCs, whereas cells with down-regulated Notch receptors up-regulate Notch-ligands followed by proneural bHLH genes, thereby progressing to terminal differentiation. In the intermediate zone (IZ), during the commitment step, downstream factors like NeuroD are switched on and cells terminally differentiate. Sox1-3 have been shown to prevent neuronal commitment and hence differentiation (Karnavas *et al.*, 2013).

E.g. during mouse neurogenesis, the so-called radial glial cells (RGCs), bipolar cells with the cell body located in the VZ and the radial fibers contacting the apical VZ and the pial surface, serve as scaffold for neurons to migrate. RGCs are multipotent and able to generate neurons as well as astrocytes and oligodendrocytes. When neurogenesis starts, the RGCs produce mostly asymmetric divisions in the VZ, to generate a RG daughter cell and either a neuron or an intermediate precursor cell (IPC). The SVZ is formed by IPCs, which divide there symmetrically to generate two or four neurons. Terminally differentiated neurons are located in the cortical plate (CP) (Lodato *et al.*, 2014). Moreover, in mouse ESCS it was shown that neuroectoderm to radial glia progression is mediated by a *Sox1* to *Pax6* switch (Suter *et al.*, 2009). Furthermore, a crucial mechanism of RGC division is the so-called Interkinetic nuclear migration (INM), mediated by apical-basal-apical cycling of the nucleus throughout the cell Cycle (e.g. Nulty *et al.*, 2015; Miyata *et al.*, 2015).

Other important players regulating the renewal of stem cells (SCs) and progenitor cells (PCs) and moreover cell fate determination are the Wnt ligands. Wnt members control the patterning of the body axes, cell fate specification, cell proliferation, and cell migration (reviewed e.g. in Clevers *et al.*, 2014), thus Wnt signaling depicts one of the most important molecular machineries in embryonic development – besides Notch, TGF- β , BMP, Hedgehog and Receptor tyrosine kinases. Hence, studying Wnt signaling has a huge impact on research since several decades.

1.4 The Wnt family

Proteins of the Wnt family are highly conserved across species like human, mice, *Xenopus*, zebrafish and the fruit fly. Wnts are secreted lipid-modified signaling glycoproteins that are 350–400 amino acids in length. Special lipid-modifications like palmitoylation and glycosylation are required for proper secretion.

Mutations in Wnts can have tremendous effects; e.g. GOF mutation can result in an oncogene and a LOF mutation may revoke the inhibitory effect of a tumor suppressor gene (Klaus and Birchmaier, 2008).

The discovery of mammalian Integrated1 to be associated to a mouse mammary tumor virus (MMTV) (Nusse and Varmus, 1982) and the description of a mouse mutant *swaying*, lacking the anterior cerebellum (Lane, 1967) was shown to be a mutant of the allele *Int1* (Thomas and Capechhi, 1990; Thomas *et al.*, 1991). Moreover, a mutant in *Drosophila*, characterized by missing the wings was named as Wingless (Wg) in 1973 (Sharma, 1973) and turned out to be the homolog of mammalian *Int1* (Rijsewijk *et al.*, 1987; Cabrera *et al.*, 1987) (both together nowadays known as *Wnt1*), meant one of the early key discoveries in Wnt research. Whereas initially Wnt signaling was just related to embryonic development for about one decade, failure in Wnt signaling was afterwards linked to play a role in human cancer. Originally, Wnt signaling was categorized in canonical (β -catenin dependent) and non-canonical (β -catenin independent). However, it has been shown that canonical Wnt ligands can also induce non-canonical Wnt signaling and the other way round (reviewed in Mikels and Nusse, 2006). Wnt1, Wnt3a and the already introduced Wnt8a are more related to the so-called canonical Wnt pathway. Additionally, e.g. the Wnt polarity (PCP), Wnt-Ca²⁺, and Wnt-atypical protein kinase C pathways are known as β -catenin independent or non-canonical Wnt pathways, with e.g. Wnt5a and Wnt11 as ligands.

Today, 19 different Wnt ligands are known in zebrafish. Moreover, the frizzled receptors and the LRP5/6 co-receptors, located in the plasma membrane, have been associated to Wnt signaling. Inhibitors like secreted frizzled-related proteins (SFRPs), Dickkopfs (DKKs) and the Wnt inhibitory factor have been identified (Klaus and Birchmaier, 2008).

In this thesis just the canonical pathway will be considered.

1.4.1 The canonical Wnt signaling pathway

In a Wnt off state (Fig.5), cytoplasmic β -catenin is bound to the destruction complex, interacting with APC and axin. The casein kinase 1 α (CK1 α) and GSK3 β mediates N-terminal phosphorylation of β -catenin. Afterwards, β -catenin becomes degraded by the proteasome, by involvement of β TrCP- (β -transducin repeat-containing protein), which is related to the E3 ubiquitin ligase complex. Hence, β -catenin levels are low in the cytoplasm and during the off state. In the nucleus, the transcription factors LEF and TCF interact which groucho repressors to inhibit expression of Wnt-specific target genes.

In the Wnt on state, phosphorylation of the co-receptors LRP5/6 is mediated by CK1 γ and GSK3 β , which leads to recruitment of Dishevelled to the plasma membrane, where it interacts with Frizzled receptors and polymerizes with other Dishevelled molecules.

The formation of the Dishevelled polymer, LRP5/6 phosphorylation and moreover internalization with caveolin result in transfer of axin to the plasma membrane and inactivation of the plasma complex. This leads to cytoplasmic stabilization and translocation of β -catenin to the nucleus, where it forms a transcriptionally active complex with LEF and TCF transcription factors by displacing Grouchos and interacting with other co-factors, finally activating transcription of Wnt target genes, e.g. the protooncogene *c-Myc* (Klaus and Birchmaier, 2008). Furthermore, it has been shown that Wnt/ β -catenin signaling mediates neural differentiation by activation of the neuron-specific transcription factors, neurog1, NeuroD and *brain-specific homeobox/POU domain protein 3A (Brn3a)* in the CNS (Kondo *et al.*, 2011).

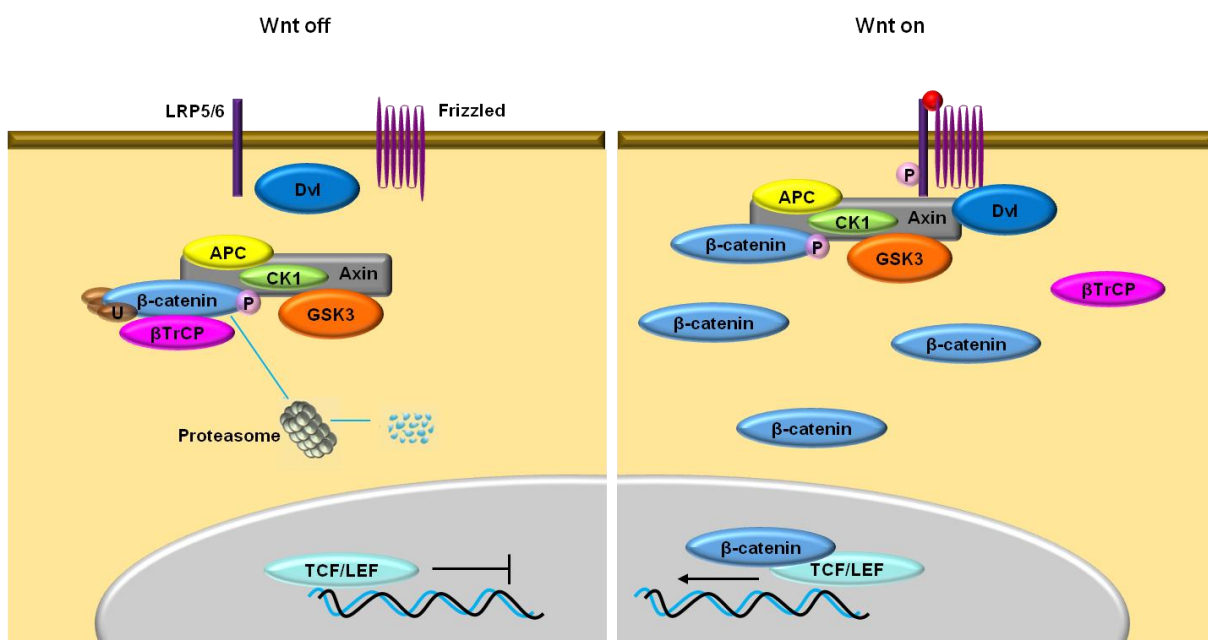


Figure 5: Simplified scheme of the Canonical Wnt pathway. In the off-state, β -catenin is degraded by the destruction complex. When the ligand Wnt binds to the Frizzled receptor and LRP5/6 coreceptors, this leads to the recruitment of Dishevelled and destruction complex to the membrane, resulting in an inactivation of the destruction complex, thereby stabilizing β -catenin. Accumulated β -catenin enters nucleus, binds TCF/LEF and activates target gene transcription.

The impact of Wnt signaling (and many other pathways) on the embryonic development of an organism and moreover its correlation to diseases (mainly cancer) was extensively studied *in vivo* (e.g. reviewed in citation) and offers still great research potential. Thereby, model organisms like the mouse, chicken, frog or the zebrafish are useful tools, since they own all essential natural conditions for normal embryonic development. Although an embryo is a well-organized system, it is very complex. In an *in vivo* scenario, immense interactions of genetic regulatory networks, cell-cell communications, cellular migration-and differentiation

steps and many influencing cues often hinder to elucidate particular developmental processes. E.g. the formation of the neural plate is induced by an interplay of signals from the underlying mesoderm. Therefore, *in vitro* systems are more suitable to add either chemical or molecular cues in a controlled way and to study their effect on the (single) cellular level, in a simplified environment more precisely.

1.5 Cell culture systems

1.5.1 The innovation of cell culture systems and its role for research and medicine

Since the last century until present, researchers try to establish a method to cultivate cells outside of an organism, thereby bothering to create conditions which mimic the natural environment of a cell. The establishment of cell culture systems over the years was influenced by continuously improved cultivating conditions, contributing to the immense progress which was made in stem cell research. The isolation and cultivation of pluripotent ESCs from mouse and human blastocysts and the generation of iPSCs from somatic cells depicted cutting-edge innovations, since they enabled access to unlimited cell material (Takahashi and Yamanaka, 2006). Thereby, the latter was enormously meaningful, since iPSC are unproblematic concerning ethical aspects. Hence, resulting in a tremendous influence and improvement on developmental and cellular studies as well as tissue engineering and regenerative medicine (Ader and Tanaka, 2014).

1.5.2 2D vs. 3D Cell Culture Systems

Nowadays an overwhelming variety of cell culture systems (CCS) is available for research. Surely, there is not “the one” CCS existing, which perfectly satisfies researchers needs. The choice to apply a certain CCS strongly depends on the researcher’s interest.

A major impact on the improvement of CCS over time was provided by the development of proper differentiation protocols for stem cells *in vitro*. In this thesis, the main focus relies on the establishment of stem cells towards neural lineages. Besides offering cells the proper conditions required to differentiate into the cell type of interest, many other components influence the behavior of cells. Cell fate decisions depend on the environment which is surrounding a cell, provided soluble factors, the connection to the ECM or substrate, the interaction between cells, mechanical forces and the curvature of a cell. All this factors vary between 2D and 3D cell culture and can influence cell behavior and gene expression.

Over time, 3D CCS interspersed, since 3D CCS resemble more the *in vivo* scenario (Altmann *et al.*, 2009; Bosi *et al.*, 2015). Thus, they are applied preferentially.

1.5.3 Soluble factors provide the differentiation towards neural lineages

Nowadays, neural differentiation protocols are well-engineered. Cells can be differentiated in a defined manner from the stem cell state towards specific neuronal and glial subtypes of forebrain, midbrain/hindbrain and spinal cord by addition of particular cues, referring to the *in vivo* scenario (reviewed e.g. in Petros *et al.*, 2011).

Neural differentiation protocols are continuously in progress, with the aim to establish most minimalistic approach sufficient for neural differentiation, thus simplifying the CCS as much as possible.

Key factors, known to be involved in neural induction have been shown to promote conversion of stem cells towards a neural progenitor fate. Addition of so-called small molecules, e.g. Wnt/BMP antagonists and FGF factors under serum free conditions leads to the development of NPCs. Moreover, e.g. inhibition of SMAD signaling and of the GSK-3 β have been used for highly efficient neural differentiation of hESCs and iPSCs: Thereby SMAD signaling was inhibited by usage of the activin-like kinase (ALK) 4,5,7 inhibitor SB-431542 (NI) together with noggin, (Chambers *et al.*, 2009) and GSK-3 β inhibitor CHIR99021 (CHIR) (Laedwig *et al.*, 2012).

The NI represents a favored tool regarding neural differentiation (programming) and is of great interest in this thesis. The NI be considered in detail in the results part.

1.5.4 Cell topography

The topography of a cell has an immense impact on the connection between the cell and the extracellular matrix (ECM). The curvature between 2D and 3D cultivated cells differs enormously, resulting in an altered mechanical forces between cells and at the cell-ECM interface. In 2D, actin stress fibers and focal adhesions are located at the basal side of a cell and contractile forces to the surface and surrounding cells. In 3D, stress fibers are limited. Moreover, the variable arrangement and clustering of membrane receptors leads to changed cell responses and finally gene expression might be varied (Schwartz and Chen 2013).

Cells in 2D grow as a flat monolayer with a fixed apical-basal polarity, whereas apical is facing the media supply where soluble factors are diluted and basal points towards a supportive surface below. 2D cells persist of a single plane of cells and thus a fixed height. Thus, interactions between neighboring cells are limited to the periphery of a cell. In a 3D cell culture, e.g. in a hydrogel, cells form spheroid structures in which epithelial cells are completely surrounded by ECM, the apical side is facing the lumen and basal is located outside. Soluble factors are enriched to the limited space in the lumen. Depending on the CCS, the arrangement of cells is more flexible in 3D, enabling the cells to generate multi-layered tissue like structures, thus enhanced contact possibilities are offered all around a

cell, resulting in increased intercellular signaling. In 3D, cell receptors and adhesion molecules are arranged more naturally (Baker and Chen, 2012; Schwartz and Chen 2013; Knight and Przyborski, 2014).

1.5.5 The substrate mimics the natural ECM

The substrate on which cells attach has a great impact on cell differentiation and has been shown to be variable in stiffness, topography and geometric confinement. ECM stiffness can influence the cell fate. E.g. the neural ECM of the brain with a stiffness of 0,1 to 1 kPA supports the differentiation of mesenchymal stem cells to neurocytes (Engler *et al.*, 2006; Lv *et al.*, 2015).

The neural ECM, which is of great interest in this thesis, depicts a dense substrate which can be found in brain and spinal cord tissue, filling up the space between neurons and glia. The neural ECM owns special components, since it is enriched in glycoproteins and proteoglycans, with a backbone created by hyaluronan. The ECM is connected to the basement membrane and constitutes the environment of blood vessels, diffuse interstitial matrix and the so-called perineuronal nets (PNNs) which surround the cell soma, proximal dendrites and axon initial segments of some neurons. Major components of the basement membrane include laminin, fibronectin and collagen IV. The densely structured PNNs consist mainly of chondroitin sulphate proteoglycans (CSPGs), Heparan sulphate proteoglycans (HSPGs), Tenascin and linker proteins (Latimer and Jessen, 2010; Giamanco and Matthews, 2012; Soleman *et al.*, 2013; Burnside and Bradbury, 2014).

Since laminin-1 and fibronectin are of special interest in this thesis, just these two components will be considered.

1.5.6 Laminin

Laminins are heterotrimeric glycoproteins, characterized by different α , β and γ subunits and 15 specific laminin isotypes in total. Laminin chains display a T-shaped structure and bind mainly to integrins, the non-integrin syndecans, dystroglycans and Lutheran blood group glycoprotein receptors. Laminins are essential for basement membrane assembly, migration and axonal pathfinding (Hohenester and Yurchenco, 2013; Burnside and Bradbury, 2014).

1.5.7 Laminin-1

Laminin-1 is responsible for permissive outgrowth by binding to growth cone integrins. A knockout of $\gamma 1$ laminin in the mouse cerebral cortex has been described to result in altered neurogenesis and neuronal migration and thus failure in cortex formation and axonal pathfinding (Chen *et al.*, 2009).

Moreover, it has been shown that laminin-1 seems to be limited to epithelial basement membranes. If either FGF signaling, β 1-integrin or laminin γ 1 chain expression are prevented in ES cells, this results in the absence of laminin-1, which is ongoing with defect BM assembly and epiblast differentiation (Ekblom *et al.*, 2003).

In the zebrafish, laminins have been shown to be essential for notochord formation, since the laminin mutants named bashful (*bal*; *lama1*), grumpy (*gup*; *lamb1*), and sleepy (*sly*; *lamc1*), have been identified due to their reduced body length and defects in notochord differentiation (Parsons *et al.*, 2002; Biehlmaier *et al.*, 2007). Moreover, the establishment of the zebrafish MHB constriction requires laminin-dependent basal constriction (Gutzman *et al.*, 2008).

1.5.8 Fibronectin

Fibronectin consists of three individual tandem repeats (I, II, III) and thus depicts a large dimeric protein. These tandem repeats contain functional domains which enable, like laminin, polymerization and interaction with cell surface receptors and other factors of the ECM. Fibronectin is also an important component of the developing CNS, suggested to be involved in adhesion, migration, proliferation and axon elongation. Additionally, fibronectin modulates the guidance function of CSPGs (Pankov and Yamada, 2002; Burnside and Bradbury, 2014). Inactivation of fibronectin in the mouse was shown to result in embryonic lethality (George *et al.*, 1993).

Laminin and fibronectin have been shown to be established in the basement membrane early during gastrulation (Latimer and Jessen, 2010). How different substrates provide ECM conditions *in vitro* and moreover how substrate topography and geometric confinement contribute to cell differentiation will be mentioned in relation to the corresponding CCS.

1.5.9 2D Cell Culture Systems

1.5.9.1 Feeder-free and feeder based substrates

Cultivation of cells *in vitro* started over a century ago, (Carrel, 1912; Harrison, 1914) by usage of glass dishes. Nowadays, the application of 2D cell culture on glass and tissue culture plastic (with minimal changes) is still common. However, as already mentioned, monolayer culture conditions have been shown to be artificial (Schwartz and Chen, 2013; Hazeltine *et al.*, 2013; Knight and Przyborski, 2014; Shao *et al.*, 2015).

2D CCS can roughly be categorized in feeder-free and feeder-based platforms. Initially, isolated human ESC colonies were plated on a feeder layer of mouse embryonic fibroblasts (MEFs), maintaining self-renewal and pluripotency *in vitro* (Thomson *et al.*, 1998; Amit *et al.*, 2000). However, due to immunogenicity, viral transmission and inconstant culture conditions (Villa-Diaz, 2013), recently a method was generated to separate feeder cells from hESCs by application of a porous membrane. Thus enabling interactions between hESCs and MEFs,

but decreased contamination from MEFs (Shao *et al.*, 2015). Moreover, in the classic two-step neural induction protocol, EBs derived from murine and human ESCs were formed at first and afterwards they were plated on an adhesive substrate like MEF cells. By addition of fibroblast growth factor 2 (FGF2) into the medium, cells differentiated into NSCs and formed so-called neural rosettes (Zhang *et al.*, 2001). Further addition of epidermal growth factor (EGF) lead to a cell population called NSC^{FGF2/EGF}, which lost the rosette shape and owned characteristics similar to the radial glia-like phenotype described in a fetal NSC population by Conti and colleagues. (Conti and Cattaneo, 2010; Conti *et al.*, 2005). These cells display posterior identity similar to an anterior hindbrain fate, which might be caused by the posteriorizing effect of FGF2. Furthermore, the cells are suitable for long-term culture (long-term neuroepithelial stem cells; It-NES), (Karus *et al.*, 2014).

However, the described neural shapes are too unstructured, due to their heterogeneous randomly mixed cell population and sphere-like structure.

Progress has been made establishing functionalized 2D surfaces with naturally derived proteins or synthetic polymers (Villa-Diaz *et al.*, 2013). The first feeder-free culture system was generated by application of a Matrigel (secreted by Engelbreth-Holm-Swarm sarcoma cells and consists of ECM proteins like laminin, collagen IV and HSPGs) for coating of 2D culture surfaces, thereby improving hPSCs renewal under MEF condition medium (Xu *et al.*, 2001). Additionally, components of ECM proteins were integrated into synthetic polymers, mimicking the natural ECM. Furthermore, pure synthetic polymers with fully defined surface chemistry were developed for long-term self-renewal of hPSCs. Another method to modify a surface for 2D cell culture has been achieved by Oxygen plasma or UV ozone treatment, respectively (Shao *et al.*, 2015).

1.5.9.2 Substrate stiffness, substrate topography and geometric confinement

Further on, referring to the variable mechanical stiffness of certain tissues in the embryo in space over time, mechanical stiffness was mimicked *in vitro*, regulating hPSC differentiation. It has been shown that hPSCs cultured on soft substrates developed a neuroepithelial fate with strongly expressing paired-homeodomain transcription factor 6 (*pax6*), whereas a stiff substrate resulted in mixed neuroepithelial and neural crest cells (*AP2*; Shao *et al.*, 2015). The neural ECM of the brain has been shown to range between 0,1-1 KPa (Engler *et al.*, 2006; Lv *et al.*, 2015). Moreover substrate nanotopography has been shown to influence cell differentiation. hPSCs cultivated on smooth glass showed strong self-renewal by enhanced *pou5f3* (an Oct4 homolog) expression, whereas hPSCs grown on nanorough glass depicted a higher differentiation rate (Shao *et al.*, 2015).

Furthermore, spatial cell fate patterning was mimicked *in vivo* by cultivating hPSCs in patterned adhesive ECM islands, resulting in patterned expression of pluripotency markers, with an increased expression from inside to outside. Additionally, when BMP4 was provided as external cue, hPSCs spontaneously built “germ-layer-like structures (Warmflash *et al.*, 2014).

Thus, 2D CCS have been shown to be suitable for long-term self-renewal and large-scale expansion of hPSCs and moreover directed differentiation towards specific lineages. However, 2D CCS are limited since resembling an artificial environment and cannot cope with 3D CCS in this regard.

1.5.10 3D Cell Culture Systems

3D CCS can be subdivided in scaffold-based and scaffold-free platforms.

1.5.10.1 Scaffold-based technologies

3D substrates consist either of natural or synthetic components. Natural biomaterials often include ECM components like fibrin and hyaluronan and moreover naturally derived silk, gelatin and alginate. Advantageous features of these materials are their biocompatibility and cell adhesion sites, as well as their biodegradability. The latter may be useful for tissue engineering, however depicts a disadvantage for cell culture, due to being a variable factor. On the contrary, synthetic materials provide more stable conditions like a defined chemical composition and mechanical properties can be modified. Synthetic substances include e.g. polymers, titanium, bioactive glasses and self-assembled peptides. The main advantage of a synthetic-based scaffold is the reproducibility, inertness and non-degradability. However, cellular adhesion sites are missing, thus a coating with ECM proteins might be necessary to imitate the natural environment of the cells.

Scaffold-based 3D systems can further on be subdivided roughly in hydrogels and solid substrates. Hydrogels provide a loose scaffold network, containing naturally-derived substances collagen, agarose, fibrin, hyaluronan and a high water content. Within hydrogels, cells are either embedded in an artificial ECM protein environment, or enabling the cells to migrate towards the inner-most region of the gel. By integration of biologically active molecules the ECM might be modified. Encapsulation of cells occurs by either radical polymerizations due to UV exposure, self-assembly of cells or ionic cross-linking.

Moreover, it has been considered, that using a single ECM component in the hydrogel is not sufficient, as it has been shown in comparison to application of a commercial Matrigel, containing various ECM components. Loss of a proper ECM environment can lead to alteration of cell proliferation, adhesion and phenotype regulation.

Furthermore, a solid scaffold enables cells to form as an organized structure, in a controllable and reproducible way. Porous scaffolds have been shown to support e.g. the formation of epidermal-like structures (Knight and Przyborski, 2014).

In a study, in which a stiff scaffold was combined with a softer ECM gel containing collagen and silk-fibroin based biomaterials cortical brain like tissue was generated. Thereby, the stiff scaffold mediated neuronal anchoring and the softer ECM gel enabled axon penetration and connectivity (Tang-Schomer *et al.*, 2013).

Moreover, the patterning of a neural tube was reconstructed in 3D. Mouse ESCs were directly embedded in matrigel or synthetic matrices (providing a scaffold) and cells were cultivated under neural induction conditions, forming clonally neuroepithelial cysts with a single lumen. By addition of retinoic acid, a complete dorso-ventral patterning was achieved (Meinhardt *et al.*, 2014).

Furthermore, with the so-called direct laser writing (DLW) photopolymerization technique, tailored 3D scaffolds can be generated. By usage of different polymers with a variation in mechanical features or adjustment of scaffold sizes, the microenvironment can be defined precisely in regard to stiffness and additionally biofunctionalized. Thus, the effect of stiffness and ECM factors on cells can be investigated in this system (Greiner *et al.*, 2015).

1.5.10.2 Scaffold- free platforms

3D CCS like low adhesion plates, micropatterned surfaces and hanging drop assays refer to this category. Scaffold-free platforms are characterized by the formation of mainly multicellular aggregates, also called spheroids, or embryoid bodies (EBs) regarding to *in vitro* differentiation of stem cells. Within these structures, the cells build their own matrix components. Spheroid structures are formed by the so-called hanging drop technique or low adherence substrates.

Within a hanging drop system, cells are cultured in a drop of media which is hanging on the lid of a cell culture dish. A main feature of this technique is the inability of cells to adhere at the surface. Thus, they form clumps. The hanging drop method is suitable for long-term cell survival, maintenance of the bone marrow stromal SCs and homogenous differentiation. Moreover, the generation of EBs is of special interest for stem cell biology to differentiate stem cells *in vitro*. EBs have been demonstrated to form as morula or blastula-like structures, however, this is hindered by the problematic long-term maintenance of EBs. Disadvantages of the hanging drop technique are the limited nutrient and gas diffusion as well as complicated media exchange, thus resulting in necrosis. Moreover, when EBs are formed using other techniques, it has been shown that the size of the EB can influence cell differentiation.

E.g. it has been shown that EBs with a diameter of 450 μ m mainly differentiated into cardiac cells, whereas EBs with 150 μ m diameter adopted an endothelial fate (Burrige *et al.*, 2007; Ungrin *et al.*, 2008).

Another method for the generation of EBs is the cultivation in a 3D microwell array, which enables the formation of uniformly sized EBs in a high throughput assay and moreover showing once more that cell-cell contact is altered in 3D (shown by modulation of Wnt/ β -catenin signaling (Azarin *et al.*, 2012).

Furthermore, EBs can be formed in a free-floating 3D suspension culture. However, EBs were not suitable to investigate formation of lineage-specific histoarchitecture, since they consist of cells from all germ layers. An important invention for the formation of neural structures was the introduction of serum-free suspension culture, which mediates the formation of specific regional identities (e.g. dorsal telencephalon) by adding morphogens implied a meaningful progress (Watanabe, 2005). The so-called serum-free floating culture of embryoid body-like aggregates (SEFB) protocol was further optimized by using ultralow-attachment 96-well plates to control EB size by quickly reaggregation (SEFBq) dissociated ESCs into an EB-like structure. Addition of Wnt and TGF β inhibitors resulted in the generation of polarized cortical epithelia in a temporally controlled manner, mimicking corticogenesis *in vivo*, although stratification was not achieved sufficiently with the SFEBq technique (Eiraku, 2008). A disadvantage of the SFEBq system is the difficulty of avoiding fusion of cellular aggregates during cultivation, resulting in variation of quality in different aggregates.

On the contrary to the described passive cultivation systems, active systems, like microfluidic devices are connected to a bioreactor, which continuously provides the cell culture with fresh medium and nutrients. A microfluidic device consists of mostly several channels of micrometer scale dimensions, filled with a volume in the nanoliter range. Microfluidic devices provide a stable and spatially, chemically and temporally controllable microenvironment. Microfluidic devices are applied e.g. to study brain cells and circuits (Millet and Gillette, 2012). Moreover, complex co-culture assays can be established in microfluidic devices, controlling various parameters like oxygen partial pressure, pulsation of fluid flow, critical flow velocity and support of the media. Microfluidic devices are used to mimic e.g. stem cell niches and enable long-term culture of cells (Gottwald *et al.*, 2015).

A microfluidic device, produced from polydimethylsiloxane (PDMS) was applied to study neuronal differentiation. Thereby, in the central channel NSCs, embedded in ECM hydrogel were cultivated and adjacent channels were filled with medium containing EGF and FGF to support neural differentiation. Afterwards, NSCs were isolated and quantified (Han *et al.*,

2012). However, disturbing factors like shear stress caused by the fluid flow might affect cell development and function. Moreover, chemicals might accumulate in the cells, influencing them (Millet and Gillette, 2012).

1.5.10.3 Combined 3D CCS

Moreover, by cultivation of 3D hPSCs, cerebral organoids (minibrains) with distinct brain regions were formed in a multiple-step method. First, neuroectoderm developed from EBs, which then were embedded in Matrigel droplets. The matrigel droplets in turn, were transferred to a spinning bioreactor to improve nutrient absorption, resulting in rapid development of brain tissues (Lancaster *et al.*, 2013). However, just in about 1:1000 cases such a minibrain develops (personal communication). Furthermore, generated cerebral organoids consisted out of variable spatially distinct “brain regions” (Karus *et al.*, 2014).

In summary, suitable 3D CCS are existing to generate neural tissues. However, none of them is optimal for the approach of this thesis.

1.5.10.4 Microcavity arrays produced by SMART

A microcavity- based CCS is characterized by accumulation of cells and moreover control of aggregate size and to determine the position of each aggregate in a reproducible manner. Giselbrecht and co-workers established a method to produce such microcavities, the so-called surface modification and replication by thermoforming (SMART).

The SMART process can be subdivided in premodification, the thermoforming step and postmodifications. During the initial step, premodifications on the planar polycarbonate film (approx. 60µm thick), fix the position of the later generated postmodifications. Polycarbonate turned out to be a suitable material for thermoforming. The site determination is performed by anisotropic directed lithographic processes. Microthermoformed devices can be provided with micro- or nanopores (to support cells with nutrients), cell adhesion micropatterns, microelectrodes or surface micro- or nanotopographies. The SMART method is realizable due to the usage of flat semi-finished films during premodification, thus allowing complete access to the surface and optimal application of all mask-based lithographic modifications. Moreover, due to the stability of the material during the thermoforming step, the melting phase is avoided, which enables maintenance of modifications. This conditions are solely provided by the SMART process. Thus, SMART provides a unique suitable method for the generation of microcavities. The microcavities are thin-walled in the range of a few micrometers and free standing.

Microstructures depict a small volume and mass, low heat capacity, they are highly flexible and thermal resistant. Additionally, they are transparent and cause only low autofluorescence, thus providing optimal conditions for imaging. 3D microcavities are eligible CCS to study 3D tissue engineering. They can be applied as passive or active systems (Giselbrecht *et al.*, 2006; Truckenmueller *et al.*, 2011). In this regard, a microcavity in the form of a microchannel, coated with collagen, was applied in an active system to study transendothelial transport to mimic a 3D porous capillary system (Hebeiss *et al.*, 2012).

Thus, the microchannel produced by SMART seems to be the most suitable platform for my approach.

1.6 Aim of this project

The complexity of neurogenesis *in vivo* hinders the detailed dissection of particular steps, due to the many diverse interactions of influencing factors, including the interplay of signals derived from the mesoderm. A simplified three-dimensional cell culture approach would be suitable to investigate neural differentiation in a controlled manner.

Therefore, the aim of my thesis was to generate a zebrafish neural tube in a three-dimensional cell culture system. Thereby, a comparative study was performed to study neuronal differentiation in the zebrafish embryo and in a 2D and 3D zebrafish primary cell culture.

In the first part of my work, the microchannel was applied to investigate neurogenesis in 3D *in vitro* and compared to the *in vivo* situation. Furthermore, I guided cells to a distinct area of interest on a polymer channel. Finally, I controlled cellular signaling in a 3D cell culture system. In summary, my project provides fundamental ground work to control the formation of the neural tube by the establishment of an advanced 3D cell culture system.

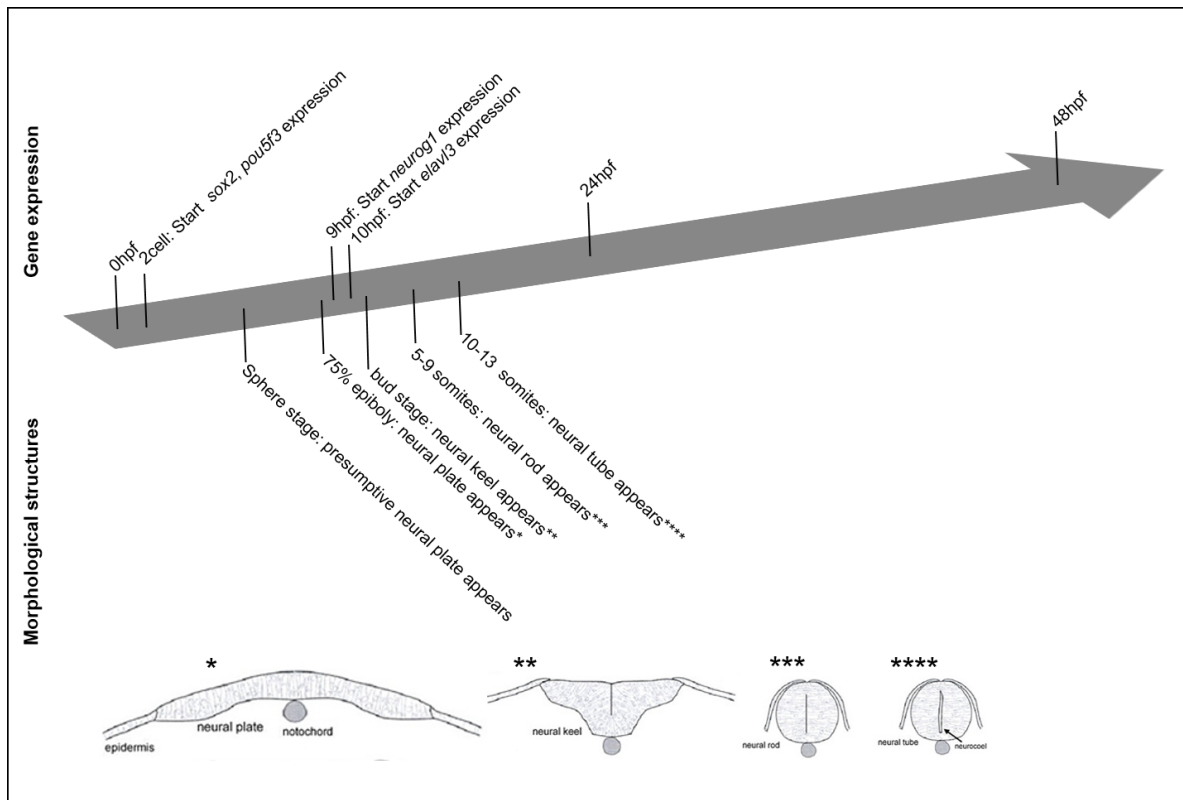


Figure 6: Time line of relevant events for this thesis. Genes and morphological structures which are described in this thesis are mentioned at their time point of appearance.

2. Material and Methods

2.1 Material

2.1.1 Equipment and Tools

Name	Description
ABI StepOnePlus	Life Technologies GmbH, Darmstadt
Dissection forceps	Fine Tip No.5 (Dumont)
Glass needle	Glass Thinw No Fil 1.0mm 3IN TW 100-3 World Precision Instruments, Inc. Sarasota, USA
Microloader tips	930001007 (Eppendorf)
Micromanipulator	Manual, M3301R (WPI Inc.)
Microscopes	Olympus SZX10/SZX16 ZEISS Axiophot Trinocular Leica SP5 X Confocal microscope Leica DMI6000 SD
Needle holder	Microelectrode holder (WPI Inc.)
Needle polisher Model EG-44	Narishige
Needle puller	P-97 Flaming/Brown Micropipette Puller (Sutter Instrument)
Photometer	pND-1000B, NanoDrop (Thermo Scientific Inc.)
Polycarbonate microchannel	provided by Dr. Stefan Giselbrecht
R100 Rotatest Shaker	Luckham,
1 ml Syringe	Braun
Teflon ring	provided by Dr. Stefan Giselbrecht
UV Ozone Cleaner – ProCleaner™ Plus	BIOFORCE Nanoscience

2.1.2 Chemicals

Name	Description
4',6-Diamidin-2-phenylindol (DAPI)	Sigma-Aldrich, Taufkirchen, Germany
Agarose	Peqlab, Erlangen, Germany

Ampicillin	Roth, Karlsruhe, Germany
Anti-Digoxigenin-Fab-fragments	Roche, Mannheim, Germany
Bacto Agar	Roth, Karlsruhe, Germany
BCIP	Roche, Mannheim, Germany
Blocking Reagent	Roche, Mannheim, Germany
Bovine serum albumine (BSA)	PAA, Coelbe, Germany
Dimethylsulfoxide (DMSO)	Fluka, Neu-Ulm, Germany
DPBS (+/+)	Invitrogen, Karlsruhe, Germany
DPBS, without calcium and magnesium (-/-)	Invitrogen, Karlsruhe, Germany
Dulbecco's modified Eagle's medium (DMEM)	Invitrogen, Karlsruhe, Germany
eGFP	Scholpp lab
Ethanol	Roth, Karlsruhe, Germany
Ethidiumbromide	Roth, Karlsruhe, Germany
Fetal Bovine Serum	BIOCHROME AG, Berlin, Germany
Fibronectin	Live Technologies, Gibco
Gentamicin Reagent Solution (50 mg/ml)	Invitrogen, Karlsruhe, Germany
Glycerol	Roth, Karlsruhe, Germany
Glycine	Roth, Karlsruhe, Germany
Hyb-	Live Technologies, Gibco
Isopropanol	Roth, Karlsruhe, Germany
Laminin-1	Invitrogen, Karlsruhe, Germany
Leibovitz' L-15	Gibco, Karlsruhe, Germany
Low melting agarose	Carl Roth GmbH, Karlsruhe, Germany
Methanol (MeOH)	Roth, Karlsruhe, Germany
NBT/BCIP solution	Roche, Mannheim, Germany
Nodal Inhibitor SB431542	Tocris
Paraformaldehyde	Merck, Darmstadt, Germany
PBST	Gibco, Karlsruhe, Germany
Penicillin/Streptomycin	Invitrogen, Karlsruhe, Germany
Phalloidin	Sigma-Aldrich, Taufkirchen, Germany
Pronase	Carl Roth GmbH, Karlsruhe, Germany
Proteinase K	Sigma-Aldrich, Taufkirchen, Germany
Triton-X-100	Roth, Karlsruhe, Germany
Trizol	Invitrogen, , Karlsruhe, Germany
Trypsin 0,25 % (w/v) EDTA	Gibco/Invitrogen, Karlsruhe, Germany

Tween20	Roth, Karlsruhe, Germany
Yeast extract	Roth, Karlsruhe, Germany

2.1.3 Software

Name	Description	Source
Adobe Photoshop CS4	Image editing	Adobe systems, San Jose, CA, USA
Cell A	Photodocumentation	Olympus, Rodgau, Germany
Imaris 7.4.2	Image processing	Bitplane AG, Zürich, Switzerland
LAS AF	Photodocumentation	Leica, Wetzlar, Germany
ND-1000 v 3.7.0	DNA/RNA measurement	
StepOne Software v2.1 and v2.3	qPCR	Applied Biosystems

2.1.4 Enzymes

Name	Source
DNaseI	Ambion Ltd, Warrington, UK
Restriction enzymes	New England Biolabs, Ipswich
Reverse Transcriptase	Promega, Mannheim
Taq-Polymerase	Promega, Mannheim

2.1.5 Marker

Name	Source
GeneRuler DNA ladder mix	Fermentas, St. Leon-Rot, Germany

2.1.6 Kits

Name	Source
SYBR® green	Life Technologies GmbH, Dresden, Germany
Direct-zol RNA Mini Prep Kit	Zymo Research, Freiburg, Germany
peqGold Gel extraction Kit	Peqlab, Erlangen, Germany
QIAGEN Plasmid Maxi purification Kit	Qiagen, Hilden, Germany

2.1.7 Overexpression constructs

Name	Description
zfWnt8aORF-GFP-pCS2+	Sequence of zebrafish Wnt8a ORF1 cloned into pCS2+ (Rhinn <i>et al.</i> , 2005)
Tg(7xTCF-Xla.Sia:nlsMCherry)	Moro <i>et al.</i> , 2013
His-CFP-pCS2+	Gift from Smith, Jim Group

2.1.8 Primer

Name	Description
pou5f3	Forward: CCC AAA CCC AAC ACT CTG G Reverse: ACG CTT TCC CTT CTG TCT ACG
sox2	Forward: GGT AAC TTC AGC AGC CTC TCC Reverse: GGC TTC AGC TCG GTT TCC
neurog1	Forward: GGA TTC TGC AAA ACC TCA AGC Reverse: CGC GAG TCC TCA TCA TCC
elavl3	Forward: AGA CAT GGA GCA GTT GTT TTC C Reverse: GCT TCG TTC CGT TTG TCG
β -actin1a	Forward: CCT TCC TTC CTG GGT ATG Reverse: GGT CCT TAC GGA TGT CCA

2.1.9 In situ probes

neurogenin1	Houart lab
-------------	------------

2.1.10 Transfection reagents

Name	Source
FuGENE® HD Transfection Reagent	Promega, Mannheim, Germany

2.1.11 Cell lines

Cell line	Description	Culture Medium	Source
HEK293T (CRL-1573)	Human embryonic kidney cells	DMEM + 10% FCS	American tissue culture collection, ATCC, Wesel, Germany
PAC2	Zebrafish fibroblasts	L15 + 15% FCS	Foulkes Laboratory

Cells	Description	Culture Medium	Source
Zebrafish primary cells	Blastula (sphere stage) embryo	L15 + 15% FCS	Fish facility

2.1.12 Bacterial strain

Name	Description
E.coli Nova Blue®	Chemical competent cells (Invitrogen) Genotype: K-12 strain

2.1.13 Fish lines

Name	Description
Tg(-8.4neurog1:GFP)	Blader <i>et al.</i> , 2003
Tg (elavl3 (huC):GFP)	Park <i>et al.</i> , 2000

2.2 Methods

2.2.1 RNA methods

2.2.1.1 RNA isolation and cDNA synthesis

For the analysis of dynamic expression of different marker genes during embryonic development a real time qPCR was performed. Therefore, RNA has to be isolated from zebrafish embryos at sphere stage, 10 somite stage, 24hpf and 48hpf. The isolated RNA was transcribed into cDNA by reverse transcription, which was performed with 20U of AMV reverse transcriptase in 80µl reactions containing 80 U RNAsin, 400ng of oligo d(T) primer and nucleotides. Following incubation for 45 min at 41°C reverse transcriptase was inactivated by heating at 70°C for 15 min. cDNA was stored at -80°C.

2.2.1.2 Real time qPCR

For qPCR analysis 4µl of 1:20 dilution cDNA were pipetted in each well of a 96 well plate together with the SYBR green Primer Mastermix (Promega). qPCR was performed in the ABI StepOnePlus Real-Time PCR system (Applied Biosystems) with a standard temperature cycle program, according to the manufacturer's conditions. The relative levels of each mRNA were calculated by $2^{-\Delta\Delta CT}$ methods (where CT indicates the cycle number at which the signal reaches the threshold of detection). Relative gene expression levels were normalized using the zf housekeeping gene β -actin mRNA.

2.2.2 *In vivo* experiments

2.2.2.1 SB431542 Nodal Inhibitor Treatment *in vivo*

Zebrafish were mated as already described. Zebrafish embryos were collected at the 2cell stage and placed in a well plate, 20 embryos each well. The embryos were treated from 2 cell stage onwards for 24h or 48h respectively in a 20 and 40mM Nodal Inhibitor solution (diluted in E3) or as Ctrl in 0,1% DMSO (diluted in E3). The embryos were incubated in the 28°C incubator in the dark. Moreover, treated and ctrl embryos were fixed in 4% PFA for in situ hybridization.

2.2.2.2 In situ hybridization

Embryos were dechorionated in 1x PBST with forceps or pronase and fixed in 4%PFA at 4°C. Then the fixed embryos were washed twice for 5 min in PBST, incubated twice for 5 min in 100% MeOH and stored in fresh MeOH at -20°C.

For the in situ hybridization the embryos were rehydrated twice for 5 min in PBST, then they were fixed again in 4% PFA for 30 min at RT and washed twice for 5 min in PBST. 24hpf embryos were digested with Proteinase K to permeabilize them to facilitate the penetration of the probe inside the embryo. This is not necessary for younger embryos. For the Proteinase K digestion the embryos were treated with 25µg/µl for 1-2 minutes and then washed twice in glycine (2mg/µl). Afterwards, the embryos were washed with PBST and then fixed again with 4% PFA for 30 min at RT. Then they were washed again three times for 5 min in PBST. Incubation in Hyb⁺ for 0,5-6h at 69°C followed. Afterwards, the Hyb⁺ was replaced with pre-warmed Hyb⁺ containing the antisense probe neurog1 and incubated over night at 69°C. The next day the probe was removed and the embryos were washed for 5 min in Hyb⁺, three times for 10 min in 25% Hyb⁻, three times for 10 min in 25% Hyb⁻, 5 min in 2X SSCT and twice for 30 min in 0,2xSSCT at 69°C. After that they were washed 5 min in 50% 0,2 x SSCT/50% MABT, 5 min in MABT and then the unspecific binding sites were blocked by incubation with 2% DIG-block for at least one hour. The blocking solution was replaced with a pre-absorbed DIG-antibody in a 1:4000 dilution in blocking solution and incubated over night at 4°C. The next day the embryos were washed five times for 15 minutes in MABT and 5-15 in NTMT. The staining solution consisted of NCP-BCIP that was diluted 1:200 in NTMT and was added to the embryos in a 12 well plate. When the staining was strong enough, the staining reaction was stopped by washing twice in PBST and the embryos were fixed again in 4% PFA for 30 min at RT. After washing again for 5 min in PBST the embryos were stored in 70% glycerol at 4°C.

Solution:

PBST:	1x PBS 0,1% Tween20
Hyb ⁻	50% Formamide 5x SSC (pH6) 0,1% Tween20
MAB:	100mM maleic acid 150mM NaCl pH 7,5
MABT:	MAB 0,1% Tween20
2% DIG-block:	2% blocking reagent in MABT
NTMT:	100mM NaCl 100mM Tris 1% Tween20

2.2.2.3 Analysis of Rohon-Beard sensory neurons

In vivo NI treatment was performed as described, with the zf neuro1:GFP transgenic line. RBs from embryos treated with 40mM NI and ctrl embryos treated with 0,1% DMSO from 2cell-24hpf and 2cell-48hpf were analyzed. Therefore, embryos were mounted in 1,5% low melting agarose and with dorsal up and analyzed by confocal microscopy.

Medium for breeding and manipulation of zf embryos:

MESAB:	400mg Tricaine powder (Sigma) 2,1ml 1M Tris (pH 9.0) to 100ml with H ₂ O adjust to pH 7.0 and store at 4°C
PTU	0,0003% 1-phenyl-2-thiourea in 1x PBS

2.3 Protein Method

2.3.1 Phalloidin/DAPI staining of cells

For visualization of the actin cytoskeleton and the nuclei, the cells were stained with Phalloidin FITC or TRITC and 4',6-diaminidino-2-phenylindole (DAPI). Therefore, the L-15 growth medium was removed from the petri dish and cells were washed twice for 5 min in PBS^{+/+}. Afterwards they were fixed with 4% PFA on ice for 30 min. Then the cells were permeabilized using 0,1% Triton X-100 solved in PBS^{-/-}. After this, the cells were stained with Phalloidin FITC or TRITC for 1h 15 min followed by 2x 5 min washing steps in PBS^{-/-}. Then the cells were stained with DAPI for 6 min and afterwards washed again in PBS^{-/-}.

2.3.2 eGFP affinity assay

The polycarbonate film was incubated for 15 min in a solution containing a 1µM concentration of enhanced green fluorescence protein (eGFP) in PBS. 1.93µl were taken from a stock solution of eGFP in PBS (154µM, 100µl) and diluted in 3ml PBS. After incubation, the polycarbonate film was washed 3x 5 min in PBS^{-/-} and finally 2x 15 min washing steps in PBS^{-/-}. The fluorescence intensity was measured on an Olympus SZX16 microscope.

2.4 Cell culture methods

2.4.1 Maintenance of PAC2 cells

Zebrafish PAC2 fibroblast cells were cultivated in Leibovitz's L-15 medium (with 15% FBS, 1% Pen/Strep and 0,1 % Gentamycin) at 28°C and without additional CO₂ supply. For passaging the cells were washed with PBS^{-/-} and detached with 0,25% trypsin-EDTA. The cells were passaged 1:3 once a week.

2.4.2 Maintenance of HEK293 cells

Human Embryonic Kidney 293T cells were cultivated in DMEM (with 10% FBS and 1% Pen/Strep) at 37°C and with 5% CO₂ supply. Passaging was performed 1:20 every 4 days.

2.4.3 Passaging cells

For passaging, the medium was removed by aspiration, cells were washed once with PBS and Trypsin-solution (0,25% Trypsin) was added to the cells. Cells were incubated at RT until they started to detach from the flask walls. Trypsination was stopped by addition of medium containing serum. Cells were collected by centrifugation. After resuspending the cells in fresh growth medium cells were seeded in new tissue culture petri dishes.

2.4.4 Seeding cells

Cells were trypsinized as described above, collected by centrifugation and resuspended in new growth medium. To obtain the number of cells per ml, 10µl of cell suspension was transferred into a Neubauer counting chamber and counted by using a bright field microscope. After adjustment of the designated cell concentration by mixing cell suspension and culture medium, cells were distributed in tissue petri dishes for the experiment.

2.4.5 Transient Transfection of cells with FuGENE HD

For the transfection of a 30mm dish of 80% confluent cells were combined with FuGENE HD Transfection Reagent, 100µl growth medium without serum and antibiotics, 1µg plasmid DNA (or 0,5µg each for co-transfection) and 4µl FuGENE HD. This mixture was vortexed shortly and spun down. The used plasmids are described in the results part. The mixture was incubated 15 min at RT. In the meanwhile, the cells were washed with PBS and the growth medium was replaced by growth medium without antibiotics but with 10% serum. Afterwards, the transfection mixture was added dropwise to the dish and the cells were cultivated as described above for 24h.

2.4.6 Primary cell culture

To gain zebrafish sphere stage embryos used for the primary cell culture experiments, male and female zebrafish were placed in tanks separated by inlays over night. The next morning female and male were mated and the female laid eggs. Zf eggs were collected and dechorionated in 1-2 cell stage by 10mg/ml pronase to remove the chorion and washed immediately three times with fish water in a beaker. Dechorionated embryos were washed fast in 70% EtOH, rinsed in sterile E3 medium and placed in calcium free Ringer's solution. Cells were transplanted by usage of a Transplantation setup, containing of a transplantation needle, connected to a vacuum syringe. Cells were transplanted into a Fibronectin/laminin-1 coated petri dish containing Leibovitz's L-15 medium with 15% FBS, 1% Pen/Strep and 0,1% Gentamycin. Then, the NI treatment was performed.

2.4.7 Biofunctionalization of the microchannel

The microchannel was produced in the SMART process (provided by Dr. Stefan Giselbrecht).

First of all, the microchannel was cleaned by a washing series in 70%,50%,35% Isopropanol, H₂O dest and PBS^{-/-}. As a prerequisite for the adherence of the coating solution, the microchannel has to be hydrophilized. Therefore, the microchannel is placed in a UV-Ozone cleaner and treated for 5 min (longer treatment is harmful for the polycarbonate). Afterwards the microchannel was coated with a mix of basal proteins; Fibronectin/Laminin-1

0,01mg/0,5ml + 0,02mg/1ml (testing of different coating conditions is described in the results part). Around the polycarbonate some drops of PBS^{-/-} were placed to avoid drying-out of the channel during the incubation in the 31°C incubator for 2h. After that the microchannel was washed 3x 10 min in PBS^{-/-} to eliminate unbound proteins. Finally the microchannel is ready to use.

2.4.8 Primary cell culture in 3D

The PC foil containing the microchannel was placed into a 60mm petri dish, weighted down with a Teflon ring and the petri dish was filled with medium. Zf sphere stage-derived cells were isolated from the embryo with the transfection needle as described and directly seeded in the microchannel. Then the SB431542 Nodal Inhibitor (NI) treatment was performed.

Transplantation capillaries:

Capillaries for transplantation were pulled on the Flaming-Brown puller with the following parameters:

Pull-heat (H)	253
Pull-force (P)	40
Pull-velocity (V)	70
Pull duration (T)	35

Medium for breeding and manipulation of zebrafish embryos:

E3 medium:	0,1% NaCl
	0,003% KCl
	0,004% CaCl ₂ x 2H ₂ O
	0,016% MgSO ₄ x 7H ₂ O
	0,0001% Methylene blue
Calcium free Ringer solution:	55mM NaCl
	1,8 mM KCl
	1,25 mM NaHCO ₃

2.4.9 SB431542 Nodal Inhibitor (NI) treatment of primary cells

Zf blastula-derived primary cells from the transgenic neurog1:RFP line were treated with SB431542 NI to inhibit mesendoderm formation. Control cells were treated with 0,1% DMSO. Cells were transferred into a petri dish as already described. 1µM SB431542 was added to the medium and cells were incubated at 28°C for 48h in the dark (due to the light sensitivity

of the NI). Control cells were treated with 0,1% DMSO. Afterwards, cells were fixed with 4% PFA for 30 min on ice and stained with the nuclei marker DAPI and the actin cytoskeleton marker phalloidin as described.

2.4.10 Cell Guidance in 2D

In the 2D cell guidance experiment PAC2 fibroblasts were seeded on the PC film and cultivated in Leibovitz's L-15 medium with 15% FBS, 1% Pen/Strep and 0,1% Gentamycin at 28°C for 24h. Afterwards, the cells were washed in PBS^{-/-} for 2x 5 min to remove non-adherent cells. Next, the cells were fixed with 4% PFA for 30 min and stained with the nuclei marker DAPI and the actin cytoskeleton marker phalloidin as described.

2.4.11 Cell guidance in a 3D microchannel

The microchannels were coated with a Fibronectin/Laminin-1 0,01mg/0,5ml + 0,02mg/0,1ml solution for 2h at 31°C. Afterwards the coating solution was removed and unbound proteins were washed out by incubation with PBS^{-/-} for 2x 5 min to remove non-adherent cells. Next, the cells were fixed with 4% PFA for 30 min and stained with the nuclei marker DAPI and the actin cytoskeleton marker phalloidin as described.

2.4.12 Co-Culture assay

2D HEK293T cells were used for the co-culture experiment (since they showed a higher transfection rate than PAC2 fibroblasts. Cells were transfected with 1µg zfWnt8aORF-GFP-pCS2+ were cultivated for 24h. In another petri dish 2D cells co-transfected with 7xTRE-mCherry-NLS/His-CFP-pCS2+ were cultivated for 24h Then, the cells were trypsinized and seeded together for co-culture into a 3D microchannel, whereas cells inside the microchannel were analyzed for 3D cell culture and cells attached outside of the microchannel were analyzed for 2D cell culture. Cells were cultivated for another 24h. As control, 7xTRE-mCherry-NLS/His-CFP-pCS2+ transfected cells were seeded in the 3D microchannel. Again, cells inside the microchannel were considered for 3D analysis, cells outside in the petri dish for 2D analysis. Living cells were imaged by confocal microscopy.

2.5 Image Acquisition

For phenotype analysis the embryos were anaesthetized with Mesab and for ISH analysis the embryos were embedded in 70% glycerol/PBS. Pictures were taken with an Olympus SZX16 microscope equipped with a DP71 digital camera by using Cell A imaging software.

For confocal analysis, living embryos were embedded in 1,5% low melting agarose in 1x E3. Confocal images were obtained using a Leica TCS SP5 X microscope with a 40x dip-in objective for embryos and a 63x dip-in objective for cells. Images of the SB431542 NI

treatment of primary cells in 2D were taken with the inverted Leica DMI6000 SD microscope, using the 20x objective. The images were processed using Imaris 7.4.2 software. Fluorescence intensity of eGFP protein was measured by carrying out five linear scans passing non-irradiated and irradiated areas across the PC film and compared with the fluorescence intensity measured in a non-irradiated zone on the same film.

2.5.1 Image Processing

The Phalloidin/DAPI z-stack data recorded at the Leica SP5 confocal microscope was processed using the Leica Application Suite Advanced Fluorescence (LAS AF).

2.5.2 Quantification of Fluorescence Intensity

For the quantification of neurog1 pos. nuclei and RBs the Imaris 7.4.2 software was used. Nuclei were quantified using the spots tool. Marking of the spots was adjusted by manually marking neurog1 pos. nuclei if necessary. For comparison, total nuclei were counted as well with the spots tool.

In the 2D cell guidance experiment, nuclei of PAC2 cells were also quantified using the spots tool. For evaluation of the surface area covered by cells the surface of cells was calculated using the surface tool.

In the Co-culture assay, Tcf nuclei were counted with the spots tool and compared to His-CFP (total) nuclei.

2.6 Statistical analysis

The double-sided student's *t*-test was used for comparison of two samples. Calculation of the mean averages and standard deviation was performed using at least three biological replicas. P-values <0,05 were considered as significant. Error bars indicate standard error (SD).

3. Results

Neurogenesis is an important and complex process, which requires the integration of various molecular mechanisms, including the regulated activity of multiple signaling pathways, e.g. Wnt, FGF, Shh and TGF- β /BMP. These signaling pathways in turn govern neural induction, cell fate specification, differentiation and morphogenesis of the nervous system. Due to the complexity in an intact embryo, a simplified three-dimensional cell culture approach would be suitable to investigate neural differentiation in a controlled manner.

Therefore, the aim of my thesis was to generate a zebrafish neural tube in a three-dimensional microchannel. Thereby, a comparative study was performed to study neuronal differentiation in the zebrafish embryo and in a 2D and 3D zebrafish primary cell culture.

The microchannel was applied to answer the following questions:

- 3.1. Can I control neurogenesis *in vitro*?
- 3.2. Can I guide cells in a polymer channel to an area of interest?
- 3.3. Can I control cellular signaling *in vitro*?

In all this contexts the 3D platform was compared to 2D culture and in the neurogenesis part additionally to the *in vivo* scenario.

3.1 Control of neurogenesis

3.1.1 Expression analysis of relevant dynamic markers during zebrafish embryonic development (with Anna Geenen)

For the investigation of dynamic markers for neurogenesis during zebrafish embryonic development a real time quantitative PCR was performed. The *in vivo* cell fate during embryonic development was analyzed by quantifying expression of dynamic markers at different time points of interest, important for neurogenesis (sphere stage, 10 somite, 24hpf and 48hpf; Fig.7). At sphere stage the prospective neuroectoderm is generated, at 10 somites the neural keel appears and at 48hpf the central nervous system is established.

Pou5f3 (a Oct4 homolog) was evaluated as a pluripotent marker for embryonic stem cells (ESCs), *sox2* as neural stem cell marker (NSCs), *neurog1* to analyze neural progenitor fate (NPCs) and *elavl3* (a HuC homolog) for mature neurons (MN).

The relative gene expression was evaluated within a marker but not between the different markers, since the expression of a marker was analyzed in correlation to the 24hpf stage (just pou5f3 was correlated to the expression at sphere stage, since sphere stage expression was higher than the normalizing factor).

Normalization was calculated in relation to the housekeeping gene β -actin.

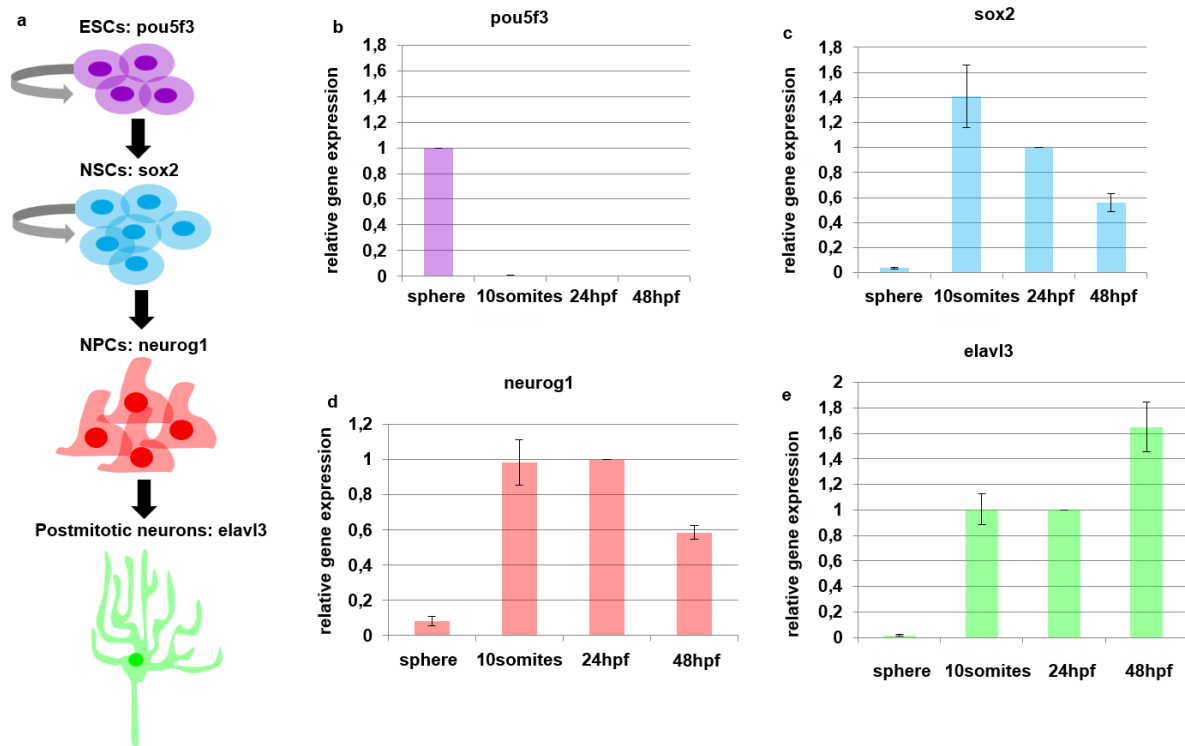


Figure 7: Expression analysis of relevant dynamic markers during zebrafish embryonic development. Scheme of stem cell differentiation during embryonic development (a). Relative gene expression of pou5f3 (b) (ESCs), Sox2 (c) (NSCs), neurog1 (d) (NPCs) and elavl3 (e) (postmitotic neurons) shown by qPCR (right). Data represent for pou5f3: n=3, sox2: n=3, neurog1: n=4 and elavl3: n=5 embryos.

The ESC marker pou5f3 (Fig.7b) was highly expressed at sphere stage and decreased until the 10 somite stage, where pou5f3 was still detectable with 0,8% (SEM 0,3%) at 24hpf with 0,2% (SEM 0,04%) and 48hpf with 0,1% (SEM 0,02%).

Sox2, the NSC marker (Fig.7c), was not detectable at sphere stage, but showed the highest expression at the 10 somite stage. At the 10 somite stage, sox2 expression was 40,8% higher than at 24hpf (SEM 24,8%). At 48hpf a decrease of 44,2% compared to 24hpf was observed (SEM +/- 24,8%).

Neurog1, the indicator for neural progenitor fate (Fig.7d), depicted a minor expression at sphere stage and increased until 10 somite stage.

The highest expression was detected at 24hpf. *Neurog1* expression was 1,8% lower (SEM 12,8%) at the 10 somite stage compared to 24hpf. At 48hpf a decrease of 41,3% was detected (SEM 4%) compared to 24hpf.

Early postmitotic neurons are indicated by *elavl3* expression (Fig.7e), which was not detectable at sphere stage, but increased obviously until the 10 somite stage, keeping this expression level until 24hpf with just a slight decrease of 0,6% (SEM 12,2% for 10 somite). Until 48hpf, once again a dynamic increase of *elavl3* expression 64,9% (SEM 19,5%) was observed compared to 24hpf.

The analysis of characteristic markers for ESCs, NSCs, NPCs and mature neurons displayed the process of cell fate during embryonic development.

Thus, the qPCR data showed that *neurog1* reflects the dynamics of neurogenesis.

Moreover double transgenic Tg(-8.4*neurog1*:RFP)/ Tg (*elavl3* (huC):GFP) expressing zebrafish embryos are shown at 24 hpf (Fig.8a, a`) and 48 hpf (Fig.8b, b`), respectively.

The expression of *neurog1* and *elavl3* is partly overlapping, since *neurog1* expression starts at 9hpf in the three longitudinal stripes of the neural plate. *Elavl3* is expressed from 10hpf onwards, just in a subset of neural plate cells (Kim *et al.*, 1997; Park *et al.*, 2000).

Neurog1 is expressed in all primary neurons and *elavl3* indicates all postmitotic neurons in the forebrain, midbrain and hindbrain at 24hpf (Fig.8a,a`) and 48hpf (Fig.8b,b`).

Neurog1 dynamically reflects neurogenesis *in vivo*. Within this thesis, a comparative study was performed to evaluate controllability of neuronal differentiation in the zebrafish embryo compared to 2D and 3D zebrafish primary cell culture.

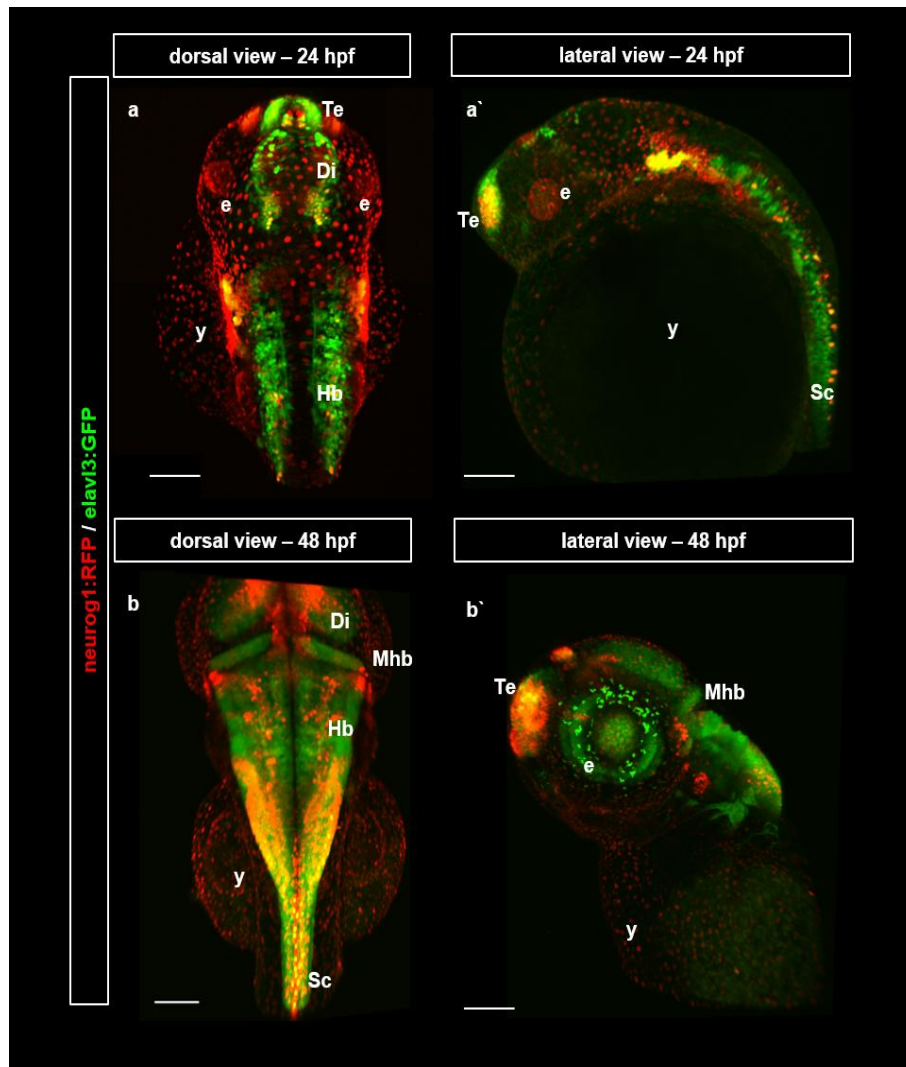


Figure 8: Expression of *neurog1*:RFP/*elav3*:GFP in a 24hpf and 48hpf zebrafish embryo. Dorsal view (a) and lateral view (a') of *neurog1*:RFP/*elav3*:GFP expression at 24hpf and in a 48hpf zebrafish (b,b'). Scale bar = 100 μ m. Di = Diencephalon, E = eye, Hb = Hindbrain, Mhb =Midbrain-hindbrain boundary, sc = spinal cord, Te = Telencephalon, y = yolk.

3.1.2 Neural differentiation *in vivo*

For the formation of a neuroepithelium ESCs have to differentiate from a pluripotent state to a proneural fate. It has been shown, that by inhibition of nodal signaling (*ndr1/ndr2* in zebrafish) mesendoderm formation is blocked, thus enhancing ectoderm formation, which partly will give rise to the prospective nervous system. In this regard, a Nodal Inhibitor (NI) - SB431542 - blocks kinase activity by binding to the ATP binding sites of the activin-like kinase (ALK) 4,5 and 7 receptors of the TGF- β pathway (Fig.9), thus blocking phosphorylation of downstream effectors Smad 2 and 3.

Hence, mesendoderm formation is inhibited (Inmann *et al.*, 2002; Sun *et al.*, 2006; Hagos and Dougan, 2007; Lippmann *et al.*, 2014).

Zebrafish embryos were treated with the NI and Dimethylsulfoxide (DMSO) as a control. Alteration of neurogenesis was observed by *in situ hybridization* with *neurog1* as indicator for a proneural fate.

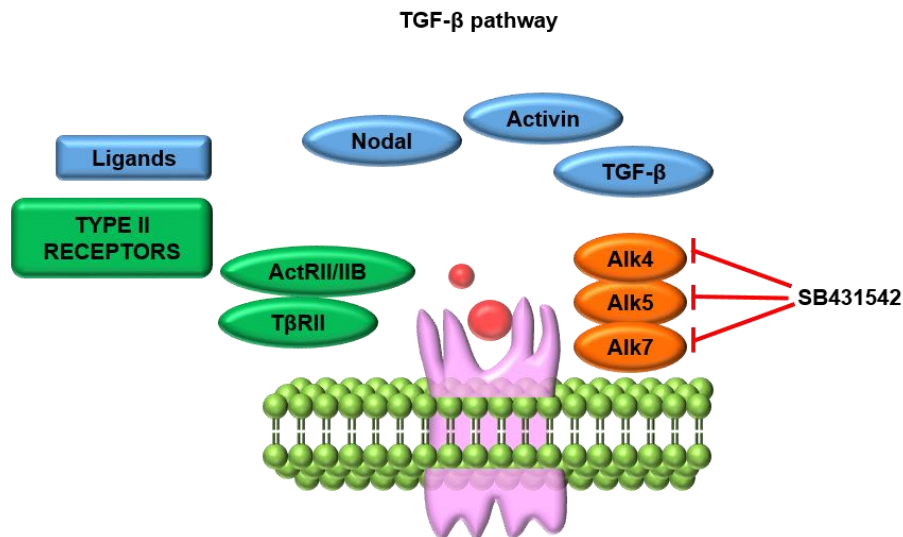


Figure 9: Inhibition of mesendoderm formation by the SB431542 Nodal Inhibitor. Blockage of the ALK 4,5,7 receptors leads to inhibition of nodal signaling (Simplified scheme).

3.1.3 Analysis of *neurogenin1* expression

Zebrafish wildtype embryos were collected and placed in a well plate, 20 embryos each well. The embryos were treated from 2-cell stage until 24hpf and from 2-cell stage to 48hpf, with concentrations of 20mM and 40mM Nodal Inhibitor solution (diluted in E3) or 0,1% dimethylsulfoxide DMSO; diluted in E3). The embryos were incubated in the 28°C incubator in the dark, due to the light sensitivity of the NI. After the NI *in vivo* treatment, embryos were fixed and *in situ* hybridization was performed with *neurog1* as a marker (Fig.10). Whole mount embryos were imaged by stereomicroscopy from the lateral side (Fig.10a,b,c). Afterwards the trunk region of the spinal cord (indicated by black cutting lines in Fig.10.a,b,c) was cut out and is shown in Fig.10a` ,b` ,c` in a dorsal view. In the 2-cell-24hpf control embryo *neurog1* was expressed in the dorsal telencephalon, diencephalon, hindbrain and spinal cord (Fig.10a,a`). In the 20mM NI treated embryo from 2-cell-24hpf a stronger *neurog1* expression was observed in the dorsal telencephalon and diencephalon (yellow arrows), hindbrain and spinal cord (Fig.10b). Moreover, the spinal cord increased in width (Fig.10b`, red arrows) compared to the spinal cord of the control embryo (Fig.10a`).

Additionally, a more broadly *neurog1* expression in the dorsal telencephalon was observed. In the 40mM NI treated embryo from 2-cell-24hpf also a strong *neurog1* expression is visible in the dorsal telencephalon and diencephalon and these expression domains expanded further (Fig.10c, yellow arrows). Furthermore, *neurog1* was strongly expressed in the spinal cord which notably increased in the width (Fig.10c', red arrows) compared to the control embryo (Fig.10a').

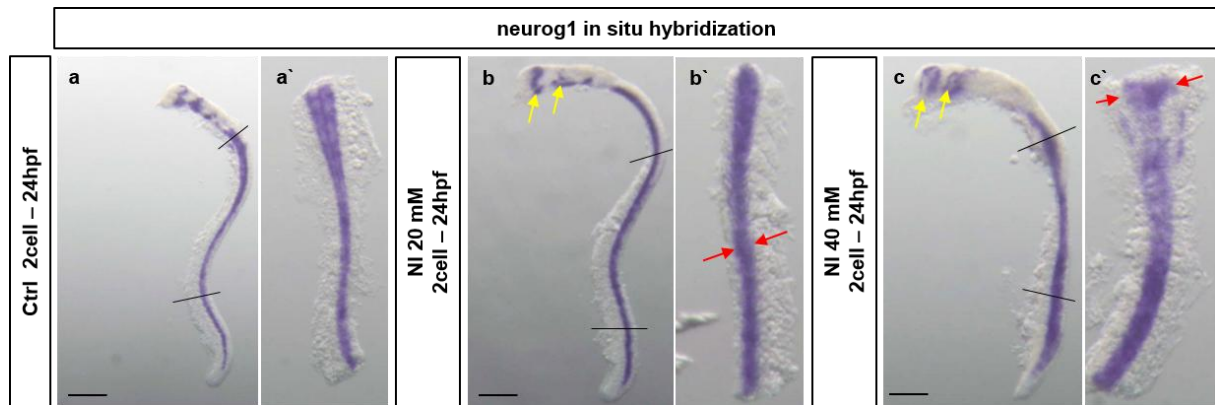


Figure 10: Neurogenin1 in situ hybridization. *Neurog1* expression was evaluated in 2cell-24hpf ctrl; n=20 (a,a') and treated embryos; n=20 (b,b',c,c'). Black lines in a,b,c indicate cut out spinal cord parts in the trunk region; shown in a dorsal view (a',b',c'). Yellow arrows show changes in the expression of dTe and Di in treated embryos, red arrows indicate widening of the spinal cord. Scale bar = 50µm. dTe = dorsal Telencephalon, Di = Diencephalon.

Thus, by inhibition of nodal signaling, the NSC population was increased *in vivo*.

3.1.4 Analysis of Rohon-Beard sensory neurons

Involvement of *neurog1* has been shown to be crucial for the development of Rohon-Beard (RB) sensory neurons and inhibition of *neurog1* resulted in failure of RB sensory neuron formation (Cornell and Eisen, 2002). Therefore, I investigated if NI treatment results in alteration of neurogenesis, reflected by a change in RB sensory neurons. Since in the *in situ hybridization* it was shown that 40mM NI treated embryos from 2cell-24hpf showed the strongest effect reflected by the *neurog1* expression, *neurog1*:GFP embryos were treated with this concentration and compared to control embryos (DMSO treated).

After NI treatment, RB sensory neurons of the *neurog1*:GFP transgenic embryos were imaged by confocal microscopy (Fig.11a,b). The average numbers (Fig.11a',b') of RB sensory neurons were analyzed with the Bitplane Imaris software. Quantification resulted in an average number of 52,8 RBs for control and 68,6 for NI treated RBs, meaning a 1,3 fold increase for 2cell-24hpf (Fig.11c). Significance was determined as n.s. (not significant) with the Student's T-Test.

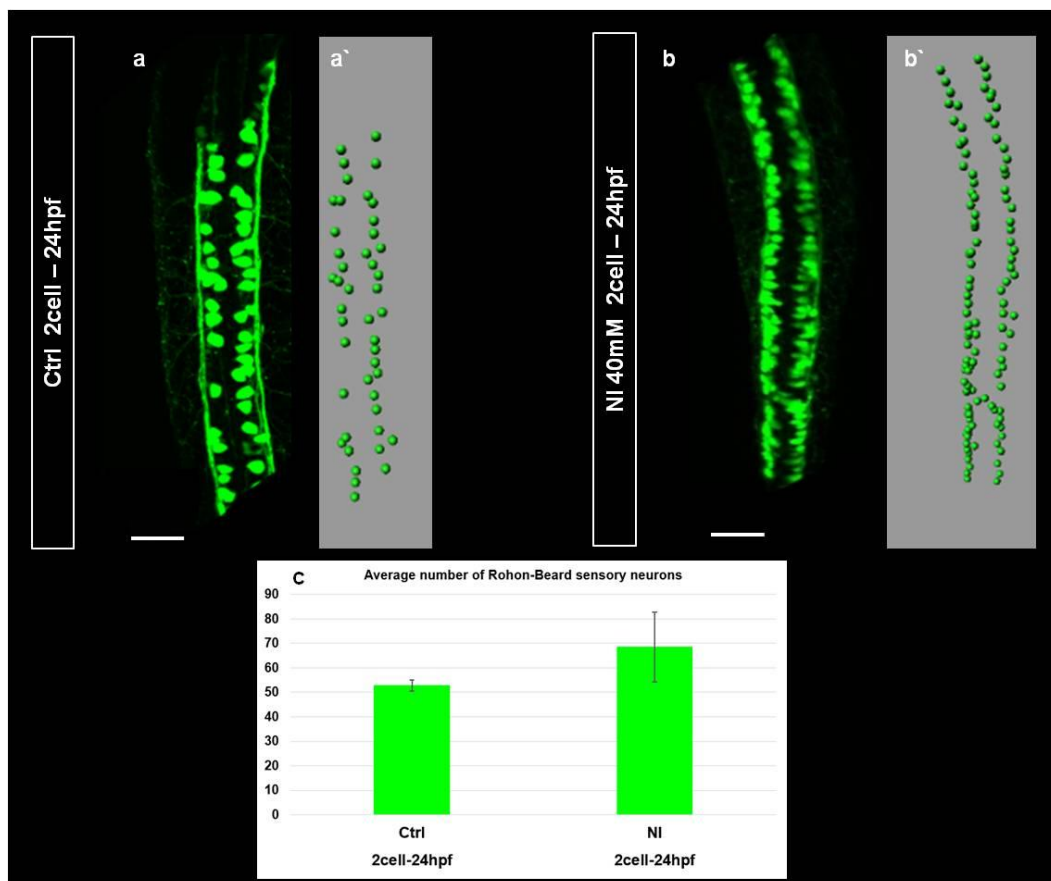


Figure 11: Analysis of Rohon-Beard sensory neurons. Confocal (**a,b**) and schematic (**a',b'**) pictures of ctrl (**a,a'**) and NI treated (**b,b'**) embryos. Scale bar = 50µm. The average numbers of RB sensory neurons are shown in (**c**). Data represent an average from n=11 control embryos and n=5 NI treated embryos with the indicated standard deviations (n.s. = not significant, statistical significance was determined by using the student's t-test).

Thus, inhibition of nodal signaling *in vivo* was at first visualized by an increase in the NSC population, shown by the neurog1 *in situ hybridization*. This hint was then further validated by a significant increase in the average number of RB sensory neurons.

Since the complex environment of an intact embryo hinders the detailed dissection of particular signaling steps, a 3D cell culture approach would be more suitable to investigate neural differentiation in a controlled manner.

At first, it was investigated if in 2D *in vitro* cultivated primary cells, derived from zebrafish blastula embryos can adopt a proneural fate.

3.1.5 Cultivation of neural progenitor cells *in vitro*

Pluripotent cells of blastula sphere stage embryos from the transgenic neurog1:RFP line (with a nuclear localization) were cultivated for 48h and stained with Phalloidin/ DAPI to visualize the nuclei (blue) and the actin cytoskeleton (green). Neurog1:RFP negative cells were indicated as blue nuclei whereas cells expressing neurog1:RFP are shown in red with a variation in intensity (Fig.12a,a`).

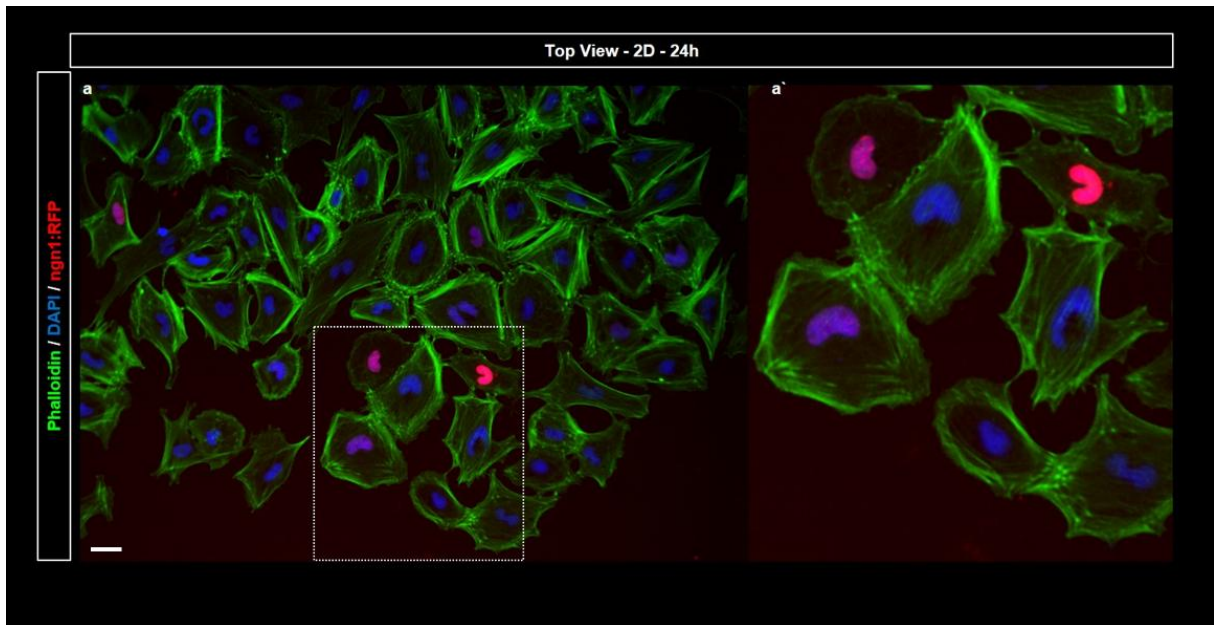


Figure 12: Cultivation of neurog1:RFP cells in 2D. Neurog1:RFP blastula-derived cells were cultivated for 24h. Nuclei of neurog1:RFP negative cells are shown in blue, positive nuclei in red (**a**). Zoom-in is shown in (**a`**). Staining was performed for nuclei (DAPI, blue) and actin (Phalloidin, green). Scale bar = 10µm.

Thus, it was shown that some of the sphere-stage derived cells developed into a proneural fate.

Although primary cells developed a proneural fate *in vitro*, observed NPCs were not so abundant. To enrich this cell population and to commit more cells towards the proneural fate, cells were treated with the NI to enrich ectoderm and prospective neuroectoderm formation.

3.1.6 Control of neurogenesis in 2D

Cells from the transgenic neurog1:RFP zebrafish line were seeded on a petri dish and treated with 1µM NI for 48h (control cells were treated with 0,1% DMSO). The treated cells showed obviously an increase in the number of neurog1:RFP positive cells (Fig.13b) compared to control (DMSO; Fig.13a). Neurog1:RFP positive nuclei were quantified with the Bitplane Imaris Software and evaluated in relation to total nuclei (Fig.19,20a).

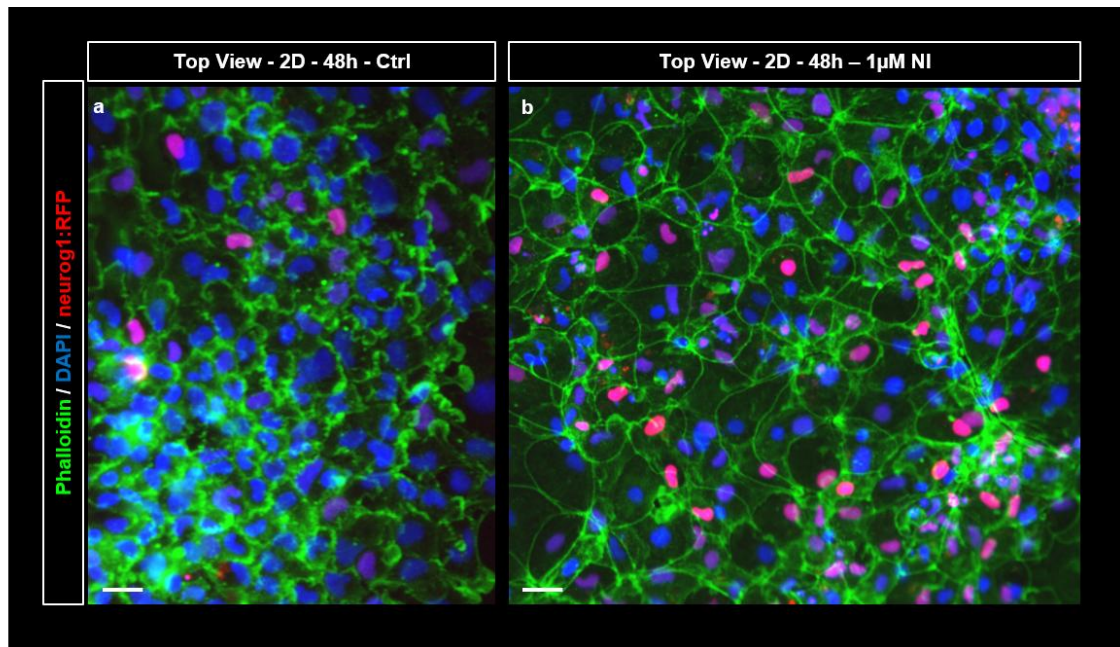


Figure 13: Control of neurogenesis in 2D. Neurog1:RFP blastula-derived cells were treated with DMSO as ctrl (a) or the NI (b) and cultivated for 48h. Nuclei of neurog1:RFP negative cells are shown in blue, positive nuclei in red. Staining was performed for nuclei (DAPI, blue) and actin (Phalloidin, green). Scale bar = 20µm. Three independent experiments were performed (for statistics see Fig. 20a).

Thus, pluripotent zf blastula-derived cells were forced to develop a proneural fate. Hence, by inhibition of nodal signaling a NPC population was increased *in vitro*.

One important aspect of developing a cell culture system (CCS) is to create conditions which mimic the *in vivo* scenario as realistic as possible. For a long time period, exclusively 2D cell culture systems were used for *in vitro* studies. However, in 2D cells are cultured in an artificial environment, since cells depict a different curvature, resulting in an altered arrangement of membrane receptors, which may result in different cellular responses and thus to changes in gene expression (Schwartz and Chen, 2013; Ader and Tanaka, 2014; Knight and Przyborski, 2014; Shao *et al.*, 2015).

Therefore, 3D CCSs are more suitable, because they enable cells are more natural behavior like in the *in vivo* scenario. Nowadays, various 3D CCS are existing, e.g. scaffold-free systems like the hanging drop technique, low adhesion substrates and scaffold-based CCS like various hydrogels and matrigels, microarrays and microfluidic devices (systems discussed in the introduction).

However, none of the CCS was perfectly fitting for the 3D cell culture approach investigated in this thesis.

The most suitable platform, the polycarbonate microchannel developed by Stefan Giselbrecht and co-workers, was therefore biologically modified to optimize it for my approach to generate a zebrafish neural tube.

3.1.7 Establishment of a 3D cell culture system to generate a neural tube

This part of the project was performed in collaboration with S.Giselbrecht and P.Nikolov (MERLN Institute for Technology-Inspired Regenerative Medicine, Maastricht University and Institute for Biological Interfaces, KIT). I thank them for thermoforming of the PC film and discussions about the design of the microchannel.

3.1.7.1 Design and production of a 3D microchannel by SMART

Since I was interested to investigate the formation of a neural tube *in vitro*, I needed a 3D platform to support the formation of a tubular shape and to fit in size with a zebrafish neural tube. Our collaboration partners Stefan Giselbrecht and Pavel Nikolov developed a three-dimensional microchannel which is produced by Surface Modification and Replication by Thermoforming (SMART; Fig.14a). This process consists of three steps, including premodification, the thermoforming step and postmodifications. Multiple microchannels can be formed in one polycarbonate foil (Fig.14b). Moreover, the microchannel is visualized by confocal microscopy (Fig.14c) and SEM (Fig.14d). The microchannel can be modified in size and shape to support the formation of tubular structures. Moreover it is possible to modify the polymer film in a physical, chemical or biological way (Giselbrecht *et al.*, 2006; Truckenmueller *et al.*, 2011). A similar 3D microchannel produced by SMART was already applied to mimic transendothelial transport in a blood vessel (Hebeiss *et al.*, 2012).

The microchannel was designed and modified to be suitable for our investigations, as described in the following paragraphs.

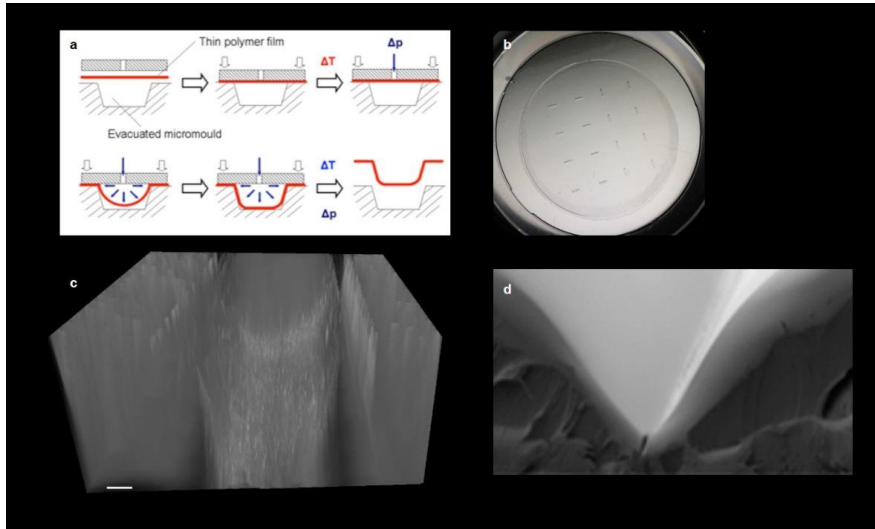


Figure 14: Production and visualization of the microchannel. Production of the microchannel by SMART (a). The formed microchannel is shown in an overview image (b), Confocal BF (c) and SEM (d).

3.1.7.2 Functionality of the microchannel

The functionality of the microchannel was tested by cultivation of zebrafish PAC2 fibroblast cells. After 24h the cells were adherent, covering the complete surface inside the microchannel. Fibroblasts were fixed with 4%PFA and stained to visualize nuclei (DAPI; blue) and the cytoskeleton (Phalloidin; green; Fig.15).

Moreover, zebrafish primary cells attached almost in the complete microchannel (Fig.18).

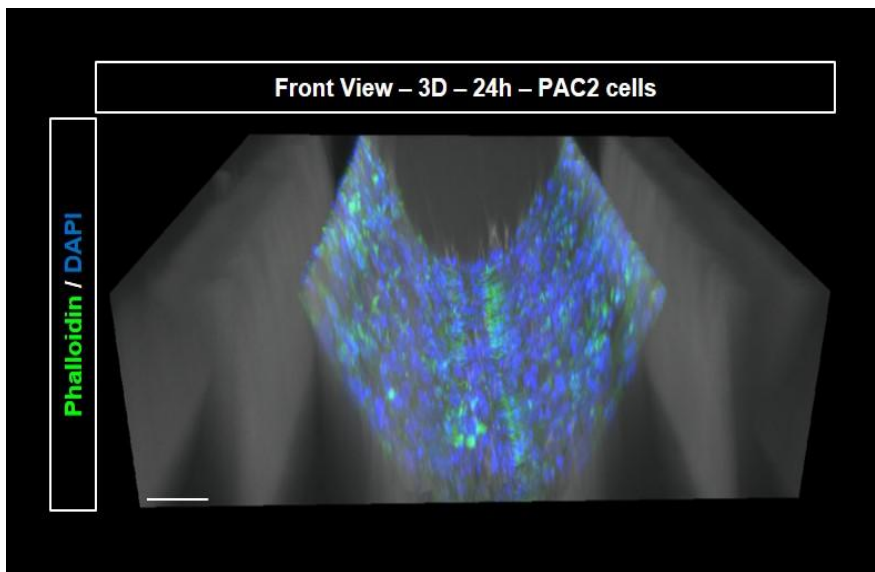


Figure 15: Biofunctionality test of the microchannel with PAC2 cells. Zebrafish PAC2 fibroblast were cultivated for 24h and stained for nuclei (DAPI, blue) and actin (Phalloidin) green. Scale bar = 100 μ m.

Thus, the microchannel is functional for cell lines (also HEK293 and neuro2a cells were tested) and zebrafish primary cells.

3.1.7.3 Coating with basal proteins laminin-1 and fibronectin

Since a main feature of a neuroepithelium is its apico-basal polarity, the microchannel was coated with the basal proteins laminin-1 and fibronectin to determine the basal side for the cells. Laminins were shown to be essential for basement membrane assembly (Ekblom *et al.*, 2003; Hohenester and Yurchenco, 2013) and moreover laminin-1 to be essential for the developing neocortex (Burnside and Bradbury, 2014). Fibronectin is as well a major component of the developing CNS, suggested to be involved in adhesion, migration and axon elongation (Pankov and Yamada, 2002; Burnside and Bradbury, 2014). Inactivation of fibronectin in the mouse was shown to result in embryonic lethality (George *et al.*, 1993). In cell culture, e.g. on coverslips, it was shown that when the surface is coated with fibronectin or laminin, cell attachment was improved (Cooke *et al.*, 2008). Hence, in my approach laminin-1 and fibronectin were tested in various concentrations (Table 1; Fig.16). Moreover, Cyclo olefin polymer (COP) and Polycarbonate (PC) was tested. It was shown that from the COP as well as from the PC foil coating solution persists as roundish drops (which were also not relevantly changed by a 2h incubation at 31°C). This might be due to the hydrophobicity of the foil. It has been shown that by UV/ozone treatment e.g. carbon nanotube surfaces can be turned to be hydrophilic, enabling attachment of the ECM proteins (e.g. laminin and fibronectin) and thus improve cell attachment (Pryzhkova *et al.*, 2014). Therefore, it was tested if a UV-ozone treatment could hydrophilize the PC or COP foil respectively, thus improving the adhesion of the coating.

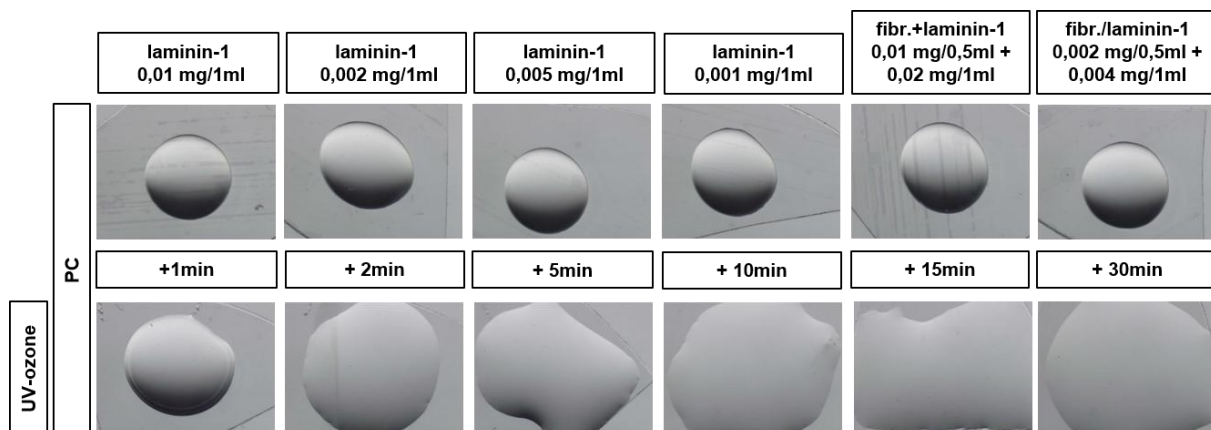


Figure 16: Testing of different coating conditions with and without UV-ozone treatment. PC foil was coated with different laminin-1 conditions or laminin-1/ fibronectin mixed. Coating was tested without UV-ozone treatment and after UV-ozone treatment for different times.

A combination of different UV-ozone treatment times and coating solutions were analyzed on the PC or COP foil respectively (Table 1; Fig.16).

Table 1: UV only, UV ozone and coating conditions. PC and COP foil was tested with various coating and UV-ozone conditions.

Foil Type	UV only	UV ozone	Concentration Laminin-1	Concentration Fibronectin
PC	-	-	1mg/1ml	-
PC	-	-	0,01mg/1ml	-
PC	-	-	0,005mg/1ml	-
PC	-	-	0,002mg/1ml	-
PC	-	-	0,001mg/1ml	-
PC	-	-	-	1mg/0,5ml
<hr/>				
COP	-	-	1mg/1ml	-
COP	-	-	0,01mg/1ml	-
COP	-	-	0,005mg/1ml	-
COP	-	-	0,002mg/1ml	-
COP	-	-	0,001mg/1ml	-
COP	-	-	-	1mg/0,5ml
<hr/>				
PC	-	-	0,02mg/1ml	0,01mg/0,5ml
PC	-	-	0,004mg/1ml	0,002mg/0,5ml
<hr/>				
PC	30 min	-	0,005mg/1ml	-
PC	30 min	-	0,02mg/1ml	0,01mg/0,5ml
PC	30 min	-	0,004mg/1ml	0,002mg/0,5ml
PC	-	30 min	0,005mg/1ml	-
PC	-	30 min	0,02mg/1ml	0,01mg/0,5ml
PC	-	30 min	0,004mg/1ml	0,002mg/0,5ml
<hr/>				
COP	30 min	-	0,005mg/1ml	-
COP	30 min	-	0,02mg/1ml	0,01mg/0,5ml
COP	30 min	-	0,004mg/1ml	0,002mg/0,5ml
COP	-	30 min	0,005mg/1ml	-
COP	-	30 min	0,02mg/1ml	0,01mg/0,5ml
COP	-	30 min	0,004mg/1m	0,002mg/0,5ml
<hr/>				
PC	-	1 min	0,02mg/1ml	0,01mg/0,5ml
PC	-	2 min	0,02mg/1ml	0,01mg/0,5ml
PC	-	5 min	0,02mg/1ml	0,01mg/0,5ml
PC	-	10 min	0,02mg/1ml	0,01mg/0,5ml
PC	-	15 min	0,02mg/1ml	0,01mg/0,5ml
PC	-	30 min	0,02mg/1ml	0,01mg/0,5ml

Indeed, the UV-ozone treatment resulted in an improved adhesion of coating solutions. Finally, a UV-ozone treatment time of 5 min (Pryzhkova *et al.*, 2014) and a laminin-1/fibronectin mixed coating solution of 0,02mg/1ml (laminin-1) + 0,01mg/0,5ml (fibronectin) was considered as working concentration, since it reflected the best conditions for cell attachment.

3.1.7.4 Schematic visualization of a neural tube in the microchannel

The illustration in Figure 17a (Front view) and Figure 17c (side view) shows the vision of a zebrafish neural tube in a 3D microchannel. The microchannel is modified in size (60µm width, 100µm depth) and shape (tubular) to mimic the dimensions of a zebrafish neural tube (Fig.17b). One characteristic feature of neural tube formation is the establishment of a solid lumen and apical/basal polarity, whereas the apical side is located towards the lumen and the outer basal side (yellow) is connected to the ECM (e.g. Araya *et al.*, 2016). As described in the previous paragraph, a coating with basal proteins (pink) – laminin-1/fibronectin – determines the basal side for the cells.

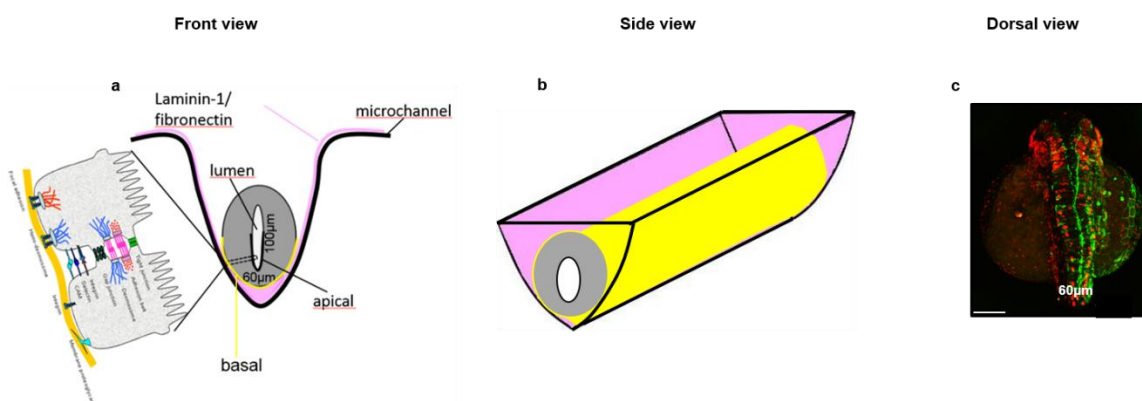


Figure 17: Vision of the establishment of a neural tube inside the microchannel. The scheme of a microchannel, coated with the basal proteins laminin-1/fibronectin is shown in Front View (a) and Side View (b). The microchannel was designed in the dimensions of a zebrafish neural tube (c), also supporting formation of the tubular structure. Pink = coating, yellow = basal side.

3.1.8 Control of neurogenesis in a 3D microchannel

Since cell behavior in 2D is artificial, I investigated if there is a difference in neuronal differentiation in 3D compared to 2D. Can I enrich a NPC population by defined NI treatment as well?

I seeded neurog1:RFP primary cells in the microchannel and treated them with 1µM NI. Cells were cultivated for 48h.

Confocal images of NI treated cells (Fig.18b,b`) showed clearly more neurog1:RFP positive cells compared to control cells (Fig.18a,a`). Neurog1:RFP positive nuclei were quantified with the Bitplane Imaris Software and evaluated in relation to total nuclei (Fig.19,20b).

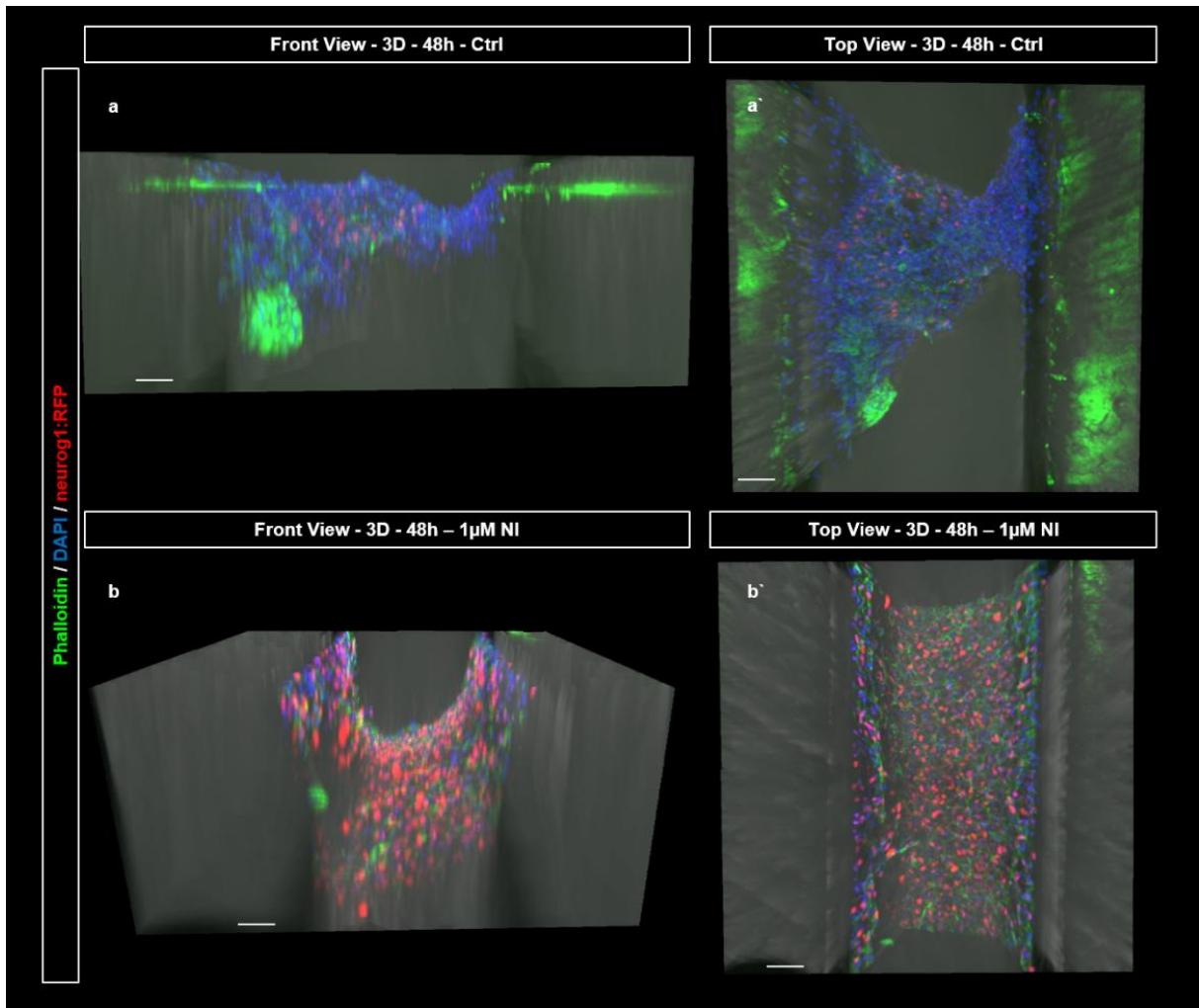


Figure 18: Control of Neurogenesis in 3D. Front View (a) and Top View (a`) of ctrl neurog1:RFP cells treated with DMSO and NI treated neurog1:RFP cells (b, b`). Cells were stained for nuclei (DAPI, blue) and actin (Phalloidin, green). Pos. neurog1:RFP nuclei show a red color.. Channel width = 300 μ M at the top, 100 μ m at the bottom. One experiment was performed (quantification is shown in Fig.20b). Scale bar = 100 μ M.

Fig.19 illustrates the relation of neurog1:PFP nuclei to total nuclei of the 2D and 3D experiment in confocal pictures (19a,b,c,d) and schematic nuclei analysis (19a`,b`,b``,c`,d`,d``; detected with the Bitplane Imaris Software).

Statistics of the NI *in vivo* and *in vitro* experiments are compared and shown in Fig.20.

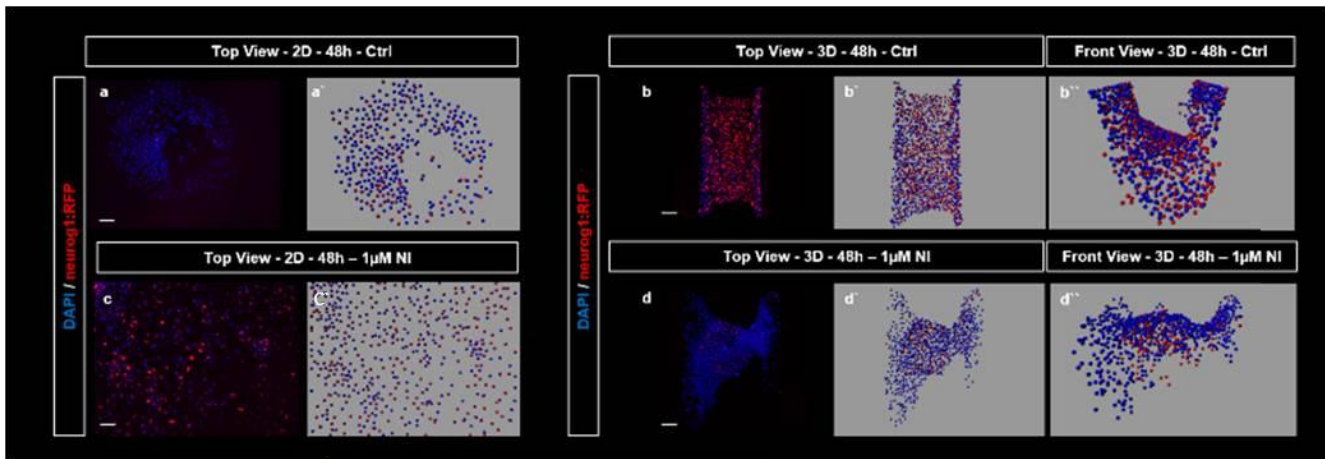


Figure 19: Acquisition of neurog1:RFP pos. nuclei in 2D vs. 3D. Confocal (a,b,c,d) visualization and schematic acquisition (a',b',b'',c',d',d'') of neurog1:RFP ctrl cells cultivated in 2D (a,a') and 3D (b,b',b''). NI treated cells are shown in 2D (c,c') and 3D (d,d',d''). Staining is shown for nuclei (DAPI, blue). Pos. neurog1:RFP nuclei are visualized in red. (For statistics see Fig.20). Scale bar = 50µm.

3.1.9 Comparison of *in vitro* altered neurogenesis to the *in vivo* scenario

In this part of the thesis a comparative study was performed, investigating neuronal differentiation *in vivo* and in a 2D and 3D zebrafish primary cell culture.

In the *in vivo* experiment, a NI treatment with 40mM from 2cell-24hpf enhanced the NSC population as it was indicated by a stronger *neurog1* expression in dorsal Telencephalon, Diencephalon and spinal cord. Additionally, a broader spinal cord of the NI treated embryo was observed compared to control (as it was shown in the *in situ hybridization*; Fig.10). Moreover, an increase in the average number of RB sensory neurons expressing neurog1:RFP in the nuclei (Fig.11) from 52,8 for control embryos to 68,6 RB sensory neurons for NI treated embryos was observed meaning a 1,3 fold increase (Fig.20c). Significance was determined as n.s. (= not significant) with the Student's T-Test.

In the 2D *in vitro* experiment, 87,5% neurog1:RFP positive and 12,5% neurog1:RFP negative nuclei were counted from NI treated cells. 32,7% neurog1:RFP positive nuclei and 67,3% neurog1:RFP negative nuclei were detected from control cells; (Fig.20a), displaying a 2,7 fold increase of neurog1:RFP positive nuclei. However, when neurog1:RFP positive control cells were compared to neurog1:RFP positive NI treated cells, the increase was detected as n.s. (= not significant, determined with the Student's T-Test).

In 3D I quantified 73,0% neurog1:RFP positive and 27,0% neurog1:RFP negative nuclei from NI treated cells and 29,1% neurog1:RFP positive and 70,9 % neurog1:RFP negative nuclei from control cells, which resulted in an 2,5 fold increase of neurog1:RFP positive nuclei (Fig.20b).

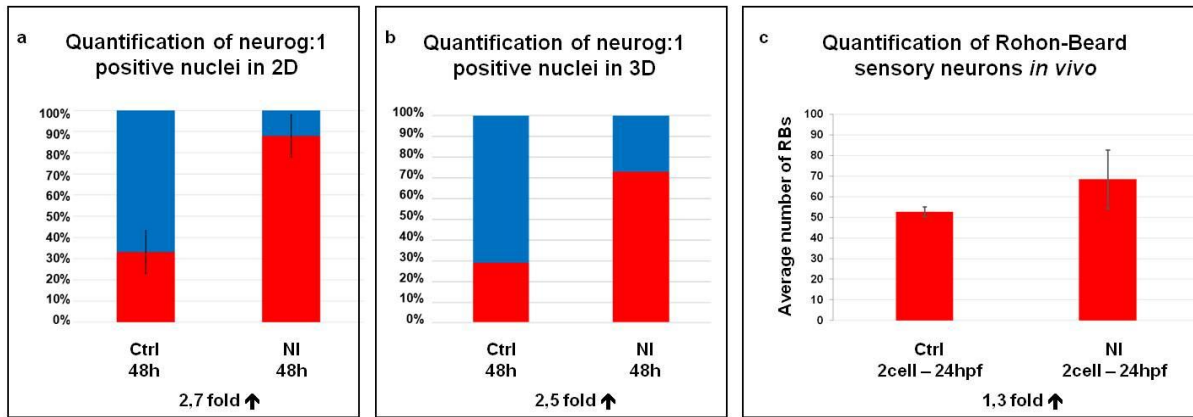


Figure 20: Quantification of neurog1:RFP pos. nuclei of the 2D (a) and 3D (b) *in vitro* experiment and RB sensory neurons expressing neurog1 *in vivo*. Graphs in (a) show the quantification of the NI 2D *in vitro* experiment shown in Fig.13, graphs in (b) show the NI 3D *in vitro* experiment performed in Fig.18 and graphs in (c) visualize the NI RB sensory neurons *in vivo* experiment shown in Fig. 11. Percentage of neurog1:RFP pos. nuclei (red) and neurog1:RFP neg. nuclei (blue) from control and NI treated cells (a,b) were evaluated and normalized to the total number of cells. Results from (a) and (b) were compared to the average number of RB sensory neurons expressing neurog1:RFP from control and NI treated embryos (c). Data shown in (a) represent an average from 3 independent experiments with the indicated standard deviations (neurog1:RFP pos. ctrl cells were compared to neurog1:RFP pos. NI treated cells; n.s. = not significant, statistical significance was determined by using the student's t-test). Data shown in (b) represent one experiment (significance was not determined). Results in (c) represent an average of 11 control and 5 NI treated embryos (analysis was performed from a constant area of the spinal cord) with the indicated standard deviations (n.s. = not significant; statistical significance was determined by using the student's t-test).

Although a neural tube could not be generated, the NSC population was enriched by defined NI treatment. Thus, the established 3D CCS resembles most the *in vivo* scenario, reflects better the dynamics of neurogenesis *in vivo* and is well controllable.

For the establishment of a complex neural tube and moreover its patterning, precise tissue organization, depending on the generation of a sharp interface of neighboring compartments is crucial. At specific borders it regulates the organization of key signaling centers like the mid-diencephalic organizer and the midbrain-hindbrain boundary. At a later stage of boundary formation, cell intermingling is prevented between two adjacent subdivisions (Kiecker and Lumsden, 2005; Xu and Wilkinson, 2013).

In vitro studies investigating boundary formation are rare, but would be suitable to clarify signaling events during boundary formation.

3.2 Guided Cell Attachment

The following part of my thesis was performed in collaboration with A. Hirschbiel and C. Barner-Kowollik (Institute for technical chemistry and polymer chemistry, KIT). The functionalized wave pattern was produced by A. Hirschbiel and C. Barner-Kowollik. Testing of eGFP capability was performed together with A. Hirschbiel. ToF-SIMS measurements were performed by A. Welle (Institute of Functional Interfaces, KIT). The thermoforming of the PC film was carried out by P. Nikolov and S. Giselbrecht (Institute for Biological Interfaces, KIT; MERLN Institute for Technology-Inspired Regenerative Medicine, Maastricht University). B. Yameen (Harvard Medical School, Boston, MA, USA) and G. Delaittre (Institute of Toxicology and Genetics, KIT) are thanked for discussion. Parts of this chapter were reproduced with permission from Hirschbiel, A. F.; Yameen, B., Welle, A.; Nikolov, P.; Giselbrecht, S.; Scholpp, S.; Delaittre, G.; Barner-Kowollik, C.; *Adv. Mater.* 2015, 27, 2621-2626 (DOI: 10.1002/adma.201500426). Copyright 2015 Wiley.

The generation of boundaries *in vitro* depicts an advantageous approach regarding the investigation of neural cells and networks and moreover to study co-cultivation and intercellular communication. In an organism, boundaries are formed e.g. between to compartments, preventing the migration of cells from one compartment to the other. This cell separation is important for regionalizing the brain. Therefore, boundaries are generated e.g. in brain organizing centers; the zona limitans intrathalamica (ZLI) and the midbrain hindbrain boundary (MHB). The MHB e.g. separates the midbrain from the hindbrain (Kiecker and Lumsden, 2005).

In these days guided cell attachment is a well-established and common method to analyze the behavior of cells in a distinct environment (e.g. Jung *et al.*, 2008).

Patterning of a cell repellent polymer, characterized by a cell repellent and a cell attractant area, displays an effective way to guide cells into a specific area of interest on a solid substrate. This approach depicted a basic step for the investigation of boundary formation *in vitro*.

Therefore, we investigated cellular guidance to a functionalized wave pattern (area of interest). Our collaboration partners developed a process to functionalize a thin PC film into a resolved surface spatially by UV irradiation and subsequent passivation with poly oligo(ethylene glycol) methyl ether methacrylate (MeOEGMA).

3.2.1 Synthetic strategy for the development of a functionalized wave pattern by Astrid Hirschbiel

By combination of photopatterning via *o*-nitrobenzyl-mediated cleavage – and reversible-deactivation radical polymerization micropatterns of an oligo(ethylene glycol) (OEG) derivative and carboxylic acid moieties were generated. OEG is an effective biopassivating/antifouling compound and a useful to avoid non-specific protein/biomolecule adsorption (Cheng and Cao, 2010; Rodriguez-Emmenegger *et al.*, 2013). Moreover carboxylic acid functional groups on the polycarbonate film improve adhesion of proteins and cells on the surface (Lee *et al.*, 1994).

3.2.2 Testing of adhesion capability of the functionalized wave pattern

3.2.2.1 Protein adhesion

First of all, protein adhesion was tested by treatment with fetal calf serum (FCS) (Fig. 21b). FCS consists of various proteins and is often used as a highly fouling complex biological fluid to test surface resistance to biofouling. FCS attached exclusively in the non-passivated pattern (irradiated area). A strong ToF-SIMS signal was given by the FCS layer for the CN- and CNO- fragments, reproducing the distinct wave-shaped pattern of the photomask (measurement by Alexander Welle).

3.2.2.2 eGFP adhesion

Moreover the affinity of enhanced green fluorescent protein (eGFP) was proven by measuring the fluorescent intensity inside the irradiated area and next to it. Fig.21c shows the bright field and fluorescence image of a film after treatment with an eGFP solution. Straight through an area of about one millimeter the fluorescent intensity was measured (Fig.21d). This particular surface was previously partly irradiated before SI-ATRP (e.g., patterned –white arrows in Fig. 21c, bottom) and compared to that of a non- irradiated zone on the same film. We recognized that eGFP favors the wave pattern, whereas the non-irradiated area showed significantly less fluorescent protein adsorption (Fig.21c). A quantitative evaluation of the fluorescence intensity (min = 0; max = 256) shows an average fluorescence value of 90.40 ± 5.61 (mean \pm S.E.M.) in the irradiated area compared to the non-irradiated control surface with an intensity of 59.80 ± 5.12 (Fig. 28d).

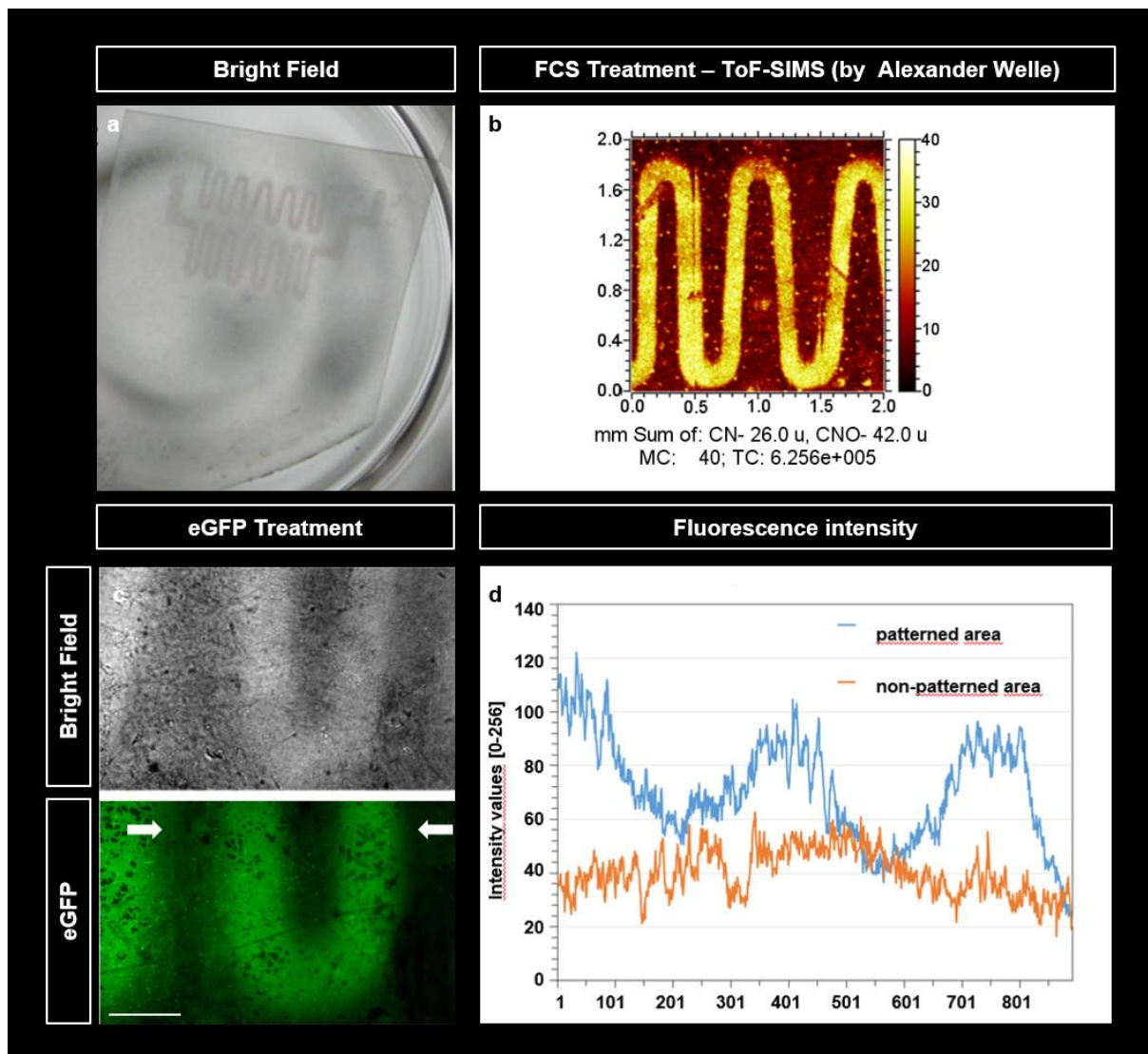


Figure 21: Testing of adhesion capability of the functionalized wave pattern. BF image of the polycarbonate film clearly showing the irradiated area **(a)**. ToF-SIMS map of the CN – and CNO – signals of FCS **(b)**. eGFP attachment to the wave pattern **(c)**. Fluorescence intensity of eGFP in the patterned area compared to the non-patterned area. The intensity shown in **(d)** is based on an average of 5 measurements. Scale bar = 200 μ m. Reprinted and modified from *Hirschbiel and Geyer et al., 2015*.

3.2.3 Cellular guidance in 2D

Further on, we confirmed our strategy regarding guided cell adhesion by cultivating cells from a solid zebrafish fibroblast line (PAC2) on the polymer films. Such a cell line was already applied for cell chip experiments (Efremov *et al.*, 2013). PAC2 fibroblasts cells were seeded on the PC film, cultivated for 24 h and stained with markers for cell nuclei (DAPI) and actin cytoskeleton (Phalloidin). We noticed that fibroblasts attached mainly to the irradiated areas, thus respecting the pattern.

The cells avoided the non-irradiated areas (Fig.22a-c). The density of cells (Fig.22d) was evaluated by quantification of cell nuclei (DAPI), whereas the actin cytoskeleton (Phalloidin) reflects the surface area covered by cells (Fig.22e). Quantification of the cell density strikingly evidenced a significant increase of nuclei on the irradiated areas, with $0.0004 \text{ cells } \mu\text{m}^{-2}$ (blue bar) compared to the non- irradiated surface, where we saw a density of only $0.0001 \text{ cells } \mu\text{m}^{-2}$ (red bar). Moreover we observed that cells attached to the irradiated surface differed in their morphology from the few cells adhering next to the pattern (Fig.22c). Whereas the cells on the passivated surface show a small round morphology, fibroblasts on the non passivated surface display a flatter shape. By pseudo-coloring this phenomenon was highlighted (Fig.22c). Quantification of the surface coverage (Fig.22e) indicated that $70.3 \pm 6.3\%$ (mean \pm SEM) of the non- irradiated surface was covered with cells compared to $15.1 \pm 4.9\%$ of the passivated surface. In general, we observed that the cells cover a much larger area in the non- passivated areas of the substrate. For the determination of the significance of difference between the data sets, a Student's T-Test was used and a p -value of $p < 0.0001$ (***) was calculated.

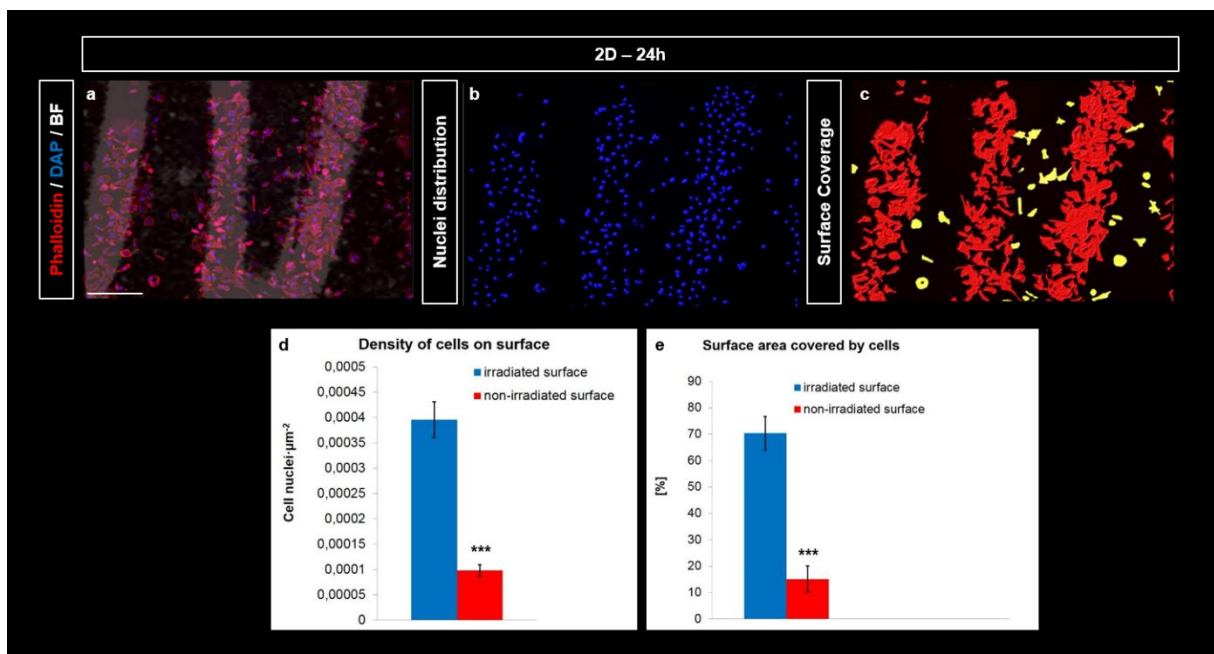


Figure 22: Attachment of PAC2 fibroblast cells to a surface patterned polycarbonate film. a) PAC2 fibroblast cells, stained with nuclei marker (DAPI), actin cytoskeleton (Phalloidin) and merged with the corresponding bright field picture. **b)** Quantification of the cell distribution, by surface rendering of the nuclear DAPI signal and localization of cell nuclei. **c)** Pseudo coloring of the cells: irradiated area (red) and non-irradiated area (yellow). **D)** Density of cells on the surface: irradiated area (blue) and non-irradiated area (red). **e)** Percentage of surface covered by cells: irradiated area (blue) and non-irradiated area (red). The cells were stained and measured after 24 h. Data represent an average from 3 independent experiments performed in triplicates with the indicated standard deviations (***) $p < 0.0001$, statistical significance was determined by using the student's t-test). Scale bar = : $200 \mu\text{m}$. Reprinted and modified from *Hirschbiel and Geyer et al., 2015*.

The cell division rate for PAC2 fibroblasts in culture may be too slow to explain the observed cellular distribution. Hence, we suggest that fibroblasts migrate from the non-irradiated surface onto the irradiated surface supported by cellular shape analysis.

3.2.4 Cellular guidance in 3D

Moreover we investigated guided cell adhesion of zebrafish PAC2 fibroblasts in a three dimensional microchannel (Figure 23). A combination of the above-mentioned SMART process and photolithographic patterning was applied to generate a non-irradiated (cell repellent) stripe in a 3D microchannel (Fig.23a). This novel platform enables the generation of a cell attractant/cell repellent 3D surface, inducible by light. PAC2 fibroblasts were seeded in a non-patterned control channel (Fig.23b), in which we found an all-over coverage of the channel surface by fibroblasts after 5 days. On the contrary, fibroblasts which were cultivated similarly in a patterned microchannel were almost exclusively found in the irradiated areas and avoided the non-irradiated zone, demonstrating the effectiveness of our photolithographic method in combination with thermoforming to produce discrete cell-populated zones inside a single 3D microchannel (Fig.23c).

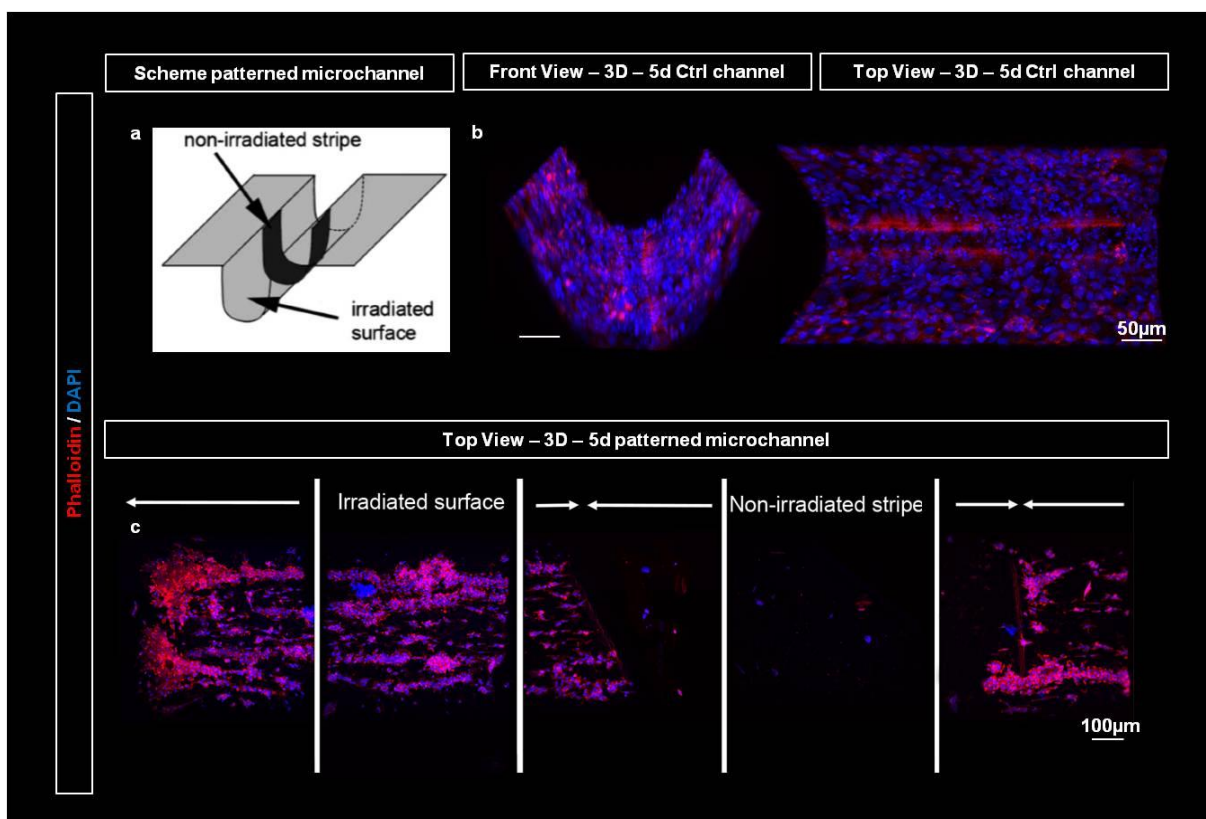


Figure 23: Attachment of PAC2 fibroblast cells to a surface patterned 3D polycarbonate microchannel. Scheme of a thermoformed 3D microchannel with an irradiated surface interrupted by a non-irradiated zone (a). Front view and top view of an untreated microchannel (ctrl) with PAC2 fibroblast cells stained with DAPI and Phalloidin (b). Top view overview of PAC2 cells in the patterned microchannel (c). Data represent one experiment (statistical significance was not determined). Channel width = 600 µm. The cells were cultivated in both cases for 5 d.

Thus, by employing a mild UV lithographic patterning approach we have developed a facile methodology to pattern cells onto a flexible polymer substrate. Further, we evidenced that specific areas of our polymeric substrate can be opened for biological impact, including strongly fouling sera such as FCS or eGFP. The introduced methodology is to date the only avenue for cell guiding on a thin, thermoformable polycarbonate substrate making use of a simple photochemical approach. This work paves the way for a patterned surface functionalization of thermoformed microstructures which could serve as a base for applications ranging from simple patterned cell culture systems to advanced tissue culture systems in 3D.

This work represents a first step towards the investigation of boundary formation *in vitro*. One cell population can already be cultivated in an area of interest. If further on cultivation of two distinct cell populations next to each other would be possible, like it is the case during boundary formation, e.g. investigation of the compartmentalization at the MHB of the neural tube would be possible.

Moreover, for neural tube formation coordinated movements of many cells in both time and space are crucial and regulated by an appropriate communication of cells. In general, intercellular interactions determine cell fate and have been shown to be dependent on the cell microenvironment, influenced by altered clustering of membrane receptors in 2D compared to 3D.

3.3 Cellular signaling

Intercellular interactions by cell adhesion molecules and membrane receptors have been shown to be different in 2D compared to 3D and result in altered cellular signaling and gene expression (Schwartz and Chen 2013; Knight and Przyborski, 2014) and thus are crucial in determining cell fate. However, how these interactions on pathways influence human embryonic stem cell (hESC) behavior is still poorly understood. 3D culture of hESCs affects cell fates, including self-renewal and differentiation to a variety of lineages. Therefore, alteration of cell-cell contact on canonical Wnt/ β -catenin signaling in hESCs in a microwell array producing 3D colonies was investigated. In the 3D microwell culture, a higher E-cadherin expression, ongoing with a Wnt downregulation, was observed in comparison to cultivation on 2D substrates. However, EBs grown in microwell cultures displayed higher Wnt signaling (despite the reduction) than EBs from hESCs cultured on 2D substrates. Moreover, in Wnt upregulated cells, an upregulation of genes connected to cardiogenesis was shown in EBs (Azarin *et al.*, 2012).

Thus, I performed a Co-culture assay with zfWnt8aORF-GFP-pCS2+ (an important player in patterning the neuroectoderm) and Tg(7xTCF-Xla.Siam:nlsCherry) in 2D and the 3D microchannel to investigate if I observe changes in cellular signaling, indicated by altered Wnt reporter activation.

3.3.1 Comparison of Wnt reporter activation in 2D compared to 3D

HEK293T cells were transfected with Wnt8a-GFP and Tcfmcherry/HisCFP (co-transfected). After 24h of cultivation the cells were co-cultured in 2D (Fig.24a; Top View) and 3D (Fig.24 b; Front View) for another 24h. Additionally, Tcfmcherry/HisCFP co-transfected cells were cultivated alone to serve as control. Cells were visualized by Confocal imaging.

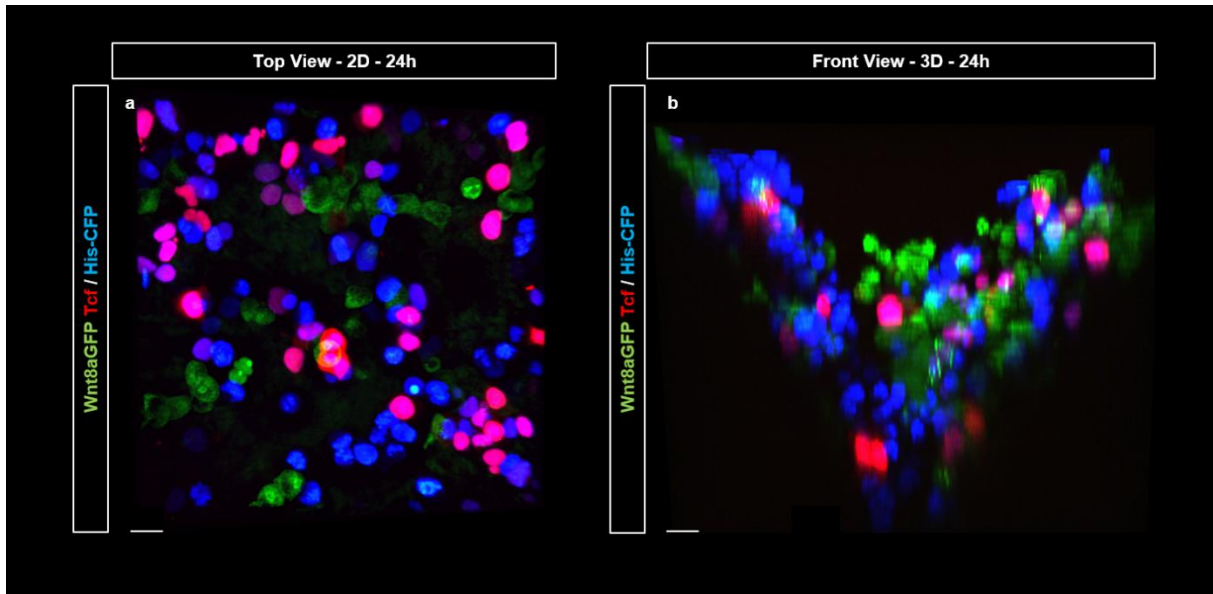


Figure 24: Co-cultivation of Wnt8a-GFP and TcfmCherry/His-CFP transfected HEK293T cells in 2D and 3D. 2D (a; Top View), and 3D (b; Front View) Co-culture of HEK293T cells visualized by Confocal imaging after 24h. Wnt8a=green, TcfmCherry=red, His-CFP=blue. Channel width 175µm at the top, 60µm at the bottom. Scale bar = 20 µm.

Thereby the Wnt reporter activation (Fig.25e) and the Tcf intensity mean (Fig.25f) were analyzed and compared between 2D vs. 3D and moreover between TcfmCherry/His-CFP and Wnt8a-GFP co-cultured cells with TcfmCherry/His-CFP (control). The Wnt reporter activation was visualized by Confocal images (Fig.25a,b,c,d) and analyzed with the Bitplane Imaris Software. Nuclei of cells expressing TcfmCherry are shown in red, whereas His-CFP nuclei are shown in blue (Fig.25b`,b```,c`,d`,d```).

Quantification of activated Tcf nuclei (Fig.25e) showed a 26,1% activation in 2D and a 13% activation in 3D (controls). Analysis from the co-cultivation resulted in 56% activation in 2D and 44,7% activation in 3D. Hence, co-cultivation resulted in a significantly higher Wnt reporter activation (* $p < 0,05$). Furthermore, cultivation in 3D showed a lower Wnt reporter activation compared to 2D, both in the TcfmCherry/His-CFP culture (control) and the Co-culture with Wnt8a.

The evaluation of the Tcf Intensity Mean (Fig.25f) showed clearly an increase in the 2D Co-culture compared to control (* $p < 0,05$) and 3D Co-culture compared to control (* $p < 0,05$). When TcfmCherry/His-CFP cells were cultured alone, they showed an intensity mean of 9,4% in 2D and 7,2% in 3D. In the 2D Co-culture, 68,7% Tcf intensity was observed compared to 46,6% in the 3D Co-culture (* $p < 0,05$).

Thus, Wnt reporter activation and the Tcf intensity mean were clearly higher in the co-culture than in TcfmCherry/HisCFP cultured alone.

Significance of the data sets was determined with a Student's T-Test and a p-value of $p < 0.05$ (*) was calculated.

Moreover, Wnt reporter activation and Tcf intensity mean were higher in 2D than in 3D, in the co-culture and in TcfmCherry/HisCFP cultured cells. Thus, cellular signaling is higher in 2D than in 3D.

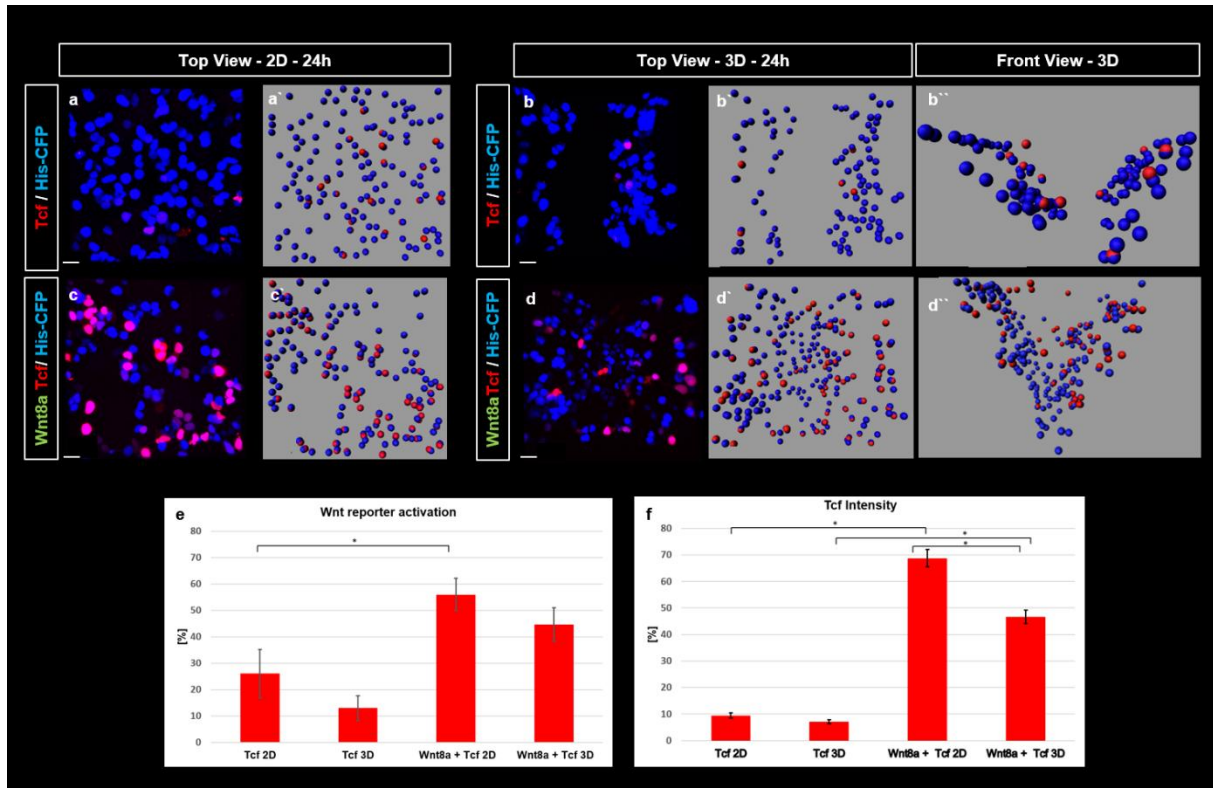


Figure 25: Analysis of Wnt reporter activation and Tcf Intensity-Mean. Confocal (a,b,c,d) and schematic analysis (a',b',b'',c',d',d'') pictures of Tcf/His-CFP cells cultivated in 2D (a,a') and in 3D (b,b',b''). Wnt8a and TcfmCherry/His-CFP transfected cells were co-cultured in 2D (b,b',b'') and 3D (d,d',d''). Wnt8a=green, TcfmCherry=red, His-CFP=blue. Wnt reporter activation (e) and Tcf Intensity-Mean (f) were quantified. Scale bar: 20µm. Data represent an average from three independent experiments performed in triplicates with the indicated standard deviations (* $p < 0.05$, statistical significance was determined by using the student's *t*-test).

Summary

In this thesis I investigated the formation of a neural tube in a 3D microchannel, thereby establishing a novel three-dimensional biofunctional cell culture system. This platform was used to study all the steps involved in the process of neurogenesis, focusing in particular on guided cell attachment and cellular signaling.

Although it could not be possible to mimic all the stages of neural tube *in vitro*, it was possible to enrich pluripotent zebrafish blastula- derived cells towards a NSC population by defined NI treatment. In my work, I could show for the first time that the established 3D CCS resembles most the *in vivo* scenario and reflects the dynamics of neurogenesis in an embryo, as shown by the comparison of neuronal differentiation in the zebrafish embryo and in a 2D and 3D zebrafish primary cell culture. Moreover, since it is not possible to study and dissect a single pathway *in vivo*, the big advantage of the 3D CCS is that it is well controllable. This will allow us to study singularly the effect of each molecule involved in the process of neurogenesis.

Furthermore, guided cell attachment on a polymer substrate was investigated in 2D and 3D. A cell attractant/cell repellent platform was generated, inducible by light, by combination of photolithographic patterning (Christopher Barner-Kowollik, Astrid Hirschbiel) and the formation of a polycarbonate microchannel by SMART (Stefan Giselbrecht, Pavel Nikolov). Thus, we created a functionalized surface, to which we can attach a particular protein or guide cells to this region of interest. The non-functionalized surface had a cell-repellent effect. Thus we could guide cells to a specific region of interest. This platform can now be used as tool for biological applications, e.g. cell-cell communication, with the long-term regard to investigate boundary formation. Boundary formation was shown to be very important during embryonic development, since e.g. it's important for the compartmentalization of the different brain parts – forebrain, midbrain and hindbrain (Kiecker and Lumsden, 2005; Rhinn *et al.*, 2005).

Moreover, it has been shown that cells in a 3D cell culture mimic the *in vivo* environment more realistic than 2D cells, which display an artificial environment. In 2D cells grow as flat monolayer, whereas in 3D cells are shaped in a spherical or tubular form. Thus, cell adhesion proteins and membrane receptor arrangement differs drastically between 2D and 3D cells, which leads to changes in signaling and finally gene expression (Schwartz and Chen 2013; Knight and Przyborski, 2014).

Thus, in the last part of my thesis I investigated in a co-culture approach differences in cellular signaling between 2D and 3D cell culture. When I analyzed the effect of Wnt releasing cells on reporter cells, I could indeed observe that Wnt reporter activation and Tcf

intensity mean showed higher values compared to the control. Moreover, Wnt reporter activation has been shown to be higher in 2D compared to 3D in the co-culture.

Thus, this cell culture approach shows that also for Wnt the cellular signaling is higher in 2D compared to 3D, underlying the importance of mimicking a more physiological environment for cells when studying signaling pathways, as it has been shown for surface stiffness (Dupont *et al.*, 2011).

4. Discussion

The establishment of the central nervous system (CNS) represents a complex process during embryonic development and has been extensively studied mainly in mammalian, avian and non-amniote vertebrates (Schoenwolf and Smith, 2000; Colas and Schoenwolf, 2001). During patterning of complex tissue like the CNS, a tremendous number of cells have to arrange themselves in a spatially and temporally precise way. Thereby cells have to rapidly change their features, due to distinct requirements during proceeding development (e.g. maturation into a neuron from a neural precursor cell). However, the machinery generating neural tissue architectures is still far from being completely understood (Karus *et al.*, 2014).

The zebrafish is a suitable model to study the development of the CNS in its entirety, due to the transparency of the zebrafish embryo and the fact that the CNS is generated in 48hpf. However, due to the complexity of neurogenesis *in vivo* the detailed elucidation of particular steps is hindered due to the many diverse interactions of influencing factors, including the interplay of signals derived from the mesoderm. Therefore, a simplified three-dimensional cell culture platform was established to investigate neural differentiation in a controlled manner.

The dynamic of gene expression we studied *in vivo* was taken in account to gauge the controllability of neurogenesis in 3D cell culture to the *in vivo* scenario.

Neurogenesis is regulated by a gene cascade, mediating the differentiation from embryonic stem cells (ESCs) and moreover self-renew to maintain the stem cell pool. Neural stem cells (NSCs) further on differentiate into neural progenitor cells (NPCs) and some of the NSCs self-renew and reside in the stem cell pool as well. NPCs finally differentiate into postmitotic neurons (Fig.26). One important gene in this cascade is *neurogenin1* (*neurog1*). *Neurog1* acts early in this gene cascade by determining which cells of the NSCs will be NPCs and differentiate further into postmitotic neurons. The proneural gene *neurog1* has been shown to act as an activator of neurogenesis (Korzh and Straehle, 2002; Blader *et al.*, 2004) and inhibitor of gliogenesis (Yuan and Hassan, 2014). *Neurog1* is expressed in primary neurons and *neurog1* misexpression leads to ectopic neuron formation in non-neural ectoderm (Kim *et al.*, 1997). Moreover, *neurog1* is crucial for the formation of Rohon-Beard (RB) sensory neurons, and misexpression of *neurog1* results in a loss of Rohon-Beard sensory neurons (Cornell and Eisen, 2002).

4.1 Neurog1 reflects the dynamics of neurogenesis

My qPCR data showed that *neurog1* was slightly detectable at sphere stage, but increased rapidly until 10 somite stage, resulting in a maximal expression at 24hpf, followed by a rapid decrease until 48hpf. Thus, *neurog1* reflects the dynamics of neurogenesis and was used as an indicator for proneural fate in this thesis.

Following the analysis of neurogenesis dynamics in the *in vivo* situation, I investigated if I can modulate and thereby control neurogenesis by forcing ectoderm formation. In the embryo, the dorsal ectoderm receives inductive signals from the adjacent mesoderm. Ectodermal cells respond to inducing signals, adopt a neural fate and form the neural plate, which gives rise to the neural tube. The remaining ectoderm develops into skin (epidermis) and derivatives.

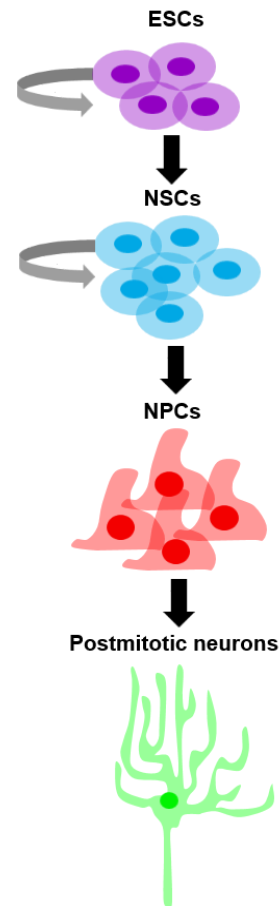


Figure 26: Neuronal differentiation.

During embryonic development, ESCs self-renew and differentiate into NSCs. NSCs renew themselves and further on differentiate into NPCs, which finally differentiate into postmitotic neurons.

Genetically, the formation of the germ layers ectoderm, mesoderm and endoderm, is regulated by nodal signaling (Hagos and Dougan, 2007). To this aim a Nodal Inhibitor was used.

4.2 Nodal signaling initiates and patterns mesendoderm formation

In all vertebrates the nodal-related subclass of the TGF- β superfamily initiates and patterns mesoderm and endoderm. In the zebrafish, these nodal-related genes are called *nodal-related1* (*ndr1*) - previously known as *squint* (*sqt*) and *nodal-related2* (*ndr2*) – previously named *cyclops* (*cyc*).

Since my aim was to force ectoderm formation, which partly adopts a neural fate to generate the CNS, I prevented mesoderm formation in the zebrafish embryo by pharmacological inhibition of nodal signaling mediated by treatment with the SB431542 Nodal Inhibitor (NI). The NI blocks the activin-like kinase (ALK) 4,5 and 7 receptors of the nodal signaling pathway, which in turn prevents phosphorylation of downstream effectors Smad 2 and 3 (Callahan *et al.*, 2002; Inmann *et al.*, 2002). Hence, mesendoderm formation is inhibited (Sun *et al.*, 2006; Hagos and Dougan, 2007; Lippmann *et al.*, 2014) and solely ectoderm is generated which will give rise to epidermis and neural tissue.

By NI treatment of zebrafish embryos it has been shown that the formation of structures derived from mesendoderm - like somites, notochord, blood, heart and Kupffer's vesicle - was prevented and moreover embryos displayed cyclopia, mimicking the severe phenotype of the *ndr1/ndr2* double mutant (Hagos and Dougan, 2007).

In my *in vivo* experiment, in which zebrafish embryos were treated with the NI, I observed the same effects of mesendoderm inhibition resulting in this severe phenotype.

The NI has been applied in several studies to inhibit mesendoderm formation. However, the concentration which was used varied. A NI concentration of 50 μ M failed to mimic the *ndr1/ndr2* double mutant phenotype (Sun *et al.*, 2006). A much higher dose of 800 μ M and additional perforation of the embryos at the margin guaranteed complete penetration of the NI into the embryos, resulting in a *ndr1/ndr2* double mutant phenotype, thus completely blocking nodal signaling. Moreover, it has been shown that anterior trunk spinal cord was lost in double *ndr1/ndr2* mutants but more anterior and posterior neural fates were present. Nodal signaling has been suggested to mediate the generation of trunk and antagonizes anterior fates. Therefore, nodal signaling might act through an intermediary posteriorizing signal to initiate trunk spinal cord. Posteriorizing signals are located at the lateral margin, and the posteriorizing influence might be due to absent nodal signaling (Feldmann *et al.*, 2000).

Lower concentrations showed a more mild phenotype similar to *teratocarcinoma-derived growth factor 1* (*tdgf1*; previously known as one-eyed pinhead; Hagos and Dougan, 2007).

The milder phenotype was also observed by treating cleavage stage embryos with 50 μ M NI (Sun *et al.*, 2006).

In my study, I tested higher concentrations of the NI; 20mM and 40mM, since NI treatment was performed through the chorion.

Moreover, it has been shown that the time in which embryos are exposed to the NI is playing an important role. In the embryo, nodal signaling acts in a time window from mid-to-late blastula stages. Thus, specification of cell fates along the animal-vegetal axis by nodal signaling occurs in a time-dependent way. When nodal signaling was blocked at a later time point (after mid-to-late blastula stages) just the specification of margin-derived cell types was inhibited, whereas animal-region derived cell types specified. Thus, cell fate also depends on how long cells receive nodal signals and a uniform nodal dose results in more marginal cell fates (Hagos and Dougan,2007).

In my *in vivo* experiment, zebrafish embryos were treated with the NI from 2-cell stage until 24hpf and from 2-cell stage until 48hpf. In my qPCR data it was shown that the highest *neurog1* expression was detected at 24hpf with a rapid decrease until 48hpf (due to differentiation of NPCs into mature neurons). Therefore, I analyzed the effect of the NI on neurogenesis on these stages by *neurog1 in situ hybridization*.

4.3 By inhibition of nodal signaling the neural progenitor cell population is increased *in vivo*

With a working concentration of 40mM and a treatment time from the 2-cell stage until 24hpf not only mesendoderm formation was inhibited. Loss of derivatives of mesoderm and endoderm as well as cyclopia were recognizable with a working concentration of 40mM NI and treatment from 2-cell until 24hpf, comparable to the severe *ndr1/ndr2* double mutant phenotype described by Hagos and Dougan. Ectoderm and future neuroectoderm formation was enhanced, reflected by a stronger *neurog1* expression in the dorsal telencephalon, diencephalon and spinal cord compared to the control embryo (DMSO treated). Additionally, the spinal cord of the treated embryo (Fig.10c`) was obviously wider than the spinal cord of the control embryo (Fig.10a`). Since the cut out spinal cord parts (cut surface indicated by black lines in the whole mount embryos; Fig.10a,b,c) are shown in the dorsal view under a cover slip (Fig.10a`,b`.c`), this might have minimally changed the shape of the spinal cord pieces.

Thus, in my experiment it was shown that by inhibition of nodal signaling the NPC population is increased *in vivo*.

Treatment with NI concentrations of 20mM and 40mM from the 2-cell stage until 48hpf resulted in massive malformation of the embryos, indicated by an immense shortened and tilted body axis and a clumpy head and seemed to have a toxic effect on the embryos.

Furthermore, since *neurog1* has been shown to be crucial for the formation of RB sensory neurons I treated transgenic *neurog1:GFP* zebrafish embryos with 40mM NI from the 2cell stage until 24hpf. An 1,3 fold increase in the average number of RB sensory neurons was observed (Fig.11).

Thus, after visualization of an enrichment of the NSC population *in vivo* (shown in the *in situ hybridization*) an increase of NSCs was additionally quantitatively confirmed by the upregulation in the average number of RB sensory neurons, both due to inhibition of nodal signaling.

Hence, ectoderm and neuroectoderm formation is controllable *in vivo*, resulting in an enrichment of the NSC population and an increase in the number of RB sensory neurons, due to defined NI treatment.

Since the aim of my study was to generate a neural tube in a simplified 3D controllable cell culture system, I investigated in the next step if I can force zebrafish primary cells to adopt a proneural fate *in vitro*, first of all in 2D cell culture.

In various *in vitro* studies an involvement of the already described NI promotes hESCs conversion into a neuronal cell type. Mostly by the so-called dual SMAD inhibition (Chen *et al.*, 2015). Thereby, the NI and the bone morphogenetic protein (BMP) antagonist noggin inhibit the SMAD pathway synergistically (Chambers *et al.*, 2009; Wattanapanitch *et al.*, 2014). Moreover, by combination of dual SMAD inhibition with the Glycogen synthase kinase 3 β (GSK-3 β) inhibitor CHIR99021 human fibroblasts can be converted into postmitotic neurons with morphological, immunocytochemical and functional characteristics. It was hypothesized, that TGF- β inhibition promotes mesenchymal-to-epithelial transition (Ladewig *et al.*, 2012).

Furthermore, a combination of the NI and LDN-193189 (LDN) was tested. LDN acts as an inhibitor of BMP type I receptors ALK2 and 3 and prevents phosphorylation of Smad1,5 and 8. Dual inhibition with the NI and LDN for one day and an additional day with LDN was sufficient to force generation of Pax6⁺ (a neuroectoderm marker) cells efficiently (Surmacz *et al.*, 2012; Rodrigues *et al.*, 2014).

Nevertheless, compared to the described methods, using combined factors to generate neuronal cell types, in my approach I tested solely one factor, the NI, to keep experimental conditions simple and thus more controllable.

4.4 By inhibition of nodal signaling the neural progenitor cell population is increased *in vitro*

In my studies, I used not murine or human ESCs, but ESCs derived from the transgenic *neurog1* zebrafish line. The aim of my study was to generate a zebrafish neural tube *in vitro*, since the spinal cord of the zebrafish as a lower vertebrate is not as complex as a mammalian spinal cord. Moreover, since I performed a comparative study of neuronal differentiation *in vitro* to neuronal differentiation in the *in vivo* scenario I took advantage of the transparency of the zebrafish embryo, which enables investigation of nervous system development in the living organism which is rapidly established until 48hpf.

Initially, I investigated if pluripotent zebrafish sphere-stage derived primary cells differentiate to NPCs *in vitro*. Indeed, a minor population of NPCs was observed. Since I showed that *in vivo* a NPC population was enriched by NI treatment, I tested if the NI is also applicable for neuronal differentiation of zebrafish primary cells *in vitro*.

In neuronal differentiation studies using mouse and human ESCs mostly a concentration of 10 μ M was used (Chambers *et al.*, 2009; Wattanapanitch *et al.*, 2014). I tested 1 μ M, 5 μ M and 10 μ M NI concentration and treated cells from sphere stage to 24h and 48h respectively. By usage of 1 μ M NI and a treatment time of 48h I observed the highest enrichment of *neurog1:RFP* positive nuclei. Thus, I used a concentration of 1 μ M Nodal Inhibitor and a treatment time of 48h. Moreover, whereas for mouse and human ESC neuronal differentiation mostly Dulbecco`s modified eagle medium (DMEM) medium was used as basis, I figured out that for sphere-stage derived zebrafish primary cells the Leibovitz`L-15 medium is more suitable. Moreover, zebrafish sphere-stage derived cells required fetal calf serum (FCS) at least at the beginning of cultivation: In contrast, in neuronal differentiation studies in mESCs and hESCs, neuronal differentiation was improved in serum-free culture conditions, due to instruction of specific regional identities by adding potent morphogens. However, with the culture conditions I used an 2,7 fold enrichment of the NPC population, indicated by *neurog1:RFP* positive nuclei, was achieved compared to *neurog1:RFP* positive nuclei of control cells (treated with DMSO; Fig.13).

Thus, by inhibition of nodal signaling the neural progenitor cell population is increased *in vitro*. Hence, the NI is applicable for zebrafish primary cells as well. Compared to the NI *in vivo* treatment where a treatment time until 24hpf showed the highest enrichment of NPCs, the *in vitro* NI treatment required a treatment time until 48hpf. This delay in cellular

differentiation might be due to a disturbance of the cell cycle, which was probably caused by the change of cell culture medium.

Since in this thesis I investigated the establishment of a zebrafish neural tube in 3D cell culture system, the next paragraphs describe the generation of neural tissues *in vitro*, thereby comparing 2D and 3D cell culture systems.

4.5 Generation of neural tissue architectures *in vitro*

NSCs have been shown to be capable forming neural structures *in vitro* (Han *et al.*, 2012; Zhu *et al.*, 2013), and in advanced 3D cell culture systems they can even build multilayered complex architectures (Tang-Schomer *et al.*, 2013; Meinhardt *et al.*, 2014; Karus *et al.*, 2014; Muguruma *et al.*, 2015). The ability of NSCs to generate complex neural structures *in vitro* is mainly based on the self-organizing properties of NSCs. Beside the access to unlimited cell material, the continuously improving neural differentiation protocols and progress in the establishment of novel optimized cell culture systems induced a new dimension for studying initial steps of neural development and brain diseases *in vitro* (Karus *et al.*, 2014). *In vitro* generate neural tissues can be roughly categorized in unstructured shapes and more complex and structured architectures. The so-called neural rosette, long-term neuroepithelial stem cells (lt-NES) and neurospheres display unstructured neural tissues.

Developing NSCs maintained proliferative characteristics when fibroblast growth factor (FGF) was added to the medium and formed neural rosette structures. The neural rosette generates apical-basal polarity (indicated by the apical proteins zona occludens 1 and N-cadherin in the core) and seem to undergo interkinetic nuclear migration (INM, a periodically movement of the nucleus of a cell between the apical and basal membrane during cell cycle; Falk *et al.*, 2012; Nasu *et al.*, 2012). When epidermal growth factor (EGF) was added, so-called NSC^{FGF2/EGF} cells were generated, which own features similar to the radial glia-like phenotype described in a fetal NSC population (Conti and Cattaneo, 2010; Conti *et al.*, 2005). These cells are suitable for long-term culture (long-term neuroepithelial stem cells; lt-NES), and display posterior identity similar to an anterior hindbrain fate, which might be caused by the posteriorizing effect of FGF2 (Karus *et al.*, 2014).

Neural rosettes can be generated classically with the two-step neural induction protocol. Thereby, ESCs are cultivated without adhesion to a substrate at first. Due to their round shape in this phase they are called embryoid bodies (EB). After the EB forming phase, EBs are plated on an adhesive substrate, like mouse embryonic fibroblast (MEF) feeder cells and are cultivated with FGF/EGF to generate lt-NES.

Although neural self-organization can be achieved in monolayer culture, a 3D suspension culture is more suitable for spontaneous generation of complex neural histoarchitectures, since they allow 3D growth. In the early 1990s, the first studies were performed applying 3D

culture, cultivating NSCs with FGF and EGF from fetal and adult rodent brain as free-floating aggregates named neurospheres, thereby establishing classical 3D neurosphere culture (Reynolds *et al.*, 1992). Neurospheres formed from primary cells have been described as primitive, consisting of a heterogeneous mixture of randomly distributed mitotic cells and moreover NSCs and NPCs. Cells within a neurosphere have been shown to be primitively separated from each other, due to their regional origin of their primary tissue (e.g. nestin-positive NSCs/NPCs located at the neurosphere edge and glial fibrillary acidic protein (GFAP) and β III-tubulin-positive neurons in the neurosphere core; Campos *et al.*, 2004; Jensen and Parmar, 2006; Sirko *et al.*, 2007; von Holst *et al.*, 2006). However, authentic neural tissue architectures like a layered cortical neuroepithelium do not generate in a neurosphere. Cells establishing neurospheres have been compared with a radial glia-like stem cell (Karus *et al.*, 2011, Reynolds and Rietze, 2005) and might be similar to the NSC^{FGF2/EGF} cell. Thus, the neurosphere-forming cell is presumably a late-stage neural precursor cell, displaying inability to contribute to complex pattern formation (Karus *et al.*, 2014).

Thus, the described neural shapes are too unstructured, due to their heterogeneous randomly mixed cell population and sphere-like structure. In my thesis, the aim was to generate a structured, tubular-shaped zebrafish neural tube. However, the classical two-step neural induction protocol and 3D suspension culture do not support the generation of a tubular shape, due to a lack of a scaffold. Therefore, a 3D cell culture system, providing a scaffold is required to support the formation of a tubular shape.

4.6 Complex neural tissue architectures

Classically, EBs were cultivated in medium containing fetal calf serum when detached from mouse embryonic fibroblast feeder cells. These EBs were not suitable to investigate formation of lineage-specific histoarchitecture, since they consist of cells from all germ layers. The introduction of serum-free suspension culture enabled the formation of specific regional identities (e.g. dorsal telencephalon) by adding morphogens implied a meaningful progress (Watanabe, 2005). The so-called serum-free floating culture of embryoid body-like aggregates (SEFB) protocol was further optimized by using ultralow-attachment 96-well plates to control EB size by quickly reaggregation (SEFBq) dissociated ESCs into an EB-like structure. Addition of Wnt and TGF β inhibitors resulted in the generation of polarized cortical epithelia in a temporally controlled manner, mimicking corticogenesis *in vivo*, although stratification was not achieved sufficiently with the SFEBq technique (Eiraku, 2008).

A drawback of the SFEBq system is the difficulty of avoiding fusion of cellular aggregates during cultivation, resulting in variation of quality in different aggregates.

Moreover, by cultivation of 3D hPSCs, cerebral organoids (minibrains) with distinct brain regions were formed in a multiple-step method. First, neuroectoderm developed from EBs, which then were embedded in Matrigel droplets. The matrigel droplets in turn, were transferred to a spinning bioreactor to improve nutrient absorption, resulting in rapid development of brain tissues (Lancaster *et al.*, 2013). However, just in about 1:1000 cases such a minibrain develops (personal communication). Furthermore, generated cerebral organoids consisted out of variable spatially distinct “brain regions” (Karus *et al.*, 2014).

Whereas neural tissues like neural rosettes and neurospheres represent a too unstructured architecture, complex neural tissues like multilayered cortical epithelia display complex and structured systems. However, they are rarely reproducible. The generation of complex structures requires strict following of cell culture guidelines. Moreover, complex architectures display a spherical structure as well, since existing advanced cell culture systems including 3D suspension culture combined with cultivation of neural architectures in a well plate, matrigel and/or bioreactor do not support the formation of a tubular structure as well, due to a lack of scaffold.

Recently, the patterning of a neural tube was reconstructed in 3D. Mouse ESCs were directly embedded in matrigel or synthetic matrices (providing a scaffold) and cells were cultivated under neural induction conditions, forming clonally neuroepithelial cysts with a single lumen. By addition of retinoic acid, a complete dorso-ventral patterning was achieved (Meinhardt *et al.*, 2014). However, this approach resulted as well in the generation of neural cysts, since a scaffold supporting the formation of a tubular shape is missing.

Thus, none of the described CCS is suitable to generate a controllable 3D CCS to support the formation of a zebrafish neural tube. Therefore, a reproducible platform is required to enable the cultivation of a complex 3D tubular neural architecture, still guaranteeing controllability of neural differentiation.

4.7 Establishment of a three-dimensional cell culture system

A 3D microchannel (provided by S. Giselbrecht and colleagues) thermoformed from a polycarbonate foil by the Substrate modification and replication by thermoforming (SMART) technology (Giselbrecht *et al.*, 2006; Truckenmüller *et al.*, 2011) served as basic structure for the 3D cell culture system. The microchannel was modified in size and shape to support the formation of a zebrafish neural tube (60µm width, 100 µm depth). First of all, the functionality of the microchannel was tested with robust PAC2 cells, which attached and covered completely inside the microchannel. Zebrafish primary cells were more difficult to cultivate, probably because the composition of their ECM is not as strong as the ECM of zebrafish fibroblasts.

Since the generation of a neuroepithelial structure requires the establishment of apical/basal polarity, the microchannel was biofunctionalized with basal proteins to determine the basal side for the zebrafish primary cells.

4.8 Biofunctionalization of the microchannel provides basal information for the cells

Proteins of the ECM, like laminin, fibronectin, gelatin and collagen have been shown to promote cell attachment and differentiation. Especially laminin-1 (Ekblom *et al.*, 2003; Hohenester and Yurchenco, 2013) and fibronectin (Pankov and Yamada, 2002; Burnside and Bradbury, 2014) are enriched in the neural ECM and have been shown to be essential for basement membrane assembly and adhesion, migration and axon elongation. The biological performance of a substrate has been shown to be due to different conformations of laminin on a substrate. Laminin domains mainly act through integrin and non-integrin binding proteins. Integrins in turn have been described as primary mediators of neural cell behavior on ECM components (Martinez-Ramos *et al.*, 2007).

Due to the importance of laminin-1 and fibronectin for the neural ECM and neuronal cell behavior, I used a laminin-1 and fibronectin coating to determine the basal side for the cells on the PC. Thereby, different coating conditions of laminin-1 alone and in combination with fibronectin were tested, with and without UV-ozone treatment (Pryzhkova *et al.*, 2014; Table 1). It was shown that a UV/ozone treatment on carbon nanotubes hydrophilized their surfaces, ECM proteins were attached and thus cell attachment was improved. Thereby, the best result was achieved with a treatment time of 5 min (Pryzhkova *et al.*, 2014). In my approach, with a UV/ozone treatment time of 5 min I observed the best effect as well. Moreover, by Cooke and co-workers it was shown that a coating with the ECM proteins laminin (0,01mg/ml) and fibronectin (0,05mg/ml) on coverslips cell attachment was improved. However, I gained the best cell attachment with a laminin-1/fibronectin mixed solution of 0,02mg/1ml (laminin-1) + 0,01mg/0,5ml (fibronectin).

4.9 By inhibition of nodal signaling the neural progenitor cell population is increased in 3D

In various studies it has been shown that an involvement of the already described NI mediates neuronal conversion of ESCs (Chambers *et al.*, 2009; Ladewig *et al.*, 2012; Wattanapanitch *et al.*, 2014; Chen *et al.*, 2015; Liu *et al.*, 2015).

In my 3D CCS, I investigated controllability of neuronal differentiation applying the NI with the same conditions as in the 2D CCs. An 2,5 fold increase of *neurog1:RFP* positive nuclei was observed compared to control cells (DMSO treated; Fig.18,19,20).

Thus, by inhibition of nodal signaling the NPC population was increased in 3D.

4.10 The 3D cell culture system reflects better the dynamics of neurogenesis *in vivo* and is well controllable

A comparative study was performed investigating neural differentiation in the zebrafish and in 2D and 3D zebrafish primary cell culture. Although a zebrafish neural tube could not be generated *in vitro*, it was shown that by defined NI treatment the inhibition of nodal signaling resulted in an enrichment of the NPC population *in vivo*, as it was reflected by an increase of *neurog1* expression and an expansion of the spinal cord of treated embryos (Fig.10b,b`c,c`) compared to control embryos (Fig10.a,a`). Moreover, an 1,3 fold increase in the average number of treated RB sensory neurons (Fig.11a,a`) was observed compared to control embryos (Fig.11b,b`). Furthermore, by defined NI treatment the NSC population was enriched *in vitro*, as it was indicated by an 2,7 fold increase of *neurog1:RFP* positive nuclei in 2D and 2,5 fold enrichment in 3D compared to controls (Fig.20).

Thus the established 3D CCS approaches closer to the *in vivo* scenario than the 2D CCS, which displays an artificial environment. Hence, controllability of neurogenesis can be achieved in the established 3D CCS, which reflects better the dynamics of neurogenesis *in vivo* and is well controllable.

4.11 Advantages and limitations of the established three-dimensional cell culture system

S. Giselbrecht and co-workers established a three-step process, consisting of premodification, thermoforming and postmodification for the establishment of 3D functionalized microstructures for 3D cell culture applications called SMART. The main advantage of the SMART technology is that polymer foils are thermoformed not in a melting phase but in a softened state (in contrast to e.g. microinjection moulding), thus guaranteeing maintenance of previously generated modifications due to the highly material coherence. Moreover, modifications established in 2D are even available on vertical side walls of the microchannel in high resolution and in depth of the material. The SMART technology enables the production of thin-walled flexible microstructures, which can be adjusted in surface modifications, size and shape – e.g to mimic the dimensions of a zebrafish neural tube and support the tubular shape due to the tubular microchannel.

A limiting factor is the thickness of the polymer film, which has to be stretched and bend around mould structures. Smallest thermoformable structures range in the low ten-micrometers. Another limitation is the depth of a microstructure, meaning the ability of a film to be stretched without tearing, which depends on wall thickness distributions (Giselbrecht 2006; Truckenmueller *et al.*, 2011).

The SMART technology was also used to produce so-called microcontainer arrays, which are 3D chips for cell culture applications (Giselbrecht *et al.*, 2008).

Moreover, by the SMART technique, a similar microchannel was applied to study transendothelial transport *in vitro*. S. Giselbrecht, U. Schepers and co-workers established a 3D porous capillary system, coated with collagen, which enabled grow of HUVEC endothelial cells on the inner walls of the microchannel, mimicking the natural curvature of a blood vessel. This 3D porous capillary system, which was created by a combination of microscale thermoforming and ion track technology, was used to study transendothelial transport of drug-like molecules (Hebeiss *et al.*, 2012).

Since I observed that in my 3D cell culture approach the cells favored to attach on the walls of the microchannel, I suppose the stiffness at the bottom of the microchannel might be too rigid for the cells. Since it was shown that the stiffness of the neural ECM of the brain ranges between 0,1-1 kPa (Lv *et al.*, 2015), cultivation of cells in a hydrogel inside the microchannel might support further neuronal differentiation, providing a softer substrate and moreover would support three-dimensional growth of cells. Additionally, to exclude a zebrafish-specific cross-reaction, neuronal differentiation should be studied with a mammalian cell line as well, e.g. mouse neuroblastoma derived neuro2a cell line.

Moreover, further differentiation should be forced by cultivation of zebrafish primary cells in neuronal differentiation medium by addition of soluble factors driving further differentiation into mature neurons, e.g. FGF8 to induce midbrain/hindbrain fate (Petros *et al.*, 2011).

Nevertheless, the established 3D CCS described in this thesis provides the most suitable platform to generate a simple neural tube under controllable conditions, further enabling to investigate singularly the effect of each molecule involved in the process of neurogenesis. Recently, Meinhardt and colleagues (2014) reconstructed a patterned neural tube in 3D, resulting in neuroepithelial cysts. On the contrary, our established 3D microchannel allows the formation of tubular structures, which additionally can be modified in size and shape to mimic the dimensions of a zebrafish neural tube. Takahashi and colleagues (2016) cultivated neuron bundles without precoating in a longitudinal way and named them “neural microtubes”. Compared to this study, in my approach I investigated neuronal differentiation in a 3D tubular platform from the beginning, additionally determining the basal side for the cells by coating with the basal proteins laminin-1 and fibronectin. Moreover, 3D CCSs generating more complex neural architectures (like minibrains; Lancaster *et al.*, 2013) require often a multi-step fabrication process, which is often hardly reproducible. Furthermore, although gradients of developmental morphogens in neural tube patterning were investigated (Demers

et al., 2016) we preferred a simplified, controllable and thus reproducible scaffold which allowed us to focus on single molecules and their effect on the process of neurogenesis.

Formation and further on patterning of the neural tube requires precise tissue organization, depending on the generation of a sharp interface of neighboring compartments. At specific borders it mediates the organization of key signaling centers like the mid-diencephalic organizer and the midbrain-hindbrain boundary. At a later stage of boundary formation, cell intermingling is prevented between two adjacent subdivisions (Kiecker and Lumsden, 2005; Xu and Wilkinson, 2013).

In vitro studies investigating boundary formation are rare, but would be suitable to clarify signaling events during boundary formation. Therefore, guided cell attachment *in vitro* was investigated in collaboration with A. Hirschbiel and C. Barner-Kowollik, creating a cell attractant/ cell repellent polymer.

4.12 By establishment of a functionalized (cell attractant) surface area distinct are by light cells can be guided to this specific are in 2D and 3D

By light inducible photolithographic patterning a functionalized, cell attractant area was created on a polycarbonate film, which is advantageous due to its amenability to thermoforming, e.g. into thin-walled 3D microchannels. The surface outside of the functionalized (irradiated) area had a cell repellent effect, due to the biofouling properties of the oligoethylenglycol (OEG; Nan Cheng, 2010; Rodriguez-Emmenegger et al., 2013), as it was indicated by fetal calf serum (FCS) adhesion (Fig.21b). Moreover, enhanced green fluorescent protein (eGFP) attached primarily to the wave pattern, whereas the non-irradiated area displayed significant less eGFP adsorption (Fig.21c). Furthermore, PAC2 cells were guided to the functionalized wave pattern and attached densely almost exclusively there displaying an expanded cell surface (Fig.22). As the cell division rate for PAC2 fibroblasts in cell culture may be too slow to explain the observed cellular distribution, I suggest that fibroblasts migrate from the non-irradiated surface to the irradiated surface supported by cellular shape analysis. Moreover, a non-irradiated, cell repellent stripe was designed in a microchannel, to investigate if cells can be guided in 3D as well. PAC2 cells avoided the non-irradiated stripe and attached almost solely in the irradiated surface (Fig.23).

Thus, cells can be guided to an area of interest on a polycarbonate film in 2D and 3D.

In another approach, Irvine and colleagues (2001) made use of Arg-Gly-Asp (RGD) peptides for control of cell adhesion (instead of OEG), thus clustering these peptides on comb polymer films. On the contrary, in our method we created a micropattern of cell-repellent OEG and cell attractant carboxylic acid moieties; which increased adhesiveness, resulting in protein/

cell attachment on the film. Furthermore, in a similar study cell-repellent polyethyleneglycol (PEG) was sulfonated to generate a comb-like polymer for highly resolved cell micropatterns. NIH 3T3 fibroblasts attached into the comb structure, whereas the sulfonated PEG areas were avoided by the cells (Jung *et al.*, 2008).

However, compared to the method of e.g. Jung and colleagues, our introduced approach reflects up to now the only possibility for cell guiding on a thin, thermoformable polycarbonate substrate produced by a simple photochemical approach. This enables a patterned surface functionalization of thermoformed microstructures allowing applications from simple patterned CCS to advanced tissue CCS in 3D (Hirschbiel and Geyer *et al.*, 2015).

A further modification of the photolithographic technique would be to generate two adjacent surfaces, with distinct functionalization. This might enable cultivation of two cell populations next to each other and would be an interesting approach to study boundary formation *in vitro*. Another opportunity would be to cultivate cells in a hydrogel inside the microchannel, filling the microchannel in three steps, with an intermediate polymerization step in between. Thus, cultivation of different cell populations next to each other would be possible, mimicking a border between two cell populations at the interface between two adjacent hydrogels (Fig.27). The hydrogel contains proteins of the neural ECM, like laminin, fibronectin, chondroitin sulphate proteoglycans and heparan sulfate proteoglycans (Soleman *et al.*, 2013; Burnside and Bradbury, 2014). Thus, it would be possible to study cellular communication at a boundary *in vitro*.

Moreover, for neural tube formation coordinated movements of many cells in both time and space are crucial and regulated by an appropriate communication of cells.

In general, intercellular interactions determine cell fate and have been shown to be dependent on the cell microenvironment, influenced by altered clustering of membrane receptors in 2D compared to 3D.

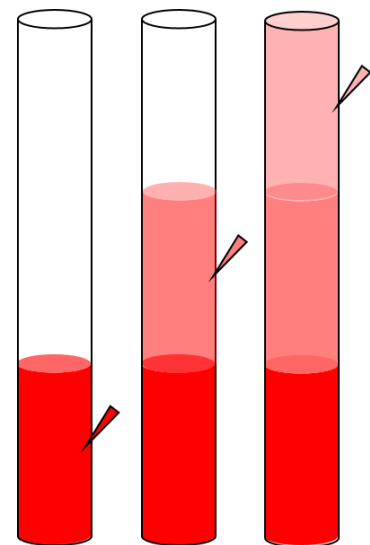


Figure 27: Model for the formation of a boundary *in vitro*. Hydrogel, enriched with cells (e.g. neuro2a) is filled in the microchannel in three-steps, with intermediate polymerization steps in between. The hydrogel contains proteins of the neural ECM.

4.13 Intercellular interactions modulate Wnt/ β -catenin signaling

Wnt/ β -catenin and FGF signaling has been shown to influence the specification and maintenance of a neuromesodermal axial progenitor in mouse ESCs. In amniotes, a specialized population of cells (called long-term neuromesodermal precursor; NMP), mediated by Wnt and FGF signaling at the end of gastrulation, widens and forms the spinal cord and paraxial mesoderm. In an adherent cell culture approach with mouse ESCs, it was shown that by controlled increase of Wnt/ β -catenin and FGF signaling cells adopt features of the NMP. Moreover, the effect of Wnt/ β -catenin and FGF signaling was increased when mESCs were cultivated as 3D aggregates and the population self-organized, underwent growth and axial elongation mimicking partly the behavior of embryonic spinal cord and paraxial mesoderm (Turner *et al.*, 2014).

Hence, Wnt/ β -catenin signaling was increased in 3D microwell culture compared to 2D adherent culture.

Furthermore, in a 3D cell culture system, control of EB size and shape has been shown to regulate cell-cell contacts on canonical Wnt/ β -catenin signaling in hESCs. Moreover, variations in EB size has been described to affect efficiency of cardiogenesis (BurrIDGE *et al.*, 2007; Ungrin *et al.*, 2008). Azarin and colleagues investigated the involvement of β -catenin between Wnt signaling and cadherin-mediated-cell-cell-interactions, which influences various developmental processes. Thereby, hESCs were cultivated on a 2D substrate and compared to cultivation in a 3D microwell array. In the 3D microwell culture, a higher E-cadherin expression, ongoing with a Wnt downregulation, was observed in comparison to cultivation on 2D substrates. However, EBs grown in microwell cultures displayed higher Wnt signaling (despite the reduction) than EBs from hESCs cultured on 2D substrates. Moreover, in Wnt upregulated cells, an upregulation of genes connected to cardiogenesis was shown in EBs (Azarin *et al.*, 2012).

Thus, Wnt signaling was downregulated in 3D compared to 2D. The aberrant activation of the pathway could lead to misinterpretation of results underlying the importance of finding the right condition to study developmental process in environment that mimic as close as possible the *in vivo* situation but more controllable in terms of molecular pathway activation.

4.14 Wnt reporter activation is higher in 2D than in 3D cell culture

To confirm this results in my system, I performed a similar study investigating Wnt/ β -catenin signaling in a co-culture approach with Wnt8a (since it is an important factor for neuroectoderm patterning; Kelly *et al.*, 1995; Erter *et al.*, 2001 ;Rhinn *et al.*, 2005) co-cultivated with 7xTCFCherry/HisCFP, serving as Wnt reporter. Cells were cultivated in 2D

and in 3D in the microchannel. In the 2D culture higher Wnt reporter activation was detected compared to 3D, confirming the results from Azarin and co-workers.

Hence, existing cellular signaling studies which have been performed in 2D should be reconsidered.

These results open up the possibility to use the system established in this thesis for more precise study of neurodevelopment.

Conclusion and Outlook

In this thesis a 3D CCS was established to support the formation of tubular structures (e.g. a neural tube). In contrast to existing CCS, which support the formation of spherical structures, the established 3D microchannel supports the formation of tubular structures and can be modified moreover in size to mimic the dimensions of a zebrafish neural tube. Moreover, the microchannel provides a reproducible scaffold, to study neuronal differentiation in a controllable manner. Hence, the established 3D microchannel represents a ground-breaking system to generate a complex and structured neural tube. Furthermore, the tubular shape would support the investigation of gradient formation in the neural tube and is suitable to mimic a NSC niche. Moreover, further modification of the cell guidance approach would enable to study boundary formation *in vitro*, in e.g. at the mhb.

5. References

Ader, M. & Tanaka, E.M. (2014). Modeling human development in 3D culture. *Curr Opin Cell Biol* 31, 23–28.

Altman, J. (1962). Are new neurons formed in the brains of adult mammals? *Science* 135, 1127-1128.

Altmann, B., Welle, A., Giselbrecht, S., Truckenmüller, R. & Gottwald, E. (2009). The famous versus the inconvenient - or the dawn and the rise of 3D-culture systems. *World J Stem Cells* 1, 43-48.

Amit, M., Carpenter, M.K., Inokuma, M.S., Chiu, C.P., Harris, C.P., Waknitz, M.A., Itskovitz-Eldor J, & Thomson, J.A. (2000). Clonally Derived Human Embryonic Stem Cell Lines Maintain Pluripotency and Proliferative Potential for Prolonged Periods of Culture. *Dev Biol* 227, 271–278.

Araya, C., Tawk, M., Girdler, G.C., Costa, M., Carmona-Fontaine, C. & Clarke, J.D. (2014). Mesoderm is required for coordinated cell movements within zebrafish neural plate in vivo. *Neural Dev* 9,9.

Araya, C., Ward, L. C., Girdler, G. C., & Miranda, M. (2016). Coordinating cell and tissue behaviour during zebrafish neural tube morphogenesis. *Dev Dyn* 245, 197-208.

Azarin, S.M., Lian, X., Larson, E.A., Popelka, H.M., de Pablo, J.J. & Palecek, S.P. (2012). Modulation of Wnt/ β -catenin signaling in human embryonic stem cells using a 3-D microwell array. *Biomaterials* 33, 2041–2049.

Bae, Y.-K., Shimizu, T. & Hibi, M. (2005). Patterning of proneuronal and inter-proneuronal domains by hairy- and enhancer of split-related genes in zebrafish neuroectoderm. *Development* 132, 1375-1385.

Baker, B.M. & Chen, C.S. (2012). Deconstructing the third dimension - how 3D culture microenvironments alter cellular cues. *J Cell Sci* 125, 3015-3024.

Bertrand, N., Castro, D.S. & Guillemot, F. (2002). Proneural genes and the specification of neural cell types. *Nat Rev Neurosci* 3, 517–530.

Biehlmaier, O., Makhankov, Y. & Neuhauss, S.C. (2007). Impaired retinal differentiation and maintenance in zebrafish laminin mutants. *Invest Ophthalmol Vis Sci* 48, 2887–2894.

Biswas, S., Emond, M.R. & Jontes, J. D. (2010). Protocadherin-19 and N-cadherin interact to control cell movements during anterior neurulation. *J Cell Biol* 191, 1029–1041.

Blader, P., Lam, C.S., Rastegar, S., Scardigli, R., Nicod J.C., Simplicio, N., Plessy, C., Fischer, N., Schuurmans, C., Guillemot, F. & Strähle, U. (2004). Conserved and acquired features of neurogenin1 regulation. *Development* 131, 5627–5637.

Bosi, S., Rauti, R., Laishram, J., Turco, A., Lonardoni, D., Nieuw, T., Prato, M., Scaini, D. & Ballerini, L. (2015). From 2D to 3D: novel nanostructured scaffolds to investigate signalling in reconstructed neuronal networks. *Sci Rep* 5, 9562.

Burnside, E. R. & Bradbury, E. J. (2014). Manipulating the extracellular matrix and its role in brain and spinal cord plasticity and repair. *Neuropathol Appl Neurobiol.* 40, 26–59.

BurrIDGE, P.W., Anderson, D., Priddle, H., Barbadillo Muñoz, M.D., Chamberlain, S., Allegrucci, C., Young, L.E. & Denning, C. (2007). Improved Human Embryonic Stem Cell Embryoid Body Homogeneity and Cardiomyocyte Differentiation from a Novel V-96 Plate Aggregation System Highlights Interline Variability. *Stem Cells* 25, 929–938.

Cabrera, C.V., Alonso, M.C., Johnston, P., Phillips, R.G. & Lawrence, P.A. (1987).

Phenocopies induced with antisense RNA identify the wingless gene. *Cell* 50, 659–663.

Callahan, J.F., Burgess, J.L., Fornwald, J.A., Gaster, L.M., Harling, J.D., Harrington, F.P., Heer, J., Kwon, C., Lehr, R., Mathur, A., Olson, B.A., Weinstock, J. & Laping, N.J. (2002). Identification of novel inhibitors of the transforming growth factor beta1 (TGF-beta1) type 1 receptor (ALK5). *J Med Chem* 45, 999-1001.

Campo, L.S., Leone, D.P., Relvas, J.B., Brakebusch, C., Fässler, R., Suter, U. & French-Constant, C. (2004). Beta1 integrins activate a MAPK signalling pathway in neural stem cells that contributes to their maintenance. *Development* 131, 3433-3444.

Carrel, A. (1912). On the Permanent Life of Tissues Outside of the Organism. *J Exp Med* 15, 516–28.

Chambers, S.M., Fasano, C.A., Papapetrou, E.P., Tomishima, M., Sadelain, M. & Studer, L. (2009). Highly efficient neural conversion of human ES and iPS cells by dual inhibition of SMAD signaling. *Nat Biotechnol* 27, 275–280.

Chen, J., Wang, Y., Chen, C., Lian, C., Zhou, T., Gao, B., Wu, Z. & Xu, C. (2015). Exogenous Heparan Sulfate Enhances the TGF- β -Induced Chondrogenesis in Human Mesenchymal Stem Cells by Activating TGF- β /Smad Signaling. *Stem Cells Int* 2016, 1520136. Epub 2015.

Chen, Z.L. Haegeli, V., Yu, H. & Strickland, S. (2009). Cortical deficiency of laminin γ 1 impairs the AKT/GSK-3 β signaling pathway and leads to defects in neurite outgrowth and neuronal migration. *Dev Biol* 327, 158-168.

Cheng, N. & Cao, X. (2010). Photoactive SAM surface for control of cell attachment. *J Colloid Interface Sci* 348, 71–79.

Clevers, H., Loh, K.M. & Nusse, R. (2014). Stem cell signaling. An integral program for tissue renewal and regeneration: Wnt signaling and stem cell control. *Science* 346, 1248012.

Colas, J.F. & Schoenwolf, G.C. (2001). Towards a cellular and molecular understanding of neurulation. *Dev Dyn* 221, 117–145.

Conti, I. & Cattaneo, E. (2010). Neural stem cell systems: physiological players or in vitro entities? *Nat Rev Neurosci* 11, 176-187.

Conti, L., Pollard, S.M., Gorba, T., Reitano, E., Toselli, M., Biella, G., Sun, Y., Sanzone, S., Ying, Q.L., Cattaneo, E. & Smith, A. (2005). Niche-independent symmetrical self-renewal of a mammalian tissue. *PLoS Biol* 3, e283.

Cooke, M.J., Phillips, S.R., Shah, D.S., Athey, D., Lakey, J.H. & Przyborski, S.A. (2008). Enhanced cell attachment using a novel cell culture surface presenting functional domains from extracellular matrix proteins. *Cytotechnology* 56, 71-79.

Cornell, R.A. & Eisen, J.S. (2002). Delta/Notch signaling promotes formation of zebrafish neural crest by repressing Neurogenin 1 function. *Development* 129, 2639–2648.

Demers, C.J., Soundararajan, P., Chennampally, P., Cox, G.A., Briscoe, J., Collins, S.D. & Smith, R.L. (2016). Development-on-chip: in vitro neural tube patterning with a microfluidic device. *Development* 143, 1884-1892.

Dupont, S., Morsut, L., Aragona, M., Enzo, E., Giulitti, S., Cordenonsi, M., Zanconato, F., Le Digabel, J., Forcato, M., Bicciato, S., Elvassore, N. & Piccolo, S. (2011). Role of YAP/TAZ in mechanotransduction. *Nature* 474, 179-183.

Efremov, A.N., Stanganello, E., Welle, A., Scholpp, S. & Levkin, P.A. (2013). Micropatterned superhydrophobic structures for the simultaneous culture of multiple cell types and the study of cell-cell communication. *Biomaterials* 34, 1757–1763.

Eiraku, M., Watanabe, K., Matsuo-Takasaki, M., Kawada, M., Yonemura, S., Matsumura, M., Wataya, T., Nishiyama, A., Muguruma, K. & Sasai Y. (2008). Self-organized formation of polarized cortical tissues from ESCs and its active manipulation by extrinsic signals. *Cell Stem Cell* 3, 519–532.

Ekblom, P., Lonai, P. & Talts, J.F. (2003). Expression and biological role of laminin-1. *Matrix Biol* 22, 35–47.

Engler, A.J., Sen, S., Sweeney, H.L. & Discher, D. E. (2006). Matrix elasticity directs stem cell lineage specification. *Cell* 126, 677–689.

Erter, C.E., Wilm, T.P., Basler, N., Wright, C.V. & Solnica-Krezel, L. (2001). Wnt8 is required in lateral mesendodermal precursors for neural posteriorization in vivo. *Development* 128, 3571–3583.

Falk, A., Koch, P., Kesavan, J., Takashima, Y., Ladewig, J., Alexander, M., Wiskow, O., Taylor, J., Trotter, M., Pollard, S., Smith, A. & Brüstle, O. (2012). Capture of neuroepithelial-like stem cells from pluripotent stem cells provides a versatile system for in vitro production of human neurons. *PLoS One* 7, e29597.

Feldman, B., Dougan, S.T., Schier, A.F. & Talbot, W.S. (2000). Nodal-related signals establish mesendodermal fate and trunk neural identity in zebrafish. *Curr Biol* 10, 531–534.

Geling, A., Itoh, M., Tallafuss, A., Chapouton, P., Tannhäuser, B., Kuwada, J.Y., Chitnis, A.B. & Bally-Cuif, L. (2003). bHLH transcription factor Her5 links patterning to regional inhibition of neurogenesis at the midbrain-hindbrain boundary. *Development* 130, 1591–1604.

George, E.L., Georges-Labouesse, E.N., Patel-King, R.S., Rayburn, H. & Hynes, R.O. (1993). Defects in mesoderm, neural tube and vascular development in mouse embryos lacking fibronectin. *Development* 119, 1079–1091.

Giamanco, K.A. & Matthews, R.T. (2012). Deconstructing the perineuronal net: cellular contributions and molecular composition of the neuronal extracellular matrix. *Neuroscience* 218, 367–384.

Gilbert, S.F. (2000). *Developmental Biology*, 6th edition.

Girdler, G.C., Araya, C., Ren, X. & Clarke, J.D. (2013). Developmental time rather than local environment regulates the schedule of epithelial polarization in the zebrafish neural rod. *Neural Dev* 8, 5.

Giselbrecht, S., Gietzelt, T., Gottwald, E., Trautmann, C., Truckenmüller, R., Weibezahn, K.F. & Welle, A. (2006). 3D tissue culture substrates produced by microthermoforming of pre-processed polymer films. *Biomed Microdevices* 8, 191–199.

Giselbrecht, S., Gottwald, E., Truckenmueller, R., Trautmann, C., Welle, A., Guber, A. Saile, V., Gietzelt, T. & Weibezahn, K.F. (2008). Microfabrication of chip-sized scaffolds for three-dimensional cell cultivation. *J Vis Exp* 12, pii: 699

Gottwald, E., Giselbrecht, S. & Truckenmüller, R. (2015). 3D-Zellkulturmodelle auf Basis thermogeformter Polymerfolien. *BIOspektrum* 21, 169–171.

Graham, V., Khudyakov, J., Ellis, P. & Pevny, L. (2003). SOX2 functions to maintain neural progenitor identity. *Neuron* 39, 749–765.

Greiner, A.M., Klein, F., Gudzenko, T., Richter, B., Striebel, T., Wundari, B.G., Autenrieth, T.J., Wegener, M., Franz, C.M. & Bastmeyer, M. (2015). Cell type-specific adaptation of cellular and nuclear volume in micro-engineered 3D environments. *Biomaterials* 69, 121–132.

Gutzman, J.H., Graeden, E.G., Lowery, L.A., Holley, H.S. & Sive, H. (2008). Formation of the zebrafish midbrain-hindbrain boundary constriction requires laminin-dependent basal constriction. *Mech Dev* 125, 974-983.

Hagos, E.G. & Dougan, S.T. (2007). Time-dependent patterning of the mesoderm and endoderm by Nodal signals in zebrafish. *BMC Dev Biol* 7, 22.

Han, S., Yang, K., Shin, Y., Lee, J.S., Kamm, R.D., Chung, S. & Cho, S.W. (2012). Three-dimensional extracellular matrix-mediated neural stem cell differentiation in a microfluidic device. *Lab Chip* 12, 2305-2308.

Harrison, R.G. (1914). The reaction of embryonic cells to solid structures. *J Exp Zool* 17, 521-544.

Hazeltine, L., Selekman, J.A. & Palecek, S.P. (2013). Engineering the human pluripotent stem cell microenvironment to direct cell fate. *Biotechnol Adv* 31, 1002-1019.

Hebeiss, I., Truckenmüller, R., Giselbrecht, S. & Schepers, U. (2012). Novel three-dimensional Boyden chamber system for studying transendothelial transport. *Lab Chip* 12, 829–834.

Hirschbiel, A.F., Geyer, S., Yameen, B., Welle, A., Nikolov, P., Giselbrecht, S. & Barner-Kowollik, C. (2015). Photolithographic Patterning of 3D-Formed Polycarbonate Films for Targeted Cell Guiding. *Adv Mater* 27, 2621–2626.

Hohenester, E. & Yurchenco, P. D. (2013). Laminins in basement membrane assembly. *Cell Adh Migr* 7, 56–63.

Hong, E. & Brewster, R. (2006). N-cadherin is required for the polarized cell behaviours that drive neurulation in the zebrafish. *Development* 133, 3895–3905.

Inman, G.J., Nicolás, F.J., Callahan, J.F., Harling, J.D., Gaster, L.M., Reith, A.D., Laping, N.J. & Hill, C.S. (2002). SB-431542 is a potent and specific inhibitor of transforming growth factor-beta superfamily type I activin receptor-like kinase (ALK) receptors ALK4, ALK5, and ALK7. *Mol Pharmacol* 62, 65-74.

Irvine, D.J. and Mayes, A.M. (2001). Nanoscale Clustering of RGD Peptides at Surfaces Using Comb Polymers. 1. Synthesis and Characterization of Comb Thin Films. *Biomacromolecules* 2, 85-94.

Jensen, J.B. & Parmar, M. (2006). Strengths and limitations of the neurosphere culture system. *Mol Neurobiol* 34, 153-161.

Jones, S. (2004). An overview of the basic helix-loop-helix proteins. *Genome Biol* 5, 226.

Jung, J., Na, K., Shin, B., Kim, O., Lee, J., Yun, K. & Hyun, J.(2008). A cell-repellent sulfonated PEG comb-like polymer for highly resolved cell micropatterns. *J Biomater Sci Polym Ed* 19, 161-173.

Kageyama, R., Ohtsuka, T. & Kobayashi, T. (2007). The Hes gene family: repressors and oscillators that orchestrate embryogenesis. *Development* 134, 1243–1251.

Kaplan, M.S. (1979). Cell Proliferation in the Adult Mammalian Brain. *Thesis*.

Karnavas, T., Mandalos, N., Malas, S. & Remboutsika, E. (2013). SoxB, cell cycle and neurogenesis. *Front Physiol* 4, 298.

Karus, M., Blaess, S. & Brüstle, O. (2014). Self-organisation of neural tissue architectures from pluripotent stem cells. *J Comp Neurol* 522, 2831-2844.

Karus, M., Denecke, B., ffrench-Constant, C., Wiese, S. & Faissner, A. (2011). The extracellular matrix molecule tenascin C modulates expression levels and territories of key patterning genes during spinal cord astrocyte specification. *Development* 138, 5321–5331.

Kelly, G.M., Greenstein, P., Erezylmaz, D.F. & Moon, R.T. (1995). Zebrafish wnt8 and wnt8b share a common activity but are involved in distinct developmental pathways. *Development* 121, 1787–1799.

Kiecker, C. & Lumsden, A. (2005). Compartments and their boundaries in vertebrate brain development. *Nat Rev Neurosci* 6, 553–564.

Kim, C.H., Bae, Y.K., Yamanaka, Y., Yamashita, S., Shimizu, T., Fujii, R., Park, H.C., Yeo, S.Y., Huh, T.L., Hibi, M. & Hirano T (1997). Overexpression of neurogenin induces ectopic expression of HuC in zebrafish. *Neurosci Lett* 239, 113–116.

Kim, C.H., Oda, T., Itoh, M., Jiang, D., Artinger, K.B., Chandrasekharappa, S.C., Driever, W. & Chitnis, A.B. (2000). Repressor activity of Headless/Tcf3 is essential for vertebrate head formation. *Nature* 407, 913-916.

Kishimoto, Y., Lee, K.H., Zon, L., Hammerschmidt, M. & Schulte-Merker, S. (1997). The molecular nature of zebrafish swirl: BMP2 function is essential during early dorsoventral patterning. *Development* 124, 4457–4466.

Klaus, A. & Birchmeier, W. (2008). Wnt signalling and its impact on development and cancer. *Nat Rev Cancer* 8, 387–398.

Knight, E. & Przyborski, S. (2014). Advances in 3D cell culture technologies enabling tissue-like structures to be created in vitro. *J Anat* 227, 746-756.

Kondo, T., Matsuoka, A.J., Shimomura, A., Koehler, K.R., Chan, R.J., Miller, J.M., Srour, E.F. & Hashino, E. (2011). Wnt signaling promotes neuronal differentiation from mesenchymal stem cells through activation of Tlx3. *Stem Cells* 29, 836–846.

Korzh, V. & Strähle, U. (2002). Proneural, prosensory, antigial: the many faces of neurogenins. *Trends Neurosci* 25, 603–605.

Ladewig, J., Mertens, J., Kesavan, J., Doerr, J., Poppe, D., Glaue, F., Herms, S., Wernet, P., Kögler, G., Müller, F.J., Koch, P. & Brüstle O. (2012). Small molecules enable highly efficient neuronal conversion of human fibroblasts. *Nat Methods* 9, 575-578.

Lancaster, M.A., Renner, M., Martin, C.A., Wenzel, D., Bicknell, L.S., Hurles, M.E., Homfray, T., Penninger, J.M., Jackson, A.P. & Knoblich, J.A. (2013). Cerebral organoids model human brain development and microcephaly. *Nature* 501, 373-379.

Lane, P.W. (1967). *Mouse News Lett* 36, 40.

Latimer, A. & Jessen, J. R. (2010). Extracellular matrix assembly and organization during zebrafish gastrulation. *Matrix Biol* 29, 89–96.

Lee, J.H., Jung, H.W., Kang, I.K. & Lee, H.B. (1994). Cell behaviour on polymer surfaces with different functional groups. *Biomaterials* 15, 705-711.

Lekven, A.C., Thorpe, C.J., Waxman, J.S. & Moon, R.T. (2001). Zebrafish wnt8 encodes two Wnt8 proteins on a bicistronic transcript and is required for mesoderm and neurectoderm patterning. *Dev Cell* 1, 103–114.

Lippmann, E.S., Estevez-Silva, M.C. & Ashton, R.S. (2014). Defined human pluripotent stem cell culture enables highly efficient neuroepithelium derivation without small molecule inhibitors. *Stem Cells* 32, 1032–1042.

Lodato, S., Shetty, A.S. & Arlotta, P. (2014). Cerebral cortex assembly: generating and reprogramming projection neuron diversity. *Trends in Neurosci* 38, 117–125.

Lowery, L.A. & Sive, H. (2004). Strategies of vertebrate neurulation and a re-evaluation of teleost neural tube formation. *Mech Dev* 121, 1189–1197.

Lowery, L.A. & Sive, H. (2009). Totally tubular: the mystery behind function and origin of the brain ventricular system. *Bioessays* 31, 446–458.

Luz, M., Spannli-Müller, S., Özhan, G., Kagermeier-Schenk, B., Rhinn, M., Weidinger, G. & Brand, M. (2014). Dynamic association with donor cell filopodia and lipid-modification are essential features of Wnt8a during patterning of the zebrafish neuroectoderm. *PLoS One* 9, e84922.

Lv, H., Li, L., Sun, M., Zhang, Y., Chen, L., Rong, Y. & Li, Y. (2015). Mechanism of regulation of stem cell differentiation by matrix stiffness. *Stem Cell Res Ther* 6, 103.

Martínez-Ramos, C., Lainez, S., Sancho, F., García Esparza, M.A., Planells-Cases, R., García Verdugo, J.M., Gómez Ribelles, J.L., Salmerón Sánchez, M., Monleón Pradas, M., Barcia, J.A. & Soria, J.M. (2008). Differentiation of postnatal neural stem cells into glia and functional neurons on laminin-coated polymeric substrates. *Tissue Eng Part A* 14, 1365-1375.

Masui, S., Nakatake, Y., Toyooka, Y., Shimosato, D., Yagi, R., Takahashi, K., Okochi, H., Okuda, A., Matoba, R., Sharov, A.A., Ko, M.S. & Niwa H. (2007). Pluripotency governed by Sox2 via regulation of Oct3/4 expression in mouse embryonic stem cells. *Nat Cell Biol* 9, 625–635.

Maucksch, C., Jones, K.S. & Connor, B. (2013). Concise review: the involvement of SOX2 in direct reprogramming of induced neural stem/precursor cells. *Stem Cells Transl Med*, 2, 579-583.

Meinhardt, A., Eberle, D., Tazaki, A., Ranga, A., Niesche, M., Wilsch-Bräuninger, M., Stec, A., Schackert, G., Lutolf, M. & Tanaka, E.M. (2014). 3D reconstitution of the patterned neural tube from embryonic stem cells. *Stem Cell Reports* 3, 987-999.

Mikels, A.J. & Nusse, R. (2006). Wnts as ligands: processing, secretion and reception. *Oncogene* 25, 7461–7468.

Millet, L.J. & Gillette, M.U. (2012). New perspectives on neuronal development via microfluidic environments. *Trends Neurosci* 35, 752–761.

Miyata, T., Okamoto, M., Shinoda, T. & Kawaguchi, A. (2015). Interkinetic nuclear migration generates and opposes ventricular-zone crowding: insight into tissue mechanics. *Front Cell Neurosci* 8, 473.

Muguruma, K., Nishiyama, A., Kawakami, H., Hashimoto, K. & Sasai, Y. (2015). Self-organization of polarized cerebellar tissue in 3D culture of human pluripotent stem cells. *Cell Rep* 10, 537-550.

Nasu, M., Takata, N., Danjo, T., Sakaguchi, H., Kadoshima, T., Futaki, S., Sekiguchi, K., Eiraku, M. & Sasai, Y. (2012). Robust formation and maintenance of continuous stratified cortical neuroepithelium by laminin-containing matrix in mouse ES cell culture. *PLoS One* 7, e53024.

Nulty, J., Alsaffar, M. & Barry, D. (2015). Radial glial cells organize the central nervous system via microtubule dependant processes. *Brain Res* 1625, 171–179.

Nusse, R. & Varmus, H. E. (1982). Many tumors induced by the mouse mammary tumor virus contain a provirus integrated in the same region of the host genome. *Cell* 31, 99–109.

Okuda, Y., Ogura, E., Kondoh, H. & Kamachi, Y. (2010). B1 SOX coordinate cell specification with patterning and morphogenesis in the early zebrafish embryo. *PLoS Genet* 6, e1000936.

Oppenheimer, J M. (1936). Transplantation experiments on developing teleosts (*Fundulus* and *Perca*). *J Exp Zool* 72, 409-437.

Pankov, R. & Yamada, K.M. (2002). Fibronectin at a glance. *J Cell Sci* 115, 3861–3863.

Park, H.C., Hong, S.K., Kim, H.S., Kim, S.H., Yoon, E.J., Kim, C.H., Miki, N. & Huh, T.L. (2000). Structural comparison of zebrafish *Elav/Hu* and their differential expressions during neurogenesis. *Neurosci Lett* 279, 81–84.

Parsons, M.J., Pollard, S.M., Saúde, L., Feldman, B., Coutinho, P., Hirst, E.M. & Stemple, D.L. (2002). Zebrafish mutants identify an essential role for laminins in notochord formation. *Development* 129, 3137–3146.

Patten, I. & Placzek, M. (2000). The role of *Shh* in neural tube patterning. *Cell Mol Life Sci* 57, 1695-1708.

Petros, T.J., Tyson, J.A. & Anderson, S.A. (2011). Pluripotent stem cells for the study of CNS development. *Front Mol Neurosci* 4, 30.

Philpott, A. (2010). Neural Development: bHLH Genes. eLS a0000827.pub2

Pryzhkova, M.V., Aria, I., Cheng, Q., Harris, G.M., Zan, X., Gharib, M. & Jabbarzadeh, E. (2014). Carbon nanotube-based substrates for modulation of human pluripotent stem cell fate. *Biomaterials* 35, 5098-5109.

Quesada-Hernández, E., Caneparo, L., Schneider, S., Winkler, S., Liebling, M., Fraser, S.E. & Heisenberg, C.P. (2010). Stereotypical cell division orientation controls neural rod midline formation in zebrafish. *Curr Biol* 20, 1966–1972.

Radosevic, M., Fargas, L. & Alsina, B. (2014). The Role of her4 in inner ear development and its relationship with proneural genes and notch signalling. *PloS One* 9, e109860.

Reiprich, S. & Wegner, M. (2015). From CNS stem cells to neurons and glia: Sox for everyone. *Cell Tissue Res* 359, 111–124.

Rentzsch, F., Bakkers, J., Kramer, C. & Hammerschmidt, M. (2004). Fgf signaling induces posterior neuroectoderm independently of Bmp signaling inhibition. *Dev Dyn* 231,750-757.

Reversade, B. & De Robertis, E. M. (2005). Regulation of ADMP and BMP2/4/7 at opposite embryonic poles generates a self-regulating morphogenetic field. *Cell* 123, 1147–1160.

Reynolds, B.A. & Rietze, R.L. (2005). Neural stem cells and neurospheres-re-evaluating the relationship. *Nat Methods* 2, 333–336.

Reynolds, B.A. & Weiss, S. (1992). Generation of neurons and astrocytes from isolated cells of the adult mammalian central nervous system. *Science* 255, 1707–1710.

Rhinn, M., Lun, K., Luz, M., Werner, M. & Brand, M. (2005). Positioning of the midbrain-hindbrain boundary organizer through global posteriorization of the neuroectoderm mediated by Wnt8 signaling. *Development* 132, 1261–1272.

Rijsewijk, F., Schuermann, M., Wagenaar, E., Parren, P., Weigel, D. & Nusse, R. (1987). The *Drosophila* homolog of the mouse mammary oncogene int-1 is identical to the segment polarity gene wingless. *Cell* 50, 649–657.

Ring, K.L., Tong, L.M., Balestra, M.E., Javier, R., Andrews-Zwilling, Y., Li, G., Walker, D., Zhang, W.R., Kreitzer, A.C. & Huang, Y. (2012). Direct Reprogramming of Mouse and Human Fibroblasts into Multipotent Neural Stem Cells with a Single Factor. *Cell Stem Cell* 11, 100–109.

Rodriguez-Emmenegger, C., Preuss, C.M., Yameen, B., Pop-Georgievski, O., Bachmann, M., Mueller, J.O., Bruns, M., Goldmann, A.S., Bastmeyer, M. & Barner-Kowollik, C. (2013). Controlled cell adhesion on poly(dopamine) interfaces photopatterned with non-fouling brushes. *Adv Mater* 25, 6123–6127.

Rossi, C.C., Kaji, T. & Artinger, K.B. (2009). Transcriptional control of Rohon-Beard sensory neuron development at the neural plate border. *Dev Dyn* 238, 931-943.

Schmidt, R., Strähle, U. & Scholpp, S. (2013). Neurogenesis in zebrafish – from embryo to adult. *Neural Dev* 8, 3.

Schoenwolf, GC. & Smith, JL. (2000). Mechanisms of neurulation. *Methods Mol Biol* 136, 125-134.

Scholpp, S., Delogu, A., Gilthorpe, J., Peukert, D., Schindler, S. & Lumsden, A. (2009). Her6 regulates the neurogenetic gradient and neuronal identity in the thalamus. *Proc Natl Acad Sci U.S.A.* 106, 19895–19900.

Schulte-Merker, S., Lee, K. J., McMahon, A.P. & Hammerschmidt, M. (1997). The zebrafish organizer requires chordino. *Nature* 387, 862–863.

Schwartz, M.A. & Chen, C. S. (2013). Cell biology. Deconstructing dimensionality. *Science* 339, 402–404.

Shao, Y., Sang, J. & Fu, J. (2015). On human pluripotent stem cell control: The rise of 3D bioengineering and mechanobiology. *Biomaterials* 52, 26–43.

Sharma, R. P. (1973). Wingless - a new mutant in *D. melanogaster*. *D.I.S.* 50, 134.

Sirko, S., von Holst, A., Wizenmann, A., Gotz, M. & Faissner, A. (2007). Chondroitin sulfate glycosaminoglycans control proliferation, radial glia cell differentiation and neurogenesis in neural stem/progenitor cells. *Development* 134, 2727-2738.

Sirotkin, H.I., Dougan, S.T., Schier, A.F. & Talbot, W.S. (2000). Bozozok and squint act in parallel to specify dorsal mesoderm and anterior neuroectoderm in zebrafish. *Development* 127, 2583–2592.

Soleman, S., Filippov, M.A., Dityatev, A. & Fawcett, J.W. (2013). Targeting the neural extracellular matrix in neurological disorders. *Neuroscience* 253, 194–213.

Spemann, H. & Mangold, H. (1924). Induction of embryonic primordia by implantation of organizers from a different species. *Int J Dev Biol* 45, 13–38.

Stanganello, E., Hagemann, A.I., Mattes, B., Sinner, C., Meyen, D., Weber, S., Schug, A., Raz, E. & Scholpp, S. (2015). Filopodia-based Wnt transport during vertebrate tissue patterning. *Nat Commun* 6, 5846.

Stern, C.D. (2006). Neural induction: 10 years on since the “default model”. *Curr Opin Cell Biol* 18, 692–697.

Sun, Z., Jin, P., Tian, T., Gu, Y., Chen, Y.G. & Meng, A. (2006). Activation and roles of ALK4/ALK7-mediated maternal TGF β signals in zebrafish embryo. *Biochem Biophys Res Commun* 345, 694–703.

Surmacz, B., Fox, H., Gutteridge, A., Fish, P., Lubitz, S. & Whiting, P. (2012). Directing differentiation of human embryonic stem cells toward anterior neural ectoderm using small molecules. *Stem Cells* 30, 1875-1884.

Suter, D.M., Tirefort, D., Julien, S. & Krause, K.H. (2009). A Sox1 to Pax6 switch drives neuroectoderm to radial glia progression during differentiation of mouse embryonic stem cells. *Stem Cells* 27, 49–58.

Takahashi, H., Itoga, K., Shimizu, T., Yamato, M. & Okano, T. (2016). Human Neural Tissue Construct Fabrication Based on Scaffold-Free Tissue Engineering. *Adv Healthc Mater* 10.1002/adhm.201600197

Takahashi, K. & Yamanaka, S. (2006). Induction of pluripotent stem cells from mouse embryonic and adult fibroblast cultures by defined factors. *Cell* 126, 663–676.

Tang-Schomer, M.D., White, J.D., Tien, L.W., Schmitt, L.I., Valentin, T.M., Graziano, D.J., Hopkins, A.M., Omenetto, F.G., Haydon, P.G. & Kaplan, D.L. (2014). Bioengineered functional brain-like cortical tissue. *Proc Natl Acad Sci U S A*. 111, 13811-13816.

Tawk, M., Araya, C., Lyons, D.A., Reugels, A.M., Girdler, G.C., Bayley, P.R., Hyde, D.R., Tada, M. & Clarke, J.D. (2007). A mirror-symmetric cell division that orchestrates neuroepithelial morphogenesis. *Nature* 446, 797–800.

Thomas, K. R. & Capecchi, M.R. (1990). Targeted disruption of the murine int-1 proto-oncogene resulting in severe abnormalities in midbrain and cerebellar development. *Nature* 346, 847–850.

Thomas, K.R., Musci, T.S., Neumann, P.E. & Capecchi, M.R. (1991). Swaying is a mutant allele of the proto-oncogene Wnt-1. *Cell* 67, 969–976.

Thomson, J.A., Itskovitz-Eldor, J., Shapiro, S.S., Waknitz, M.A., Swiergiel, J.J., Marshall, V. S. & Jones, J.M. (1998). Embryonic Stem Cell Lines Derived from Human Blastocysts. *Science* 282, 1145-1147.

Truckenmüller, R., Giselbrecht, S., Rivron, N., Gottwald, E., Saile, V., van den Berg, A., Wessling, M. & van Blitterswijk, C. (2011). Thermoforming of film-based biomedical microdevices. *Adv Mater* 23, 1311–1329.

Turner, D. A., Hayward, P.C., Baillie-Johnson, P., Rue, P., Broome, R., Faunes, F. & Martinez Arias, A. (2014). Wnt/ -catenin and FGF signalling direct the specification and maintenance of a neuromesodermal axial progenitor in ensembles of mouse embryonic stem cells. *Development* 141, 4243–4253.

Ungrin, M.D., Joshi, C., Nica, A., Bauwens, C. & Zandstra, P.W. (2008). Reproducible, ultra high-throughput formation of multicellular organization from single cell suspension-derived human embryonic stem cell aggregates. *PLoS ONE* 3, e1565.

Villa-Diaz, L.G., Ross, A.M., Lahann, J. & Krebsbach, P.H. (2013). The evolution of human pluripotent stem cell culture: from feeder cells to synthetic coatings. *Stem Cells* 31, 1–7.

von Holst, A., Sirko, S. & Faissner, A. 2006. The unique 473HD- chondroitinsulfate epitope is expressed by radial glia and involved in neural precursor cell proliferation. *J Neurosci* 26, 4082–4094.

Wang, X., Chu, L.T., He, J., Emelyanov, A., Korzh, V. & Gong, Z. (2001). A novel zebrafish bHLH gene, neurogenin3, is expressed in the hypothalamus. *Gene* 275, 47–55.

Warmflash, A., Sorre, B., Etoc, F., Siggia, E.D. & Brivanlou, A.H. (2014). A method to recapitulate early embryonic spatial patterning in human embryonic stem cells. *Nat Methods* 11, 847-854.

Watanabe, K., Kamiya, D., Nishiyama, A., Katayama, T., Nozaki, S., Kawasaki, H., Watanabe, Y., Mizuseki, K. & Sasai, Y. (2005). Directed differentiation of telencephalic precursors from embryonic stem cells. *Nat Neurosci* 8, 288–296.

Wattanapanitch, M., Klincumhom, N., Potirat, P., Amornpisutt, R., Lorthongpanich, C., Upratya, Y., Laowtammathron, C., Kheolamai P., Pongvarin, N. & Issaragrisil, S. (2014). Dual small-molecule targeting of SMAD signaling stimulates human induced pluripotent stem cells toward neural lineages. *PLoS One* 9, e106952.

Wegner, M. (2011). SOX after SOX: SOXession regulates neurogenesis. *Genes Dev* 25, 2423–2428.

Wilkinson, G., Dennis, D. & Schuurmans, C. (2013). Proneural genes in neocortical development. *Neuroscience* 253, 256–273.

Wilson, L. & Maden, M. (2005). The mechanisms of dorsoventral patterning in the vertebrate neural tube. *Dev Biol* 282, 1–13.

Woo, K. & Fraser, S.E. (1997). Specification of the zebrafish nervous system by nonaxial signals. *Science* 277, 254–257.

Xu, C., Inokuma, M.S., Denham, J., Golds, K., Kundu, P., Gold, J.D. & Carpenter, M.K. (2001). Feeder-free growth of undifferentiated human embryonic stem cells. *Nat Biotechnol* 19, 971–974.

Xu, Q. & Wilkinson, D.G. (2013). Boundary formation in the development of the vertebrate hindbrain. *Wiley Interdiscip Rev Dev Biol* 2, 735–745.

Yang, K., Park, H.J., Han, S., Lee, J., Ko, E., Kim, J., Lee, J., Yu, J.H., Song, K.Y., Cheong E., Cho, S.R., Chung, S. & Cho, S.W. (2015). Recapitulation of in vivo-like paracrine signals of human mesenchymal stem cells for functional neuronal differentiation of human neural stem cells in a 3D microfluidic system. *Biomaterials* 63, 177–188.

Yuan, L. & Hassan, B.A. (2014). Neurogenins in brain development and disease: An overview. *Arch Biochem Biophys* 558, 10–13.

Zhang, S. & Cui, W. (2014). Sox2, a key factor in the regulation of pluripotency and neural differentiation. *World J Stem Cells* 6, 305-311.

Zhang, S.C., Wernig, M., Duncan, I.D., Brüstle, O. & Thomson, J.A. (2001). In vitro differentiation of transplantable neural precursors from human embryonic stem cells. *Nat Biotechnol* 19, 1129–1133.

Zhu, Y., Carido, M., Meinhardt, A., Kurth, T., Karl, M.O., Ader, M. & Tanaka, E.M. Three-dimensional neuroepithelial culture from human embryonic stem cells and its use for quantitative conversion to retinal pigment epithelium. *PLoS One* 8, e54552.

Žigman, M., Trinh, L.A., Fraser, S.E. & Moens, C.B. (2011). Zebrafish neural tube morphogenesis requires Scribble-dependent oriented cell divisions. *Curr Biol* 21, 79–86.